

UC Santa Barbara

UC Santa Barbara Electronic Theses and Dissertations

Title

Topological Phases of Matter: a mathematical approach

Permalink

<https://escholarship.org/uc/item/6c63q51m>

Author

Babakhani, Arman

Publication Date

2021

Peer reviewed|Thesis/dissertation

University of California

Santa Barbara

Topological Phases of Matter:

A Mathematical approach

A thesis submitted for the degree of
Masters of Science in

Chemistry

by

Arman Babakhani

Committee in charge:

Professor Vojtech Vlcek, Co-Chair

Dr. Parsa Bonderson, Microsoft, Co-Chair Professor

Mark Srednicki

Professor Bernard Kirtman

December 2021

Arman Babakhani's Master's thesis is approved by

Professor Mark Srednicki

Professor Bernard Kirtman

Dr. Parsa Bonderson, Co-Chair

Professor Vojtech Vlcek, Co-Chair

December 2021

Topological Phases of Matter

Copyright © 2021

by

Arman Babakhani

Acknowledgements

It should go without saying that no individual achievements are truly individual. If it was not for the support of my parents, and the opportunity given to me by many amazing mentors and professors including Vojtech Vlcek, Mark Srednicki, and especially Parsa Bonderson, I would not be able to learn as much as I have. Graduate school has been an immense journey of not only academic exploration, but of self-discovery. It has been quite a challenge not to be intimidated by the intellectual brilliance of many of my peers and Professors. Through the engagement and belief of many of my mentors, however, I have been able to cultivate some confidence in my knowledge and be eager to learn more. I would like to thank Bernard Kirtman for dedicating some of his time towards the development of this thesis and being on this committee. I would also like to thank many others in the chemistry department, including Trevor Hayton, Petra Van Koppen, and Frank Brown.

I have had many insightful conversations with Postdocs and graduate students in Vlcek group namely Carlos Mejuto-Zaera, Anna P. Vidal, Gwen Weng, Mariya Romanova and others. I have also tremendously benefited from participating in weekly meetings with Mark Srednicki and his former and current student (Chaitanya Murthy and Fernando Iniguez). I should also thank Hassan Shapourian at station Q for his support and engaging conversations.

Finally, I would like to especially thank my uncle, Vartan, for our long intellectual conversations on endless topics, and his encouragement for my pursuit of science.

Topological Phases of Matter:

A mathematical approach

by

Arman Babakhani

Abstract

In this work, I provide a literature review of earlier works on classification of topological phases. In doing so, we motivate the idea of topological order and phases of matter that are dependent on global geometric features of systems in consideration.

I review an algebraic formalism to categorize phases of matter containing non-abelian anyons, known as Braided Tensor Categories (BTC). With the motivation to study the relationship between non-abelian anyonic and symmetry defects, I also introduce the an algebraic formalism describing the interplay of global symmetries with the anyonic degrees of freedom. This formalism is known as G -crossed BTC. These algebraic formalism provide observable topological quantities, such as the topological S -matrix, that can be probed by interference measurements [1]. When the topological S -matrix of the BTC is unitary, it is said that the fusion theory is said to be modular. Hence, one calls the algebraic formalism a Modular Tensor Category (MTC).

I present the results of our work showing that one can construct projective representations of the mapping class group of the punctured torus from the topological formalism given by G -crossed BTC. This is pivotal in constructing a G -crossed BTC for surfaces of higher genus, as one can build surfaces of arbitrary genus by gluing many punctured tori. Throughout my mathematical

analysis, I also show that modularity of BTCs are not destroyed by the presence of symmetry defects.

Contents

I.	Introduction and Outline	1
II.	Adiabatic Theorem and Geometric Phases	8
A.	Avoided crossings	11
A 1.	Degeneracies due to symmetries	13
B.	Conical intersections	13
III.	Topology and Transport	15
A.	Topological invariants in solids	15
B.	Chern Numbers	16
C.	Anomalous velocity	18
C 1.	Hall conductivity from linear response	19
D.	Topological Insulators (TI)	22
IV.	Topological order	25
A.	The 2d Toric code	26
B.	Quantum Hall Effect	31
B 1.	IQH	31
B 2.	FQH	33
V.	Fusion and Braided Tensor Categories (BTC)	37
A.	Motivation	37
B.	Quasiparticle Fusion and Braiding	39
B 1.	Fusion	39

B 2.	Associativity and F-moves	41
B 3.	Quantum dimensions	42
B 4.	Braiding	43
C.	Topological quantities	44
VI.	Symmetries and topological defects	46
A.	Topological Defects	46
B.	G -crossed BTC	47
B 1.	G -Graded Fusion	47
B 2.	G -crossed Topological Eigenstates	48
B 3.	G -Crossed Braiding	49
B 4.	G -crossed Invariants and the S -matrix	54
VII.	Modularity of $\mathcal{C}^{\times G}$ on torus *	57
VIII.	G-crossed MTC on surfaces of arbitrary genus *	62
A.	Modular transformations	66
IX.	Proof of modular group relations *	68
A.	$(ST)^3 = \Theta_0 S^2$	68
B.	$S = CS^\dagger$	69
C.	$C^2 = Q^{-1}$	70
D.	$CS = SC$	73
E.	$CT = TC$	75
F.	$S^2 = C$	77
F 1.	$S(\mathfrak{g}, \mathbf{0})S(\mathbf{0}, \bar{\mathfrak{g}}) = C(\mathfrak{g}, \mathbf{0})$	78

F 2.	$\mathbf{S}(\mathbf{g}, \mathbf{h})\mathbf{S}(\mathbf{h}, \bar{\mathbf{g}}) = \mathbf{C}(\mathbf{g}, \mathbf{h}) \dots \dots \dots$	79
X.	Concluding Remarks	81
A	$(ST)^3 = \Theta_0 S^2$: Detailed diagrammatic steps	82
B	$S = CS^\dagger$: detailed diagrammatic steps	84
C	$CS = CS$: detailed diagrammatic steps	85

* Indicates sections containing original work by the author.

I. INTRODUCTION AND OUTLINE

Quantum mechanics has been very successful in explaining the behavior of systems in atomic scale, a scale that was not well-understood by classical theories of mechanics and electromagnetism. It has also helped explain various phenomena on larger length scales. Electronic transport properties through a process called quantum tunneling is an example of such phenomena. Quantum mechanics has also revolutionized the fields of technology and engineering, through the invention of transistors, and the most valuable of its applications might yet to be realized in quantum computers.

Even though some features of quantum mechanics, such as quantum entanglement, might seem unintuitive and complicated, the mathematical formalism describing quantum mechanics is quite straightforward: there is a single equation, namely the Schrödinger Equation (SE), that explains how a quantum system evolves as a function of time [2]. How the system evolves, depends on the types of interactions and microscopic mechanisms inherent to the system, described by a Hamiltonian. That is all it takes to do quantum mechanics. All the complicated and eerie features arise as a result of solving the SE, using a given Hamiltonian. Though, one must admit that solving the SE can be incredibly daunting.

As a result of solving the SE, one finds all the possible states (eigenstates) in which one can find the system upon measurement at a particular time¹. Each eigenstate has a well-defined energy, and sometimes multiple states have the same energy eigenvalue. These states are called energy degenerate states. In order to distinguish eigenstates, especially degenerate states, one must specify how the states project or overlap onto

¹Eigenstates are the equilibrium states of a Hamiltonian. A general quantum system can be described by a superposition of such states.

one another. In this sense, it is possible to think of eigenstates as vectors, and define an inner-product operation to specify how two states align with respect to each other. In order to consider all possible quantum states, one must then specify the space spanned by all the solutions to the SE, known as the Hilbert space.

Due to the difficulty of solving the SE, physicists and chemists, for the most part, have relied on approximation methods [3]. If the eigenstates of a particular Hamiltonian H_1 is very difficult to solve for, a possible approach is to find another Hamiltonian H_2 for which one can solve the eigenstates with ease, and relate the eigenstates of H_2 to H_1 with an approximation method, such as perturbation theory. There are various limitations to using perturbation theory, namely that the difference of energies induced by the two Hamiltonians $\Delta H = H_1 - H_2$ must be much smaller than the energy scales of the Hamiltonian H_2 . In other words, the bigger the difference between the two Hamiltonians, the poorer our estimation for the eigenstates of H_1 . Therefore, generally, most of the qualitative features of H_1 will be removed if ΔH is significantly large. This is called the breakdown of perturbation theory. One might naturally come to ask the following questions. Given two different Hamiltonians H_1 and H_2 , are there any common features between the two systems, even when ΔH falls outside of the domain of perturbation theory? What set of quantities remain unchanged upon perturbations? Are there a set of Hamiltonians that share universal characteristics, independent of the detailed description of the microscopic interactions?

These types of questions have motivated the search for the types of systems that have intrinsic features which cannot be removed upon perturbations. These features are often called topological features. This implicitly defines what most physicists

mean by a “topological” feature: a quantity that is robust under smooth deformations of the Hilbert space. To highlight why this definition is suitable, one can draw an analogy between deformation of the Hilbert space to deformation of surfaces in real space. Consider the surface of a torus: irrespective of how one smoothly² deforms the surface of this torus, the hole surrounded by the torus can never be removed. The number of holes of a surface is thus a topological quantity, known as the genus of the surface. Of course, the Hilbert space is not the real space, so I will provide more specific examples and emphasize what is meant by smooth deformations in quantum mechanical setting.

The existence of topological features was not obvious in the early days of quantum mechanics [4]. It took clever thought experiments and masterful use of physical intuition in order to hypothesize the existence of such features. One of the first such thought experiments was due to Aharonov and Bohm [5]. Contrary to classical electromagnetism, they argued that electromagnetic potentials produced physically observable effects on a quantum system. The classically held belief was that as long as there are no electric or magnetic fields in the region of a charged particle’s presence, no physical effects due to the electromagnetic gauges will be observable. However, in a set up shown in Figure 1, Aharonov and Bohm argued that the wavefunction of an electron traveling around a solenoid in a region of zero magnetic field, will pick up a phase, which can be detected upon interference measurements.

The topological feature in the Aharnov-Bohm (AB) experiment is due to the path-independence of the phase picked up by going around the solenoid. Since the phase $e^{i\gamma(\phi)}$ only depends on the angle traversed (as shown in the RIGHT figure of

²Smooth deformation refers to a deformation that does not rip or cut the surface.

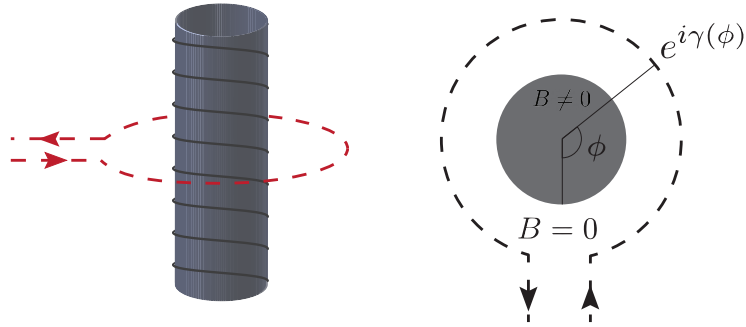


Figure 1: Aharonov and Bohm experiment showing the path of a quantum system in a region of zero magnetic field. LEFT: figure of a solenoid showing the traversed path of the particle. RIGHT: Top View of the setup. The phase picked up by the wavefunction is dependent on the angle traversed around the solenoid.

Figure 1), moving all the way around the solenoid will result in a fixed phase $e^{i\gamma(2\pi)}$, regardless of the specific path taken. In other words, this phase is robust under smooth deformations of the path chosen around the solenoid, and so one can think of it as a topological feature.

A similar path-independent phase is gained by the electronic wavefunction in chemical systems of polyatomic nature. Herzberg et al. in 1979, showed that given the presence of a certain type of degeneracy in polyatomic systems, known as a *conical intersection*(CI), the electronic wavefunction gains a minus sign upon going around the conical intersection, regardless of the specific path taken around it [6]. Figure 2 illustrates the intersection of two potential energy surfaces in a polyatomic system. CIs have been an important topic of research in molecular dynamics in the last few decades. Subtle treatments that account for effects due to the phases gained by the electronic wavefunctions must be accounted for when computing the scattering of electronic orbitals [7, 8]. These effects are typically categorized as non-adiabatic (diabatic) effects. I will explain how the presence of CIs in a molecular system introduces

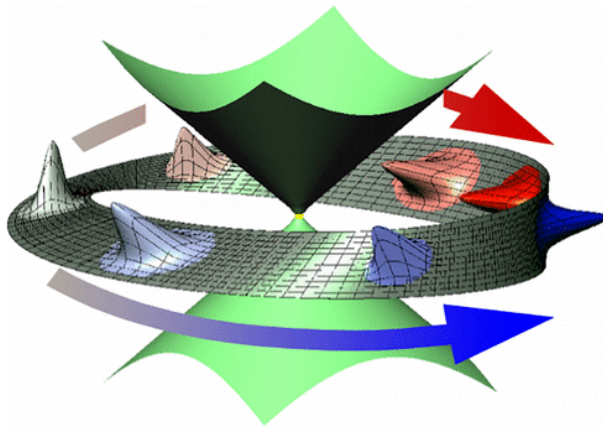


Figure 2: Conical intersection of two potential energy surfaces. The electronic wavefunction gains a minus sign upon going around the center of the intersection. The figure is taken from [7].

complications in later subsections. I mention this example to highlight the types of observation that have motivated theoretical chemists and physicists to study systems with topological features.

The systems which possess such features have gained popularity not for purely mathematical reasons, but also for their application in explaining superconductivity and other exotic phenomena such as quantum Hall effect (QHE). In this work, I will review some quantitative metrics used to capture topological features in materials. I will discuss some models containing topological features and highlight signatures of topological effects in physical systems, namely a class of material known as topological insulators. I will also emphasize topological aspects governing the QHE, and highlight the existence of excitations that are neither bosonic nor fermionic. These excitations are known as anyons, the existence of which has been experimentally verified in fractional quantum hall states [9]. Anyonic systems are attractive test grounds for studying many-body phases that are topological. This is because the path of every particle around any other particle in the system produces observable effects on the

state of the system. Therefore, to characterize the topological properties of a system, it is important to analyze the way the paths of the particles ‘thread’ around all the other ones. ‘Threading’ of particles around one another is called braiding.

It is important to emphasize that most of the discussion in this work will be limited to two spatial dimensions, $(2+1)D^3$. This is because studying the braiding of particles around one another requires specifying path of one or many particles that enclose other particles. In three spatial dimensions, one can reduce closed loops into single points, rendering the effect of enclosed particles on the closed paths trivial [10]. In sections I-IV, I will provide some background on topological character of various systems, including quantum hall states. I will provide a motivation to consider phases of matter that are known to have ‘topological order’. In doing so, I will motivate an algebraic approach that takes a fundamental step in characterizing topological phases of matter that is consistent with Quantum Field theory.

Quantum field theory (QFT) provides an alternative, but similar, approach to studying quantum systems. Instead of a Hamiltonian description and Schrödinger’s Equation, one often uses path integral formalism, describing the quantum system via Lagrangian dynamics [11, 12]. An intricate approach to studying topological aspects of quantum theory is through Topological Quantum Field Theory (TQFT) [13]. TQFT is the study of properties of quantum fields that do not depend on the details of the spacetime on which the fields live, i.e. properties that are metric independent. Prominent work has been done by Edward Witten in this field to relate the structure of certain quantum field theories to those of knots and closed links [14]. TQFTs are a general framework in which physical observables and topological

³two space and one time dimension.

quantities can be computed from a microscopic description of interaction of various types of quantum fields. Even though TQFTs provide a detailed picture of the types of interaction in a system, computation of observables and topological features of a physical system involves challenges such as evaluating Wilson loops [13].

In section V, I will delve into a simpler mathematical formalism than TQFTs, which allows one to describe excitations and the resulting topological features upon their braiding in many-body systems. This mathematical structure, known braided tensor categories (BTC), are equivalent to TQFTs for two-dimensional systems with low-energy excitations such as those of QHE [15, 16]. However, BTCs are a more pragmatic algebraic method of describing topological features of anyonic states in low-energy two-dimensional systems. Provided the types of excitations and how they interact with each other, BTCs allow for the categorization of possible anyonic phases due to the transport of excitations around one another.

The effects of global symmetries on systems with anyonic excitations is an interesting ongoing topic of research. One can use BTCs to study the topological phases arising in systems with anyonic excitations. However, applying BTCs on systems with global symmetries requires a richer structure. Violations of the global symmetries, called symmetry defects, require one to not only study the interaction of quasiparticle⁴ excitations but those of the symmetry defects themselves. In section VI, I will briefly review the mathematical structure created by the interplay of symmetry defects with electronic excitations, known as G -crossed BTC. In a recent work, Barkeshli et al. have shown that G -crossed BTCs provide a consistent mathematical structure that

⁴Quasi-particles are localized excitations that are not destroyed by small perturbations. They are called quasi-particles because they are emergent excitations and do not constitute an individual particle by themselves.

allows one to study defects and quasi-particles on a torus, a surface of genus one [17].

Finally, in sections VII and XI, I will introduce and present the results of our recent project, showing the relationship between BTCs and topological representation of a torus and surfaces with higher genus. As a result of the our mathematical analysis, we come to the conclusion that if BTCs preserve unitarity of quasi-particle processes⁵ (specifically a quantity known as the S -matrix), the G -crossed BTCs also preserve this property.

II. ADIABATIC THEOREM AND GEOMETRIC PHASES

In order to study smooth deformations and be able to characterize features that are independent of such deformations, one needs to define what is meant by smoothness. A precise approach requires one to consider adiabatic processes. In thermodynamics, an adiabatic process is one that occurs slow enough that no energy is entered or exited a closed system. In order to highlight the precise definition of adiabaticity in quantum systems, I will begin by introducing adiabatic transport using Schrödinger's Equation (SE).

For a general treatment of the problem, one could define a Hilbert space, specified by a set of parameters $\{\lambda_i\}$, $\mathcal{H}(\{\lambda_i\})$. Let us denote the Hamiltonian of the system by $H(\vec{\lambda}(t))$, where $\vec{\lambda}(t)$ is a vector in the space of parameters given by λ_i , and for generality, let us assume that this vector is time dependent. Given the initial state of the system, $|\psi(0)\rangle$, in order to describe the state $|\psi(t)\rangle$, one could use SE to write

$$H(\vec{\lambda}(t))|\psi(t)\rangle = i\hbar\partial_t|\psi(t)\rangle. \quad (1)$$

⁵This feature is called modularity of the fusion category.

If one assumes that the $\lambda_i(t)$ is a smooth function of t for all i , then the eigenstates of H , $\{|n(\vec{\lambda}(t))\rangle\}$ satisfy

$$H(\vec{\lambda}(t))|n(\vec{\lambda}(t))\rangle = E_n(\vec{\lambda}(t))|n(\vec{\lambda}(t))\rangle. \quad (2)$$

Working in the Schrödinger's picture, and writing $|\psi(t)\rangle = \sum_n c_n(t)|n(\vec{\lambda}(t))\rangle$, one can write a differential equation for the coefficients $c_n(t)$ by using SE (having set $\hbar = 1$)

$$\begin{aligned} \partial_t |\psi(t)\rangle &= \sum_n \left(\dot{c}_n(t) |n(\vec{\lambda}(t))\rangle + c_n(t) \partial_t |n(\vec{\lambda}(t))\rangle \right) \\ &= -iH(\vec{\lambda}(t))|\psi(t)\rangle = -i \sum_n c_n(t) E_n(t) |n(\vec{\lambda}(t))\rangle. \end{aligned} \quad (3)$$

Note that the dot over a variable represents a time derivative. Now, taking the inner product of the equation above with $\langle m(\vec{\lambda}(t))|$ results in the following differential equation for the coefficients $c_m(t)$

$$\begin{aligned} \dot{c}_m(t) + ic_m(t)E_m(t) + c_m(t) \langle m(\vec{\lambda}(t)) | \partial_t |m(\vec{\lambda}(t))\rangle \\ = \sum_{n \neq m} c_n(t) \frac{\langle m(\vec{\lambda}(t)) | \dot{H}(\vec{\lambda}(t)) |n(\vec{\lambda}(t))\rangle}{E_m(t) - E_n(t)}. \end{aligned} \quad (4)$$

To obtain the right hand side of the equation above, I have used the fact that $\langle m | \partial_t |n\rangle = \frac{\langle m | \dot{H} |n\rangle}{E_n - E_m}$ for $n \neq m$. To see this, one can time differentiate Eq. (2), and take the inner product of the resulting equation with $\langle m |$.

When the minimal energy differences between eigenstates are significantly larger than the rate of change of the Hamiltonian, one can simply neglect the right hand side of Eq. (4). This condition can be stated as follows

$$|\langle m(\vec{\lambda}(t)) | \dot{H}(\vec{\lambda}(t)) |n(\vec{\lambda}(t))\rangle| \ll |E_m(t) - E_n(t)|. \quad (5)$$

This is the precise adiabatic condition in quantum systems. This condition obviously fails if there are degeneracies or band-crossings along the path of transport.

Under adiabatic conditions, Michael Berry offered a solution to Eq. (4) by considering the adiabatic limit (setting the right hand side of the equation to zero) [18].

The solution, thus, is written by the following

$$c_m(t) = \exp \left[i \left(\gamma_m(t) - \int_0^t E_m(t') dt' \right) \right] \quad (6)$$

$$\gamma_m(t) = \int \mathcal{A}_m(\vec{\lambda}(t)) \cdot d\boldsymbol{\lambda} \quad (7)$$

$$\mathcal{A}_m(\vec{\lambda}(t)) = -i \langle m(\vec{\lambda}(t)) | \nabla_{\boldsymbol{\lambda}} | m(\vec{\lambda}(t)) \rangle. \quad (8)$$

This solution entails the usual phase corresponding to the energy of the system at any particular time, with an additional term, $\gamma_n(t)$, which has been popularized as the Berry's phase, due to major contributions from Michael Berry. The term $\mathcal{A}_m(\vec{\lambda})$ is known as Berry's connection, and is a vector quantity, quantifying the smooth deformations of the eigenstates. The Berry's phase is an entirely geometric contribution, as it depends on the traversed path in the parameter space. Berry's phase and connection vector will be used to account for topological effects upon smooth deformations of solid crystals upon smooth deformations in k -space, in later sections.

We must note that our analysis above is restricted to Hamiltonians that commute with themselves in the entire parameter space given by $\{\lambda_i\}$. In other words, $[H(\vec{\lambda}(t)), H(\vec{\lambda}(t')))] = 0$ for all $\vec{\lambda}(t)$ and $\vec{\lambda}(t')$. These types of systems are known as Abelian systems. In non-Abelian systems, the components of the Berry-connection vector are matrices. Thus one must also account for the order in which Berry-

connections act on the evolution of the system. Without getting into the details of such systems, we state that the non-Abelian nature of Berry's phase is captured by the following quantity (also known as 'Wilson line/loop' in topological quantum field theory context)

$$\gamma = \mathcal{P} \exp \left(\int \mathcal{A}(\vec{\lambda}) \cdot d\boldsymbol{\lambda} \right). \quad (9)$$

$\mathcal{P} \exp()$ denotes a path-ordered exponential, and the integral is along the path taken in the parameter space. References [19, 20] provide a detailed discussion of Berry-connections in non-Abelian systems.

As mentioned earlier, transport in systems with band crossings and degeneracies fails to satisfy the adiabatic condition, regardless of the speed of transport. In these instances one must also account for non-adiabatic transitions, i.e. transitions to different energy levels implied by the right hand side of Eq. (4). In most polyatomic materials, due to large number of degrees of freedom (DOF), crossing of energy levels near the valence bands are a rarity. In fact, Herzberg and Longuet-Higgins extended the eigenvalue crossings observation by von-Neumann and Wigner, and analyzed systems with eigenvalue crossings. I will review the importance of these analyses in the next few subsections and emphasize the importance of adiabatic theorem in quantum chemistry and materials.

A. **Avoided crossings**

One of the first works highlighting the relationship between symmetry and level statistics and energy level crossings was done by Wigner and von-Neumann [21]. Wigner and von-Neumann showed that in order for a system with no symmetries to have

energy level crossings, one must tune at least two parameters. This is easily demonstrated by a simple model. One can demonstrate this fact by considering a Hamiltonian specified by a parameter vector $\vec{\lambda} = (\lambda_0, \lambda_1, \lambda_2, \lambda_3)$, and Pauli matrices $\{\sigma_i\}$, represented in vector form $\vec{\sigma}$, $H(\vec{\lambda}) = \vec{\lambda} \cdot \vec{\sigma}$. Note that with this notation $\sigma_0 = \mathbb{1}$ is the identity matrix. The Hamiltonian can be written in the following matrix form

$$H(\lambda_0, \lambda_1, \lambda_2, \lambda_3) = \begin{pmatrix} \lambda_0 + \lambda_3 & \lambda_1 - i\lambda_2 \\ \lambda_1 + i\lambda_2 & \lambda_0 - \lambda_3 \end{pmatrix} \quad (10)$$

Since the Hamiltonian does not have any symmetries, λ_i s are arbitrary complex parameters. The eigenvalues of the Hamiltonian is thus given by

$$E_{\pm} = \lambda_0 \pm \sqrt{\lambda_1^2 + \lambda_2^2 + \lambda_3^2} \quad . \quad (11)$$

Thus, in order for the two eigenvalues to coincide, one must require $\lambda_1^2 + \lambda_2^2 + \lambda_3^2 = 0$. This implies that at least two of the three parameters must be specifically chosen in order to achieve this. The general argument holds for any Hamiltonian with N DOFs. Without any symmetries, one must tune $N-2$ DOFs in order to achieve level crossings. This argument can be extended to molecules. In diatomic molecules without any symmetries, the only DOF is the bond length between the two molecules. Thus, from arguments above, one might infer that no level crossings occur. Thus, systems with insufficient DOFs cannot host degeneracies or level crossings. This phenomena is referred to as avoided crossings.

A 1. Degeneracies due to symmetries

It is worth emphasizing that symmetries can often create degeneracies in a system. For instance, if one requires that the Hamiltonian in Eq. (10) be symmetric under σ_z conjugation, i.e. $[H, \sigma_z] = 0$, we must have that $\lambda_1 = \lambda_2 = 0$. This suggests that, by tuning a single parameter λ_3 , one can obtain level crossings. In general, a system H with a set of symmetries J_i could host degeneracies, when the symmetries do not commute. This can be observed by picking two non-commuting operators J_1 and J_2 , such that $[H, J_1] = [H, J_2] = 0$. Assuming that $\{|n\rangle\}$ are a complete set of eigenstates of H . One should observe that $J_{1,2}|n\rangle$ is also an eigenstate of H by the following

$$0 = [H, J_{1,2}]|n\rangle = H(J_{1,2}|n\rangle) - E_n(J_{1,2}|n\rangle) \quad (12)$$

From the relation above, we see that both states $J_1|n\rangle$ and $J_2|n\rangle$ have the same energy, however, they are not necessarily the same state. Now, repeating this argument with the states $J_{1,2}|n\rangle$

$$0 = [H, J_{2,1}](J_{1,2}|n\rangle) = H(J_{2,1}J_{1,2}|n\rangle) - E_n(J_{2,1}J_{1,2}|n\rangle) \quad (13)$$

This shows that the state $J_1J_2|n\rangle$ has the same energy $J_2J_1|n\rangle$. However, since $[J_1, J_2] \neq 0$, these two states are not necessarily identical. So, non-commuting symmetries could enforce degeneracies and level crossings in a quantum system.

B. Conical intersections

From the discussion of symmetries, one can note that in diatomic molecular systems, level crossings due to existence of different types of non-commuting symmetries are a

possibility. In complex structures, such as polyatomic molecules, due to large number of DOFs, level crossings are not contingent upon the existence of symmetries. Herzberg and Higgins went beyond diatomic molecules and analyzed triatomic structures, and highlighted the nature of the level crossings near the center of the molecular structure [6]. They observed the existence of a conical intersection of potential energy surfaces and noted that the electronic wavefunction attains a non-trivial minus sign upon transporting the system around the center of the conical intersection.

Upon the observation that the electronic wavefunction acquires a negative sign upon being transported around the center of the conical intersection, one must be wary of the implications of this observation on the single-valuedness of the total wavefunction of the system. It is clear that in order to preserve the single-valuedness of the total wavefunction of the conically intersecting systems, then the nuclear wavefunction must also acquire some phase in order to compensate for the sign gained by the electronic wavefunction upon transporting around the loop of the intersection. This indicates that our usual assumptions about the separation of the total wavefunction into electronic and nuclear parts, given by the Born-Oppenheimer approximation is invalid. Namely, one can no longer split the nuclear and electronic DOFs and write

$$|\Psi\rangle \approx |\psi_{elec}\rangle \otimes |\psi_{nuc}\rangle \quad (14)$$

$$\Psi(\{\mathbf{r}_i\}, \{\mathbf{R}_j\}) \approx \psi_{elec}(\{\mathbf{r}_i\}|\{\mathbf{R}_j\}) \psi_{nuc}(\{\mathbf{R}_j\}). \quad (15)$$

Before the work of Herzberg et al., quantum chemistry calculations relied on Eq. (15), with the justification that in non-relativistic systems, the nuclear dynamics are orders of magnitude smaller than those of electronic, and so one could neglect any

correlation between the nuclear and electronic wavefunctions. However, in the presence of entanglement between nuclear and electronic DOFs, one cannot apply the Born-Oppenheimer approximation. Therefore, adiabatic quantum chemistry calculations might be inappropriate for systems exhibiting long-range entanglement and topological order at molecular level.

In light of the signatures of breakdown of Born-Oppenheimer approximation in presence of conical intersections, Mead et al. introduced a mathematical formalism to account for non-adiabatic corrections by unitary transformations on nuclear wavefunctions [22]. Since 1980s, great progress has been made on incorporating geometric phase effects from non-adiabatic dynamics due to conical intersections. Intricate methods to go beyond Born-Oppenheimer approximation and account for non-adiabatic effects upon doing molecular dynamics simulations have been explored in the recent years [23, 24, 7, 8]. Molecular systems with CIs remain an ongoing topic of research in theoretical chemistry.

III. TOPOLOGY AND TRANSPORT

A. Topological invariants in solids

Insulators are a class of materials about which topology has helped expand our understanding. Conventionally, one thinks of insulators as systems with a band gap. This gap between the occupied and unoccupied states is large enough that no significant thermal excitations from the valence band maximum (VBM) to conduction band minimum (CBM) can occur. Thus, using band-theory one can predict insulat-

ing behavior on systems with large gaps between VBMs and CBMs. However, not all insulators are alike. In fact, there are classes of insulators exhibiting topological character. I will emphasize the importance of topological insulators after introducing Chern numbers and their role in transport properties of material.

In order to describe the topological character, we need to consider smooth deformations of the bands, keeping in mind the symmetries possessed in the system. For instance, a solid with crystal structure has translational symmetry, and one by smoothly deforming the bands, by either varying the chemical potential of each constituent or by changing the cell dimensions, still retains the translational symmetry. Therefore, when applying topological methods to studying material, one assumes that periodicity is not broken upon deformations (change of parameters).

B. Chern Numbers

In this subsection, I introduce Chern numbers and their relation to the topology of quantum systems. In order to define the mathematical form of the Chern number, let us limit ourselves to 2 spatial dimensional systems (2+1)D. The reason for this is not only to simplify some of the mathematical expressions, but to also merge our discussion with anyonic systems, which are (2+1)D phenomena. Let us start from the definition of Berry's phase, given in Eq. (7), defined in the momentum space, i.e. $\vec{\lambda} = \vec{k}$.

$$\gamma_m(\mathbf{k} \rightarrow \mathbf{k}') = \int_{\mathbf{k}}^{\mathbf{k}'} \mathcal{A}_m(\vec{k}) \cdot d\mathbf{k} \quad (16)$$

$$\gamma_m(\mathbf{k} \rightarrow \mathbf{k}) = \oint_S [\nabla \times \mathcal{A}_m(\vec{k})] \cdot d^2\mathbf{k} \equiv \oint_S \Omega_m(\vec{k}) \cdot d^2\mathbf{k} \quad (17)$$

$$C_m = \frac{1}{2\pi} \oint_S \Omega_m(\vec{k}) \cdot d^2\mathbf{k} \quad (18)$$

Eq. (18) defines Chern number C_m of a band m in a solid. It is worth noting that, in the second step of Eq. (17), we have used Stoke's theorem and $\mathbf{\Omega}_m(\vec{k})$ is called the Berry-curvature of band m . However, one must be careful to keep in mind that the integrals in Eq. (17) are contour integrals in the 2d complex plane. This means, that closed loop line integrals are not always vanishing. They vanish only if the integrand of the line integral does not contain any singularities. The number of singularities in the Berry-connection vector is a topological quantity that cannot be altered by small perturbations.

There are rigorous arguments using complex analysis that one can employ to show the quantization of the Chern number. A simple observation, however, is to require single-valuedness of the wavefunctions (bands) upon traversing along the entire Brillouin zone. This suggests that the Berry's phase, $\gamma_m(\mathbf{k} \rightarrow \mathbf{k})$ gained upon traversing through the entire Brillouin zone (a closed loop in k -space) should have a trivial phase, i.e.

$$\gamma_m(\mathbf{k} \rightarrow \mathbf{k}) = 2\pi n, \quad n \in \mathbb{Z}. \quad (19)$$

Using this argument, and the definition of the Chern number for band m from Eq. (18), we see that the Chern number of a band m could only take on integer values, namely $C_m = n$. We end this subsection by emphasizing that the Chern number, like the winding number⁶ or the genus of a surface, is quantized, and it relates many important ideas in quantum mechanics to the study of geometry and topology.

⁶In simple terms, the winding number is the number of full circular turns that a closed curve makes.

C. Anomalous velocity

To observe the geometric effects due to Berry-curvature, N. Qian and S. Ganesh analyzed the equations of motion of a semi-classical system, described by wave-packets, in presence of external electric and magnetic fields [25]. By calculating the expectation values of momentum and position operators, they obtained dynamics that closely resembles those described by classical equations of Lorentz forces in electromagnetism. These resulted in the so called semi-classical transport equations, given as follows

$$\dot{\mathbf{x}} = \nabla_{\mathbf{k}} E_m(\mathbf{k}) - \dot{\mathbf{k}} \times \boldsymbol{\Omega}_m(\mathbf{k}) \quad (20)$$

$$\dot{\mathbf{k}} = -e\mathbf{E} - e\dot{\mathbf{x}} \times \mathbf{B}. \quad (21)$$

We observe that there in addition to the usual group velocity of band m , $\mathbf{v}_m^g(\mathbf{k}) = \nabla_{\mathbf{k}} E_m(\mathbf{k})$, we have an extra term in Eq. (20), $\dot{\mathbf{k}} \times \boldsymbol{\Omega}_m(\mathbf{k})$, known as the anomalous velocity. This term is a topological contribution to the velocity, and is the only term that is due to quantum mechanical effects in the equations above. One way to rationalize the appearance of the Berry-curvature is to consider the action of the position operator on a wave-packet described in the quasi-momentum space, with $\{|\mathbf{k}, m\rangle\}$ as the complete set of quasi-momentum states with band labels m as follows

$$\begin{aligned} \psi_m(\mathbf{k}) \equiv \langle \mathbf{k}, m | \psi \rangle &= \frac{1}{V} \int d^d \mathbf{x} \langle \mathbf{k}, m | \mathbf{x} \rangle \langle \mathbf{x} | \psi \rangle = \frac{1}{V} \int d^d \mathbf{x} e^{-i\mathbf{k} \cdot \mathbf{x}} \langle b_{n,\mathbf{k}} | \mathbf{x} \rangle \\ &= \frac{1}{V} \int d^d \mathbf{x} e^{-i\mathbf{k} \cdot \mathbf{x}} f_{n,\mathbf{k}}(x) \tilde{\psi}_m(\mathbf{x}). \end{aligned}$$

In the last step we defined the functions $f_{m,\mathbf{k}}(x) \tilde{\psi}_m(\mathbf{x}) = \langle b_{m,\mathbf{k}} | \mathbf{x} \rangle$. Now, consid-

ering $\hat{\mathbf{x}}\psi_m(\mathbf{k})$, we have

$$\begin{aligned}\hat{\mathbf{x}}\psi_m(\mathbf{k}) &= \frac{1}{V} \int d^d \mathbf{x} e^{-i\mathbf{k}\cdot\mathbf{x}} f_{m,\mathbf{k}}(\mathbf{x}) \mathbf{x} \psi_m(\mathbf{x}) = \frac{1}{V} \int d^d \mathbf{x} i \nabla_{\mathbf{k}} (e^{-i\mathbf{k}\cdot\mathbf{x}}) f_{m,\mathbf{k}}(\mathbf{x}) \psi_m(\mathbf{x}) \\ &= i \nabla_{\mathbf{k}} \psi_m(\mathbf{k}) - \frac{1}{V} \int d^d \mathbf{x} e^{-i\mathbf{k}\cdot\mathbf{x}} (i \nabla_{\mathbf{k}} f_{m,\mathbf{k}}(\mathbf{x})) \psi_m(\mathbf{x}) \\ &= i \nabla_{\mathbf{k}} \psi_m(\mathbf{k}) - \frac{1}{V} \int d^d \mathbf{x} e^{-i\mathbf{k}\cdot\mathbf{x}} (i \nabla_{\mathbf{k}} f_{m,\mathbf{k}}(\mathbf{x})) \int \frac{d^d \mathbf{k}'}{(2\pi)^d} f_{m,\mathbf{k}'}^*(\mathbf{x}) e^{i\mathbf{k}'\cdot\mathbf{x}} \psi_m(\mathbf{k}')\end{aligned}\quad (22)$$

The second term in the last line of the equation above simplifies to the following

$$\begin{aligned}\int \frac{d^d \mathbf{k}'}{(2\pi)^d} \psi_m(\mathbf{k}') \int \frac{d^d \mathbf{x}}{V} e^{-i(\mathbf{k}-\mathbf{k}')\cdot\mathbf{x}} (i \nabla_{\mathbf{k}} f_{m,\mathbf{k}}(\mathbf{x})) f_{m,\mathbf{k}'}^*(\mathbf{x}) \\ = i \int \frac{d^d \mathbf{k}'}{(2\pi)^d} \psi_m(\mathbf{k}') \int \frac{d^d \mathbf{x}}{V} e^{-i(\mathbf{k}-\mathbf{k}')\cdot\mathbf{x}} \langle \nabla_{\mathbf{k}} b_{m,\mathbf{k}} | \mathbf{x} \rangle \langle \mathbf{x} | b_{m,\mathbf{k}'} \rangle \\ = i \int \frac{d^d \mathbf{k}'}{(2\pi)^d} \psi_m(\mathbf{k}') \langle \nabla_{\mathbf{k}} b_{m,\mathbf{k}} | b_{m,\mathbf{k}'} \rangle \delta(\mathbf{k} - \mathbf{k}') = i \psi_m(\mathbf{k}) \langle \nabla_{\mathbf{k}} b_{m,\mathbf{k}} | b_{m,\mathbf{k}} \rangle \\ = -\psi_m(\mathbf{k}) \mathcal{A}_m(\mathbf{k}).\end{aligned}\quad (23)$$

Therefore, we see that $\hat{\mathbf{x}}\psi_m(\mathbf{k}) = (i \nabla_{\mathbf{k}} + \mathcal{A}_m(\mathbf{k})) \psi_m(\mathbf{k})$. This is where the Berry connections enter into the equations of motion.

C 1. Hall conductivity from linear response

In order to see the observable effects of Berry connections in material conductivity, it is common to use the Boltzmann equation with relaxation time approximation to write a continuity equation for the electronic distribution function $g_m(\mathbf{x}, \mathbf{k})$ for band label m as follows [26]

$$\left(\partial_t + \dot{\mathbf{x}} \cdot \nabla_{\mathbf{x}} + \dot{\mathbf{k}} \cdot \nabla_{\mathbf{k}} \right) g_m(\mathbf{x}, \mathbf{k}, t) \approx -\frac{1}{\tau_{m,\mathbf{k}}} \left(g_m(\mathbf{x}, \mathbf{k}, t) - g_m^{(eq)}(\mathbf{x}, \mathbf{k}) \right) \quad (24)$$

where $g_m^{(eq)}(\mathbf{x}, \mathbf{k})$ is the equilibrium electronic distribution function and $\tau_{m,\mathbf{k}}$ is the average collision time between electrons of band m and momentum \mathbf{k} .

Using the equations of motion in Eqs. (20) and (21), one can find the response of the distribution functions $g_m(\mathbf{x}, \mathbf{k}, t)$ to external electric field E , in the absence of magnetic fields, by writing

$$g_m(\mathbf{x}, \mathbf{k}, t) = g_m^{(eq)}(\mathbf{x}, \mathbf{k}, t) + \delta g_m(\mathbf{x}, \mathbf{k}, t) + \dots \quad (25)$$

where $\delta g_m(\mathbf{x}, \mathbf{k}, t)$ is $O(E)$: a perturbative response due to the external electric field.

By making simplifying assumptions about $g_m(\mathbf{x}, \mathbf{k}, t)$, namely that it is a uniform distribution function in real space and time, i.e. $\nabla_{\mathbf{x}} g_m(\mathbf{x}, \mathbf{k}, t) = \partial_t g_m(\mathbf{x}, \mathbf{k}, t) = 0$. If we further assume that the equilibrium distribution is nothing but a Fermi-distribution $n_F(E_m(\mathbf{k}))$, we find that Eqs. (24),(25), and (21) imply that

$$e\mathbf{E} \cdot \nabla_{\mathbf{k}} g^{(eq)}(\mathbf{k}) = e\mathbf{E} \cdot \nabla_{\mathbf{k}} n_F(E_m(\mathbf{k})) = \frac{1}{\tau_{m,\mathbf{k}}} \delta g_m(\mathbf{k}). \quad (26)$$

This implies that the first order response of the electronic distribution function is $\delta g_m(\mathbf{k}) = e\tau_{m,\mathbf{k}} \nabla_{\mathbf{k}} n_F(E(\mathbf{k})) \cdot \mathbf{E} = e\tau_{m,\mathbf{k}} n'_F(E) \mathbf{v}_m^g(\mathbf{k}) \cdot \mathbf{E}$.

Now, in order to find the conductivity tensor $\sigma_{\mu\nu}$, we must find the electronic current due to the external electric field. Electronic current $j(\mathbf{x}, t)$ is nothing but the expectation value of the electronic velocity, i.e.

$$\mathbf{j}(\mathbf{x}, t) = -2e \sum_m \int \frac{d^d \mathbf{k}}{(2\pi)^d} \mathbf{v}_m(\mathbf{x}, \mathbf{k}) g_m(\mathbf{x}, \mathbf{k}, t). \quad (27)$$

The factor of 2 in the equation above, comes from contribution of spin. Using the results of Eq. (26) in Eq. (27), with the the equation for band velocity from Eq. (20),

we obtain

$$\begin{aligned}
& \mathbf{j}(\mathbf{x}, t) \\
&= -2e \sum_m \int \frac{d^d \mathbf{k}}{(2\pi)^d} (\mathbf{v}_m^g(\mathbf{k}) + e\mathbf{E} \times \boldsymbol{\Omega}_m(\mathbf{k})) (n_F(E_m(\mathbf{k})) + e\tau_{m,\mathbf{k}} n'_F(\mathbf{k}) \mathbf{v}_m^g(\mathbf{k}) \cdot \mathbf{E}) \\
& \qquad \qquad \qquad = \mathbf{j}_0(x) \\
&+ 2e^2 \sum_m \int \frac{d^d \mathbf{k}}{(2\pi)^d} (-\mathbf{v}_m^g(\mathbf{k}) (\mathbf{v}_m^g(\mathbf{k}) \cdot \mathbf{E}) \tau_{m,\mathbf{k}} n'_F(\mathbf{k}) + n_F(E_m(\mathbf{k})) \boldsymbol{\Omega}_m(\mathbf{k}) \times \mathbf{E}) + O(E^2).
\end{aligned} \tag{28}$$

We have defined $\mathbf{j}_0(x)$ to be the equilibrium zero-field current. From the expression above, we see that there are two types of first order contribution to the current due to applied electric field. The first simply gives a contribution to the current if the applied field \mathbf{E} is in the direction of the group velocity. However, we note that the second term in the integrand above implies that there is current generated in perpendicular direction to the applied field \mathbf{E} . This is the contribution to Hall current. Thus, in order to predict the Hall conductivity, we must only account for the contributions from the second integral.

Note that the conductivity tensor is defined as $j_\mu = \sigma_{\mu\nu} E_\nu$. The contribution from the second term in the last equality of Eq. (28) can be written as the Hall current

$$j_\mu^{Hall} = 2e^2 \sum_m \int \frac{d^d \mathbf{k}}{(2\pi)^d} n_F(E_m(\mathbf{k})) \epsilon_{\mu\nu\lambda} [\boldsymbol{\Omega}_m(\mathbf{k})]_\nu [\mathbf{E}]_\lambda. \tag{29}$$

We see that the Hall conductivity σ^H can be written as

$$[\sigma_H]_{\mu\lambda} = 2e^2 \sum_m \int \frac{d^d \mathbf{k}}{(2\pi)^d} n_F(E_m(\mathbf{k})) \epsilon_{\mu\nu\lambda} [\boldsymbol{\Omega}_m(\mathbf{k})]_\nu. \tag{30}$$

In order to predict the Hall conductivity for a planar 2d (two real-space dimensions)

system (on the x - y plane), we can assume that \mathbf{E} is along say x -direction and note that from the definition of Berry's curvature in Eq. (17), $\mathbf{\Omega}_m(\mathbf{k}) = \Omega_m(\mathbf{k})\hat{z}$ is purely in z -direction. Noting that the Hall conductivity tensor is asymmetric, i.e. $\sigma_{\mu\lambda}^H = -\sigma_{\lambda\mu}^H$, we write the Hall conductivity

$$\sigma_H = \frac{\sigma_{xy} - \sigma_{yx}}{2} = -e^2 \sum_m \int \frac{d^2\mathbf{k}}{(2\pi)^2} n_F(E_m(\mathbf{k})) \Omega_m(\mathbf{k}). \quad (31)$$

In the zero temperature limit, since $n_F(E_m(\mathbf{k})) \rightarrow 1 - \Theta(E_m(\mathbf{k}))$, in presence of a band-gap (for insulating material), the sum over all bands turns into only a sum over the occupied bands. We, thus, arrive at the following result

$$\sigma_H(T=0) = \frac{\sigma_{xy} - \sigma_{yx}}{2} = \frac{e^2}{(2\pi)^2} \sum_{m(\text{occ.})} \int d^2\mathbf{k} \Omega_m(k) = \frac{e^2}{2\pi} \sum_{m(\text{occ.})} C_m = \frac{e^2}{2\pi} n. \quad (32)$$

In the last equality, we used the fact that the Chern number is quantized, as implied by Eq. (19). We observe that Eq. (32) implies that the the hall conductivity is quantized, without presence of any magnetic field. In fact, ferromagnetic systems also exhibit this effect, known as the Anomalous Quantum Hall (AQH) effect.

D. Topological Insulators (TI)

Eq. (32) implies that certain insulating systems exhibit Hall conductivity. These insulators are classified by the sum over the Chern numbers of all of the occupied bands. For systems with time-reversal symmetry, the sum of all Chern numbers is zero. This can be seen by noting that the Berry-curvature is antisymmetric under time-reversal. Insulators with a sum of Chern numbers $\sum_m C_m = n = 0$ are called trivial insulators, and ones with $n \neq 0$ are referred to as topological, or more specifically as Chern insulators. The sum of the Chern numbers of the occupied bands, denoted by

the integer n , classifies integer quantum hall (IQH) insulators.

It is important to emphasize that Eq. (32) implies that non-trivial insulators conduct electricity. Since, we are dealing with insulators, no current can be conducted through the bulk of the material. However, one way in which Chern insulators can conduct electricity is through the edges (surfaces) of the material. The reason for this is as follows. Two Chern insulators with different sum of occupied band Chern numbers are topologically distinct. This means that one cannot smoothly deform a system of class n TI into a class $n' \neq n$ TI without introducing gapless states (band-crossings) [27]. Thus, at the boundary of the Chern insulator and the vacuum or a trivial topological state, we must have band-crossings. Due to these band-crossings, there are states at the boundary that are gapless. These are often referred to as gapless edge modes. These ‘modes’ are excitation channels that cannot be destroyed by small perturbations or disorder. Hence, they are also referred to as topologically protected surface states. In Figure 3, we show the edge states on the boundary of an IQH insulator, produced on the boundary by ‘unclosed’ quantized Landau levels. Even though, Quantum Hall effect will be discussed further in the next section, I emphasize the classification of Chern insulators and the existence of edge modes due to their topological nature.

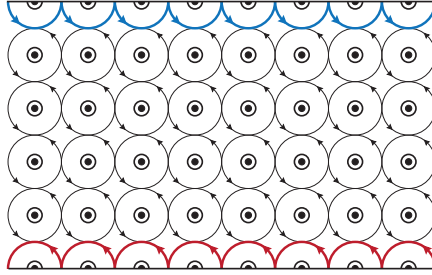


Figure 3: This figure shows a system of IQH Landau levels represented by the loops with arrows. In an IQH system, the edges of the material produce unclosed Landau levels that connect neighboring localized wavefunctions. This allows for conduction of current along the edges of the material. These states, shown in blue and red lines in the figure flow in the opposite directions and are topologically protected.

In the recent years, it has been shown that such topologically protected surface states can be realized in not only 2d Chern insulators but a more general class of 2d and 3d topological insulators, even in presence of time-reversal symmetry [28]. As mentioned above, the sum of the Chern numbers of the occupied bands is a metric that classifies insulators with broken time-reversal symmetry. However, there are various other classification metrics for a more general class of topological insulators with time-reversal symmetry [29].

Topological insulators are classes of material whose topological character manifests under breaking of time-reversal symmetry, as discussed earlier. These classes of material are known as symmetry-protected topological (SPT) phases, due to the fact that they are topologically trivial in presence of certain global symmetries. There are other classes of topological phases of matter that do not lose their topological character in presence of global symmetries. These are called symmetry-enriched topological (SET) phases. Thus in order to distinguish between systems with SPT and SET, it is important to study the influence of global symmetries on topological degrees of free-

dom of a system. The discussion of global symmetries and their effects on topological quantities will be taken up mostly in section VI, where we introduce a formalism called G -crossed modular tensor categories. One of the motivations for considering such mathematical formalism is to precisely explore the relationship between global symmetries of a system and its topological character.

IV. TOPOLOGICAL ORDER

Before the discovery of the quantum Hall effect, a typical approach to the study of phase transitions and novel phases of matter was to find a symmetry breaking mechanism for the degenerate subspace of a model that was described by Landau-Ginzburg theory. This model has been very successful in describing various symmetry-broken phases of matter, namely that of liquid-crystals and superfluids [11, 30]. However, quantum Hall effect, as shall be explained in the next sections, is not the simply a result of a symmetry-breaking mechanism. Even though breaking of time-reversal symmetry, through application of strong magnetic fields, produces the observable effects of Landau levels of Integer Quantum Hall (IQH) effect, there are more intricate relationships between fluxes and electronic occupation. Furthermore, given the fact that IQH and fractional Quantum Hall states are robust against disorder, more subtle explanations that symmetry-breaking was required to explain the electronic order. Inspired by the topological nature of IQH and many other mentioned effects such as Berry's phase, the term topological order was introduced to capture a phase of matter due to topological phenomena, robust under perturbations that did not destroy bulk properties of a system [31]. Characterizing topological order is still a topic of ongoing

research. In subsection B., we introduced Chern numbers, C_m , that characterized some topological information about the band m . In fact, C_m tells us whether there are any singularities in the Berry-connections $\mathcal{A}_m(\mathbf{k})$, upon traversing the Brillouin zone of a crystal across band m . Chern numbers are one example of a topological quantity that characterize nontrivial geometric effects. Another important characteristic describing the topology of a system is ground state degeneracy. In the following sections, we will show how the topology of a system could be characterized by the degeneracy of the ground states of a system.

A. The 2d Toric code

A toy model describing the intimate relationship between topology and degeneracy of the ground states of a system is the 2d toric code [32]. We will show that the boundary conditions⁷ of the following lattice model determines the number of ground state degeneracy. We provide a brief highlight of the model by describing the Toric code Hamiltonian describing an $N \times N$ lattice (with N^2 placquettes and junctions) as follows

$$H_{Toric} = -s \sum_i A_i - p \sum_j B_j. \quad (33)$$

Here, the operators $A_i = \prod_{k \in i^{th} \text{ junction}} Z_k$ and $B_j = \prod_{l \in j^{th} \text{ plac.}} X_l$ are operators defined on a 2d lattice containing spin- $\frac{1}{2}$ in between the junctions of the lattice. Z and X are pauli spin operators. Figure 4 demonstrates the spins on which A_i and B_j act on the 2d lattice. We must note that to build the entire lattice, one can define a unit

⁷The boundary conditions is a way of specifying the topology of the space. Open boundary conditions imply that the two ends of the lattice are not connected, describing the topology of a flat space. Periodic boundary conditions imply that the two ends of the rectangular lattice are connected, exhibiting the topology of a torus.

cell with 2 spins for each placquette. This suggests that there are $2N^2$ total spins in this model. It should be emphasized that first I will show briefly describe the ground state properties of the Hamiltonian in Eq. (33)

In order to solve for the ground state of this model, we shall first note that $[A_i, B_j] = 0$, for all i and j . This is because a placquette and a junction operator only act on even number of common spins. Either they are too far apart, in which case they do not share any common spins, or they are in immediate proximity, in which case they act on 2 common spins. Even though pauli spin generators X and Z on a specific spin anticommute, since even number of spins are shared by the placquette and junction operators, the anticommutations cancel out.

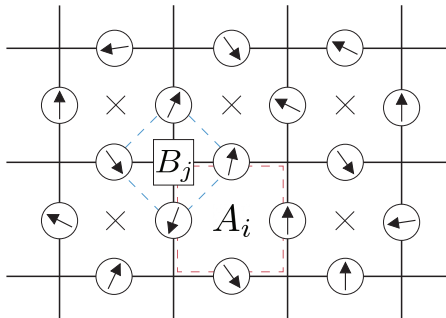


Figure 4: 2d lattice of spin- $\frac{1}{2}$. A_j is an operator acting on the spins surrounding a placquette, and B_j is an operator acting on the neighboring spins of a junction.

Since, the placquette and junction operators commute, we can simply find the ground state of the entire system by finding states that minimize placquettes and junctions terms individually. Let us work in the Z -basis, and denote $|-\rangle$ for the ground state of Z with energy -1 , and $|+\rangle$ for the excited state with energy $+1$. One can note that the following state

$$|AP\rangle = |+\rangle_1 \otimes |+\rangle_2 \otimes \dots \otimes |+\rangle_{2N^2}$$

minimizes the junction terms in H_{Toric} , i.e. $-\sum_j B_j$. We used the notation $|AP\rangle$ to denote the state with ‘All Plus’. Since, the operation of A_j term on the state $|AP\rangle$ has the effect of flipping all the spins on the i^{th} plaquette from $|+\rangle$ to $|-\rangle$, we can note that such a state has the same energy as $|AP\rangle$, since any junction will be surrounded by even number of $|-\rangle$ states. In Figure 5, we have shown the state $A_i |AP\rangle$ which has the same energy as $|AP\rangle$, i.e.

$$\left(\sum_j B_j\right) (A_i |AP\rangle) = (A_i |AP\rangle) |AP\rangle = -N^2 |AP\rangle. \quad (34)$$

In fact, any string of A_i s will not change the energy of the state $|AP\rangle$.

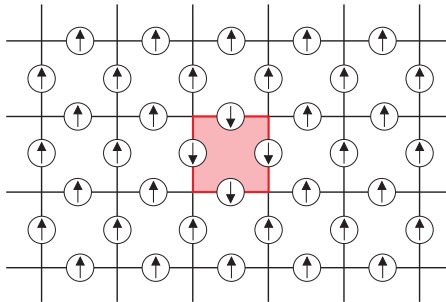


Figure 5: The state $A_i |AM\rangle$ denoted by a red loop. One can see that any of the junction terms B_j surrounding the i^{th} plaquette will have even number of spin downs.

Any state that produces even number of $|-\rangle$ will have the same energy as $|AP\rangle$.

Figure 6 shows some states satisfying this condition, and in fact, one can observe that any state with closed loops of $|-\rangle$ s will fall in this category.

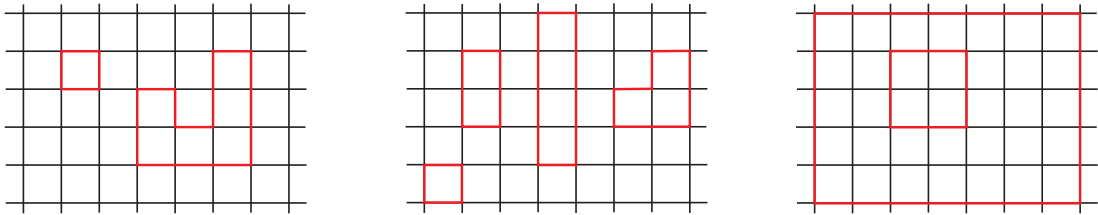


Figure 6: A few degenerate configurations with the same energy as $|AP\rangle$. In the diagram, the red lines represent and the black lines represent $|-\rangle$ and $|+\rangle$ state for a single spin respectively.

From these analysis, one can conclude that the ground state of the 2d Toric code is nothing but an equal-weight superposition of all the possible configurations with the same energy as $|AP\rangle$, i.e.

$$|G\rangle = \frac{1}{\mathcal{D}} \left(\begin{array}{c} \text{Grid 1} \\ \text{Grid 2} \\ \text{Grid 3} \\ \text{Grid 4} \\ \text{Grid 5} \\ \text{Grid 6} \\ \dots \end{array} \right). \quad (35)$$

We observe that the ground state is a highly entangled state. We further emphasize that our analysis, so far, pertained to the toric code with open boundary conditions. We shall extend the analysis to periodic boundary condition, by noting that one can count the expected number of degeneracy in the ground state, n , by considering the difference between the dimension of the Hilbert space and the number of DOF, i.e.

$$n = 2^{2(N^2 - \text{DOF})} = 4^{N^2 - \text{DOF}}. \quad (36)$$

This is because each spin has 2 configurations, $|-\rangle$ and $|+\rangle$, and for every unit cell there are 2 spins. So, the dimension of the Hilbert space for a unit cell is 4, and since there are N^2 unit cells, the dimension of the full Hilbert space is 4^{N^2} . However, the number of DOFs, i.e. independent action of string of A_i , should determine how many ways one can construct a ground state. Since, there are N^2 plaquette operators, A_i , for the

toric code with open boundary conditions, one expects that $DOF = N^2$, and so $n = 1$. However, when we require periodic boundary conditions, the situation is slightly different. The reason is that a string of A_i s along the entire horizontal and vertical dimension would act trivially, due to the periodicity of the lattice. Mathematically, this suggest the following constraint

$$\prod_{i=1}^{N^2} A_i = 1. \quad (37)$$

This suggests that the number of DOFs have been reduced by one due to the constraint imposed on the possible outcomes of the strings of A_i due to periodicity of the lattice.

This makes the ground state degeneracy $n = 4^{N^2 - (N^2 - 1)} = 4$.

The connection between the ground state degeneracy and the topology is the following. The 2d lattice with open boundary condition has the same topology as a flat space. Simply put, the ends of the space along either direction never meet. However, periodic boundary conditions suggest that the two ends of each direction loops around. This is exactly the topology of a torus: a 2d space with genus $g = 1$. As discussed above, for every additional genus, we will have to require a constraint equation on the periodic strings of A_i , so the DOF of the system is given by $N^2 - g$. This gives us the degeneracy of the toric code for a lattice on a surface of genus g

$$n = 4^g. \quad (38)$$

It is important to exclaimate the nature of ground state degeneracy of the Toric code Hamiltonian. It is not an artifact of a symmetry: it is simply due to the topology of the 2d lattice of the model. This system provides an example of the type of order that is subject to change due to global geometric properties of the system. This is an

example of topological order that we have previously mentioned.

B. Quantum Hall Effect

B 1. IQH

The theory behind IQH is well understood, and in fact, one can write a Hamiltonian and solve for the eigenstates and show that the Hall conductivity for such a system is integer quantized. The Hamiltonian given for an electron in a magnetic field given by the vector potential \mathbf{A} is as follows

$$H = \dot{\mathbf{x}} \cdot \mathbf{p} - \mathcal{L} = \frac{1}{2m}(\mathbf{p} + e\mathbf{A})^2. \quad (39)$$

We will assume that we have a 2d system, with 2 component of momentum vector p_x and p_y , and introduce a magnetic field along the perpendicular direction, i.e. $\vec{B} = \nabla \times \mathbf{A} = B\hat{z}$. We can pick a gauge, \mathbf{A} , satisfying this condition, namely $\mathbf{A} = xB\hat{y}$. Now, one can write a functional form of SE as follows

$$H\Psi(x, y) = \frac{1}{2m} (p_x^2 + (p_y + eBx)^2) \Psi(x, y), \quad (40)$$

keeping in mind that p_x and p_y are derivative operators on the spatial wavefunction $\Psi(x, y)$. Since, there is translational invariance in the y -direction, we can substitute the plane wave ansatz $\psi_k(x, y) = e^{iky} f_k(x)$ into Eq. (40), and obtain

$$H\psi_k(x, y) = \frac{1}{2m} (p_x^2 + (\hbar k + eBx)^2) \psi_k(x, y) \equiv h(k) \psi_k(x, y). \quad (41)$$

Restoring our \hbar , we note that $h(k) = \frac{1}{2m} p_x^2 + \frac{m\omega^2}{2} (x + kl_B^2)^2$, with $\omega = eB/m$ and $l_B = \sqrt{\hbar/(eB)}$, a length scale known as the magnetic length. We can note that the

Hamiltonian, with the given wavefunction ansatz, is that of a quantum harmonic oscillator, shifted along x -axis by an amount $-kl_B^2$. Similar to Harmonic oscillator, the energy eigenvalues are

$$E_n = \hbar\omega\left(n + \frac{1}{2}\right), \quad (42)$$

with the given eigenstates:

$$\psi_{n,l}(x, y) \propto e^{iky} H_n(x + kl_B^2) e^{-(x+kl_B^2)^2/2l_B^2}. \quad (43)$$

Note that in writing $\psi_{n,k}$, we have restored our units of \hbar , manifested in the magnetic length units.

The quantum number n defines the energy of the state, and we shall consider the degeneracies in such a state, given some finite length along y -direction (specified by L_y) and x -direction (specified by L_x). To count the degeneracies, we shall integrate over the phase space

$$\mathcal{N} = \int \rho(\mathbf{k}) \frac{dk}{2\pi} \approx \frac{L_y}{2\pi} \int_{-L_x/l_B^2}^0 dk = \frac{L_x L_y}{2\pi l_B^2} = \frac{eBA}{h} = \frac{\Phi}{\Phi_0}. \quad (44)$$

Due to the localization of the wavefunction around $x = -kl_B^2$, we can estimate the integral over the phase space for k given by $x = 0$ and $x = L_x$, from which we determine the bounds using $k = -x/l_B^2$. In the last equality, we have denoted the flux quantum by $\Phi_0 \equiv h/e$. The discussion of degeneracies highlights the fact that for a single electron, there is a single magnetic flux of Φ , which gives rise to the IQH states. This is summarized by defining the following quantity, known as the filling fraction

$$\nu \equiv \frac{N}{\mathcal{N}} = \frac{N}{\Phi/\Phi_0}, \quad (45)$$

and observing that $\nu = 1$ for IQH.

To highlight the similarity between the Landau levels and the wavefunctions describing FQH states, it is more convenient to work in the symmetric gauge, $\mathbf{A} = -\frac{yB}{2}\hat{x} + \frac{xB}{2}\hat{y}$. The Hamiltonian becomes

$$H(x, y; p_x, p_y) = \frac{1}{2m} \left(\left(p_x - \frac{eyB}{2} \right)^2 + \left(p_y + \frac{exB}{2} \right)^2 \right). \quad (46)$$

By introducing the complex variable $s = x + iy$ and its complex conjugate $\bar{s} = x - iy$, we can write Eq. (46) as follows

$$H(s, \bar{s}; \partial_s, \partial_{\bar{s}}) = \frac{1}{2m} \left[- \left(\partial_s - \frac{eB\bar{s}}{4} \right) \left(\partial_{\bar{s}} + \frac{eBs}{4} \right) + \frac{eB}{2} \right]. \quad (47)$$

The eigenstates of the equation above are given by Laguerre polynomials $L_n^l(s, \bar{s})$ as follows

$$\psi_{n,l} \propto s^l L_n^l(s, \bar{s}) e^{-\frac{|s|^2}{4l^2 B}}. \quad (48)$$

We note that we have restored units of \hbar in the equation above. These states give us an idea of lowest Landau levels, which is useful for the discussion of FQH. We note that, the lowest Landau level (LLL) ($n = 0$), is

$$\psi_{LLL}^l(s, \bar{s}) \propto s^l e^{-\frac{|s|^2}{4l^2 B}}. \quad (49)$$

Recall that we briefly introduced IQH states in section III.-B., through discussion of the Hall conductivity. The Landau levels described in Eq. (43) share the same properties on Hall conductivity.

B 2. FQH

Soon after the discovery of the IQH in the early 1980s, various experiments observed a fractional Hall conductivity [33, 34]. Experimentalists observed plateaux not only

near Hall conductivities with integer proportion to the universal constant e^2/h , but fractional proportions, $\frac{p}{q}$, mostly with an odd denominator. Figure 7 shows Hall resistance $R_H \propto 1/\sigma_H$, in units of h/e^2 .

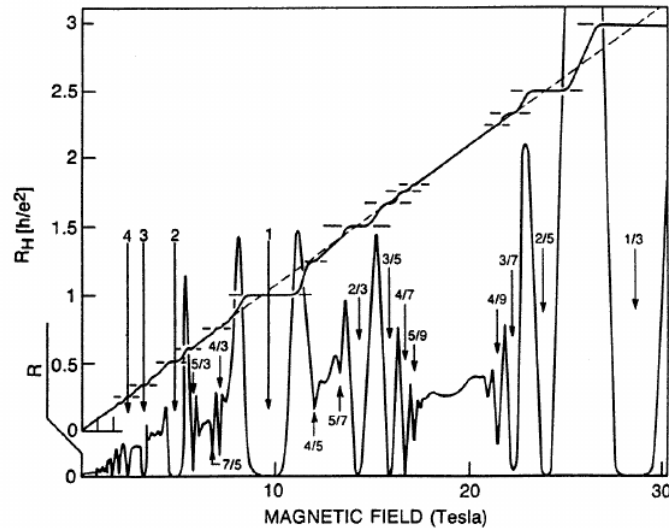


Figure 7: Observation of FQH. Plateaux observed at fractional conductivities. Observe that almost all of the fractions have an odd denominator. This figure is used taken from [34]

Many successful attempts have been made in describing most classes of FQH states, especially states with odd denominators. Since FQH states host fractional electronic charges, the fundamental attempts were to guess an antisymmetric wavefunction that allowed for fractional occupation of electrons and quasiparticle excitations. Laughlin proposed the following wavefunction ansatz for the ground states with fractional electronic occupations of $1/m$, with odd m

$$\psi_m = \prod_{i>j} (s_i - s_j)^m \prod_k e^{-|s_k|^2/4l_B^2}. \quad (50)$$

Note that since Quantum Hall effect is observable in high magnetic fields, the system is spin-polarized. Thus, the spinor part of the electronic wavefunction is symmetric by the nature of the setup. Therefore the spatial ansatz wavefunctions must be

antisymmetric in exchange of electronic exchange. Thus, for odd m , we see that Eq. (50) is antisymmetric upon exchange any two $s_i s$. We must also note that the Laughlin wavefunction in Eq. (50) is very similar to the single electronic LLL given by Eq. (49). We can estimate the fractional occupation of electrons per flux quantum by a similar analysis to Eq. (44). In Eq. (44), we had a state with zero angular momentum, since our wavefunction was purely a gaussian. However, any additional power of spatial component s in the wavefunction adds to the angular momentum of the state. A single electronic wavefunction with canonical angular momentum m will enclose an area of $2\pi l_B^2(m+1)$ [35]. Since, the highest power of a single electronic coordinate z_i in the Laughlin wavefunction in Eq. (50) is $m(N-1)$, so the occupation of electron per flux is

$$\nu = \frac{N}{\Phi/\Phi_0} = \frac{N}{m(N-1)+1} \rightarrow \frac{1}{m}, \quad (51)$$

where the last arrow indicates the thermodynamic limit. Thus, we see that, per flux, there is a fractional electronic occupation, explaining the plateaux in the Hall conductivity with $1/m$ fractional proportion.

It is important to emphasize, again, that the wavefunction proposed in Eq. (50) is for ground state of $1/m$ FQH states. In order to consider excited states, we need to create quasi-particles, or quasi-holes. One does so by adding moments of ∂_s or s into the Laughlin wavefunction ψ_m , with a given coordinate for the position of the localized quasi-particle/hole η . As an example, consider the following wavefunction specifying the $1/m$ wavefunction with excitations, given by their coordinates $\{\eta_\mu\}$ [36]

$$\Psi_m^{hole} = \psi_m \times \prod_{i=1}^N \prod_{\mu=1}^n (s_i - \eta_\mu) \prod_{\mu < \nu} (\eta_\mu - \eta_\nu)^{1/m} e^{-\frac{1}{4m} \sum_{\mu} |\eta_\mu|^2}. \quad (52)$$

This trial wavefunction not only predicts the fractional occupation of electrons correctly, but it captures the fractional charge excitations that are observed in FQH systems. To see this, one can compute the Berry connection and observe that

$$\mathcal{A}_{\eta_\mu} = -i \langle \Psi_m^{hole} | \partial_{\eta_\mu} | \Psi_m^{hole} \rangle = -i \frac{\bar{\eta}_\mu}{4m} \quad (53)$$

$$\mathcal{A}_{\bar{\eta}_\mu} = i \frac{\eta_\mu}{4m}. \quad (54)$$

Upon integrating this around a loop, one finds out that the Berry's phase is nothing but an Aharonov-Bohm contribution that is due to the flux enclosed by the area of the path of taking a quasi-hole around another [36]. However, exchanging two quasi-holes, namely η_μ with η_ν in the trial wavefunction in Eq. (52) will introduce a complex phase

$$(-1)^{1/m} = e^{i\pi/m}. \quad (55)$$

This phase is -1 if $m = 1$, which is nothing but a fermionic exchange contribution. However, when $m > 1$, we get a phase that is called an anyonic phase. Anyons are a class of 2d particles that have exchange statistics different than bosonic and fermionic systems[37]. In fact, one of the early motivations to study anyonic phases of matter came from understanding FQH states. So far, we have introduced the emergence of anyonic quasiparticle states by considering Laughlin trial wavefunctions for $\nu = 1/m$ FQH states. There are other classes of FQH states, with odd denominators. Various approaches to classifying such states have been presented over the years. One approach by Jain, known as the composite fermion, in which the physical intuition of the treatment for FQH states comes from binding electrons to even number of flux quanta [38]. However, there are a few FQH states with even denominators such

as $\nu = 1/2$ and $\nu = 5/2$, which are explained by more mathematically intricate methods [39]. Due to theoretical predictions, FQH states are also an exciting topic of research for non-Abelian statistics [37]. This means that the exchange of two quasi-particles/holes is not simply accounted for by a phase (as given by Eq. (55)) but a matrix operation. To study the statistics in systems with non-Abelian anyons, one needs to consider the entire degenerate subspace and analyze the action of braiding (exchanging) two or more quasi-particles in the entire degenerate subspace. This is one of the motivations to consider Braided Tensor Categories (BTC). BTCs provide mathematical toolkit to predict phases and quasiparticle statistics. We shall further motivate the use of BTCs through the discussion of highly degenerate excited many-body states that exhibit anyonic statistics.

V. FUSION AND BRAIDED TENSOR CATEGORIES (BTC)

A. Motivation

FQH-like systems have highly degenerate ground states that are preserved under breaking of time-reversal and many other common symmetries [34]. These are states that have low-energy excitations (quasi-particles and quasi-holes) that exhibit anyonic statistics, as discussed in the previous section. FQH quasi-particle and quasi-hole states discussed above for $\nu = 1/m$ are Abelian, i.e. the braiding of two quasi-particles/holes around one another introduces a simple phase given by Eq. (55). However, in a more general setting, due to presence of degenerate configurations, the action of braiding two quasi-particles introduces a more complicated action. In other

words, due to existence of degenerate ground states of quasi-particle configurations, systems of quasi-particles could exhibit non-Abelian statistics. One by considering all the possible ways in which a system of quasi-particles can map back onto itself, could capture the entire action of a braiding operation. As briefly mentioned in the last section, there are theoretical predictions for more exotic systems like $\nu = 5/2$ that are expected to have non-Abelian quasi-particles [40, 39]. However, existence of non-Abelian FQH states are still in need of experimental verification.

We begin our introduction to Braided Tensor Categories (BTC) with the motivation to find a suitable way to describe the ways in which the paths of quasi-particles around one another can produce physical effects on the many-body system. A quantum system of N quasi-particles is described by a wavefunction $\Psi_N(\{\eta_i\})$ that is a function of the quasi-particle coordinates. The interpretation of this wavefunction as a probability density, enforces a normalization condition on Ψ_N . The evolution of the quantum system must also preserve the normalization condition in closed systems, so that no particles/information is "leaking out" or "flowing into" our system. Of course one could consider a more general setting in which a system of N quasi-particles are allowed to interact with a thermal bath or a particle reservoir, in which case effective non-unitary dynamics could introduce significant perturbation so that the system wavefunction no longer carries the information about the N quasi-particle state. We will avoid the discussion of such topics which consider effects of open-system dynamics. A justification for the avoidance of open-system dynamics is that quasi-particle states discussed in fractional and Integer Quantum Hall systems are quite robust to perturbations and disorder. After all, this was partly why such states are thought of

as having a topological character.

B. Quasiparticle Fusion and Braiding

The underlying mathematical structure of quasiparticle excitations in two-dimensional systems is provided by Braided Tensor Categories. Since we apply this mathematical formalism on closed quantum systems, the mathematical representations used to describe actions such as braiding must be Unitary. For this reason, the specific representations of BTCs on quantum systems are called Unitary Braided Tensor Categories (UBTC) [16, 15]. This formalism requires one to specify the types of possible quasiparticles, the ways in which these excitations fuse, and the action they produce upon braiding.

B 1. Fusion

The starting point of describing a system of quasiparticles is to define fusion rules, i.e. rules about the resulting quasiparticles upon fusing two quasiparticles

$$a \times b = \sum_c N_{ab}^c c. \tag{56}$$

The indices N_{ab}^c are integers that specify the number of resulting c quasiparticles upon fusion of quasiparticles a and b . The topological charges $a, b, c, \dots \in \mathcal{C}$ are elements of the UBTC \mathcal{C} . It is natural to require that the fusion is finite, i.e. $\sum_c N_{ab}^c$ is finite for any a and b in the system. N_{ab}^c specifies the number of distinguishable ways that quasiparticle c arises as a result of fusing a and b . The states resulting from the fusion can be considered as the orthonormal basis states of a Hilbert space V_{ab}^c , more specifically referred to as the fusion space of a and b . By definition, this implies

that the dimension of the fusion space $\dim(V_{ab}^c) = N_{ab}^c$. Similarly one can consider the ways in which quasiparticle c splits into quasiparticles a and b , specified by the splitting space V_c^{ab} .

For logical and physical consistency UBTC \mathcal{C} must satisfy a few conditions. One such condition is associativity. Fusing a with b or b with a should result in the same quasiparticles, thus

$$\sum_e N_{ab}^e N_{ec}^d = \sum_f N_{af}^d N_{bc}^f. \quad (57)$$

One can adopt a diagrammatic way to represent the quasiparticles states indicating the topological events such as fusion and splitting. The following define our fusion and splitting states

$$(d_c/d_a d_b)^{1/4} \begin{array}{c} c \\ \uparrow \mu \\ a \swarrow \quad \searrow b \end{array} = \langle a, b; c, \mu | \in V_{ab}^c, \quad (58)$$

$$(d_c/d_a d_b)^{1/4} \begin{array}{c} a \swarrow \quad \searrow b \\ \uparrow \mu \\ c \end{array} = |a, b; c, \mu \rangle \in V_c^{ab}, \quad (59)$$

where $\mu = 1, \dots, N_{ab}^c$. (Many anyon models of interest have no fusion multiplicities, i.e. $N_{ab}^c = 0$ or 1 only, in which case the trivial vertex labels μ will usually be left implicit.) The bra/ket basis vectors are orthonormal. d_a , d_b , and d_c are quantum dimensions of the corresponding quasiparticles. We shall explain what is meant by quantum dimension shortly. The normalization factors $(d_c/d_a d_b)^{1/4}$ are included so that diagrams will be in the isotopy invariant convention, as will be explained in the following. Isotopy invariance means that the value of a (labeled) diagram is not changed by continuous deformations, so long as open endpoints are held fixed and lines are not passed through each other or around open endpoints.

Diagrammatically, inner products are formed by stacking vertices so the fus-

ing/splitting lines connect

$$\begin{array}{c} c \\ \uparrow \\ \mu \\ \circlearrowleft \\ \uparrow \\ a \quad b \\ \uparrow \\ \mu' \\ c' \end{array} = \delta_{cc'} \delta_{\mu\mu'} \sqrt{\frac{d_a d_b}{d_c}} \begin{array}{c} c \\ \uparrow \end{array}. \quad (60)$$

Note that the orthonormality of states imply conservation of charge.

Given the inner product defined above, one can think of an identity operation through the following diagrammatic expression

$$\mathbb{1}_{ab} = \begin{array}{c} a \\ \uparrow \\ \uparrow \\ b \end{array} = \sum_{c,\mu} \sqrt{\frac{d_c}{d_a d_b}} \begin{array}{c} a \quad b \\ \swarrow \quad \searrow \\ \mu \\ c \\ \swarrow \quad \searrow \\ \mu \\ a \quad b \end{array}. \quad (61)$$

It is also worth emphasizing that the conjugate of a topological charge a is denoted by \bar{a} and diagrammatically it is represented as follows

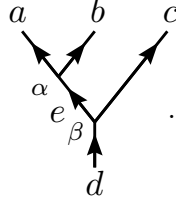
$$\begin{array}{c} \uparrow \\ a \end{array} = \begin{array}{c} \downarrow \\ \bar{a} \end{array}. \quad (62)$$

Before we end the discussion of fusion, it is important to remark that fusion associativity, coupled with consistency of fusion and splitting results in the following equalities for the dimension of the fusion spaces

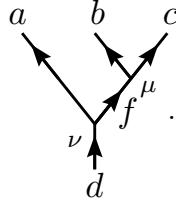
$$N_{ab}^c = N_{ba}^c = N_{ac}^b = N_{bc}^a = N_{ca}^{\bar{b}} = N_{bc}^{\bar{c}}. \quad (63)$$

B 2. Associativity and F-moves

In the previous subsection we briefly mentioned associativity. I will briefly clarify what is meant by this, and introduce what are called F -moves on anyonic charge lines. In the case of fusion of three topological charges, we obtain more complicated diagrams such as



This diagram is obtained by considering the fusion of the resulting charge e , from fusing a with b , with c . In other words, $(a \times b) \times c$. However, we could have instead considered $a \times (b \times c)$, i.e. the fusion of the resulting charge of b and c with a , which corresponds to a diagram of the following form



The two diagrams above are related through F -moves, given by the following equation

$$\begin{array}{c} a \\ \swarrow \\ \alpha \\ \swarrow \\ e \\ \swarrow \\ \beta \\ \swarrow \\ d \end{array} \begin{array}{c} b \\ \swarrow \\ \alpha \\ \searrow \\ e \\ \searrow \\ \beta \\ \searrow \\ d \end{array} \begin{array}{c} c \\ \swarrow \\ \alpha \\ \searrow \\ e \\ \searrow \\ \beta \\ \searrow \\ d \end{array} = \sum_{f, \mu, \nu} [F_d^{abc}]_{(e, \alpha, \beta)(f, \mu, \nu)} \begin{array}{c} a \\ \swarrow \\ \nu \\ \swarrow \\ f^\mu \\ \swarrow \\ d \end{array} \begin{array}{c} b \\ \swarrow \\ \nu \\ \searrow \\ f^\mu \\ \searrow \\ d \end{array} \begin{array}{c} c \\ \swarrow \\ \nu \\ \searrow \\ f^\mu \\ \searrow \\ d \end{array} . \quad (64)$$

The F -moves are isomorphisms⁸ relating different fusion spaces given by $(a \times b) \times c$ and $a \times (b \times c)$

$$V_d^{abc} \cong \bigoplus_e V_e^{ab} \otimes V_d^{ec} \cong \bigoplus_f V_f^{bc} \otimes V_d^{af} . \quad (65)$$

B 3. Quantum dimensions

We should first note that our normalization conventions for the orthonormal states (Eq. (59) and (58)) imply that the inner product of the bra and the ket states result

⁸One-to-one mappings between fusion spaces space that preserve the fusion structure.

in the following

$$\delta_{\gamma c} \delta_{\nu \mu} = \langle a, b; \gamma, \nu | a, b; c, \mu \rangle = \delta_{\gamma c} \delta_{\nu \mu} \frac{1}{d_c} \text{tr}_c \left[\begin{array}{c} c \\ \uparrow \end{array} \right] = \delta_{\gamma c} \delta_{\nu \mu} \frac{1}{d_c} \begin{array}{c} \circlearrowleft \\ c \end{array} . \quad (66)$$

This implies that we have implicitly defined the diagrammatic notation

$$\begin{array}{c} \circlearrowleft \\ c \end{array} \equiv d_c. \quad (67)$$

However, this definition is nothing but a diagrammatic convention. The physical significance of the quantum dimension can be interpreted by the following. Let us examine what happens when there are two pair-creation and pair-annihilation events. Then there are two ways in which one can recombine the opposite conjugate charges (a, \bar{a}) and (a, \bar{a}) . One is that each pair is annihilated by their corresponding pairs, the other is that the conjugates of opposite pair annihilate each other. The ratio of the probabilities of these two events is what is defined as the quantum dimension of quasiparticle a . Diagrammatically, it is the following relation

$$\begin{array}{c} \circlearrowleft \\ a \end{array} \begin{array}{c} \circlearrowleft \\ a \end{array} \equiv \begin{array}{c} \begin{array}{c} 0 \\ \vdots \end{array} \\ \begin{array}{c} a \quad \bar{a} \\ \diagdown \quad \diagup \\ a \quad \bar{a} \\ \diagup \quad \diagdown \\ \begin{array}{c} 0 \\ \vdots \end{array} \end{array} \begin{array}{c} \begin{array}{c} 0 \\ \vdots \end{array} \\ \begin{array}{c} a \quad \bar{a} \\ \diagdown \quad \diagup \\ a \quad \bar{a} \\ \diagup \quad \diagdown \\ \begin{array}{c} 0 \\ \vdots \end{array} \end{array} = \frac{1}{d_a} \begin{array}{c} \begin{array}{c} 0 \\ \vdots \end{array} \\ \begin{array}{c} a \quad \bar{a} \quad a \quad \bar{a} \\ \diagdown \quad \diagup \quad \diagdown \quad \diagup \\ a \quad \bar{a} \\ \diagup \quad \diagdown \\ \begin{array}{c} 0 \\ \vdots \end{array} \end{array} . \quad (68)$$

B 4. Braiding

The counterclockwise braiding exchange operator of two anyons is represented diagrammatically by

$$R^{ab} = \begin{array}{c} a \quad b \\ \diagdown \quad \diagup \\ \diagup \quad \diagdown \end{array} = \sum_{c, \mu, \nu} \sqrt{\frac{d_c}{d_a d_b}} [R_c^{ab}]_{\mu\nu} \begin{array}{c} a \quad b \\ \diagdown \quad \diagup \\ c \\ \diagup \quad \diagdown \\ \mu \quad \nu \\ b \quad a \end{array} , \quad (69)$$

$[R_c^{ab}]_{\nu\mu}^*$ (which are simply phases when $N_{ab}^c = 1$).

An important quantity derived from braiding is the topological twist (or topological spin) of charge a

$$\theta_a = \theta_{\bar{a}} = \sum_{c,\mu} \frac{d_c}{d_a} [R_c^{aa}]_{\mu\mu} = \frac{1}{d_a} \text{Diagram}, \quad (74)$$


which is a root of unity [41]. This quantity expressed the probability amplitude of creating to pairs of topological charges (a, \bar{a}) , braiding the conjugate charge \bar{a} of the first pair with the charge a of the second and annihilating the pair. Eq. (74) can be used to show that the R -symbols satisfy the “ribbon property”

$$\sum_{\lambda} [R_c^{ab}]_{\mu\lambda} [R_c^{ba}]_{\lambda\nu} = \frac{\theta_c}{\theta_a \theta_b} \delta_{\mu\nu}. \quad (75)$$

Another important quantity is the topological S -matrix

$$S_{ab} = \mathcal{D}^{-1} \sum_c N_{\bar{a}b}^c \frac{\theta_c}{\theta_a \theta_b} d_c = \frac{1}{\mathcal{D}} \text{Diagram} . \quad (76)$$


We emphasize the importance of the quantities described above in describing the anyonic nature of the system, as these quantities specify the way in which various topological charges braid around one another. The S -matrix, for instance, specifies the amplitude of a quasiparticle process in which two pair-annihilation and pair-creation events are intermediated by a braiding of the opposite pairs twice. More precisely, one can think of the S_{ab} as representing the amplitude of creating conjugate pair (a, \bar{a}) and (b, \bar{b}) , braid \bar{a} and b twice and annihilate the pairs.

VI. SYMMETRIES AND TOPOLOGICAL DEFECTS

We start with a brief review of the algebraic theory describing the interplay of global symmetries of a system with topological degrees of freedom (DOF), e.g. braiding and fusion.

Let us consider a system with a global symmetry group G . In short, this means that any group element of G commutes with the total Hamiltonian H of the system. Here, we do not specify any Hamiltonians, but we highlight the definition of what is meant by a global symmetry group. The local violations of this global symmetry group are thought of as defects. In real materials, defects could simply be any impurities which break the time-reversal symmetry locally. When the physical system has a symmetry G , one can consider the possibility of point-like defects associated with group elements $\mathbf{g} \in G$, which may be thought of as fluxes. In many ways, a defect behaves like a quasiparticle. However, an important distinction is that when a quasiparticle is transported around a \mathbf{g} -defect, it is acted upon by the corresponding symmetry action on the topological DOF, denoted by $\rho_{\mathbf{g}}$, possibly permuting the quasiparticle's topological charge value. These defects are externally imposed on the system by modifying the original Hamiltonian of the system, and can be thought of as confined excitations [17].

A. Topological Defects

As explained above, considering the action of extrinsic defects, thought of as symmetry fluxes, can alter the topological phases of a system. The algebraic theory describing the action of fluxes on topological phases is built by separating the original unitary

braided tensor category (UBTC) \mathcal{C} into regions with topological fluxes, represented by the group elements of G . The extended algebraic theory, C_G , now takes into account various sectors of the space which contain the symmetry flux $\mathbf{g} \in G$, and are said to represent a G -graded fusion theory

$$\mathcal{C}_G = \bigoplus_{\mathbf{g} \in G} \mathcal{C}_{\mathbf{g}}. \quad (77)$$

The fusion and other topological relations of quasiparticles in different defect sectors of C_G respect the group multiplication of G . In particular, a quasiparticle in \mathbf{g} sector and another in \mathbf{h} , fuse into a quasiparticles in \mathbf{gh} sector. It is important to emphasize that in the absence of any defects, the topological phases correspond to a $\mathbf{0}$ -defect sector, $\mathcal{C}_0 = \mathcal{C}$. The fusion algebra of the action of defect lines on the fusion channels and braiding of topological charges is thus called G -crossed extension of the UBTC \mathcal{C} , denoted by $\mathcal{C}^{\times G}$.

B. G -crossed BTC

We start the brief review of the G -crossed fusion theory by emphasizing the utility of topological data on defining the S -matrix and other topological properties of the system.

B 1. G -Graded Fusion

Fusing topological charges of a \mathbf{g} -defect with that of an \mathbf{h} -defect, resulting in charge(s) of a \mathbf{gh} -defect can be described by the following

$$a_{\mathbf{g}} \times b_{\mathbf{h}} = \sum_{c \in \mathcal{C}_{\mathbf{gh}}} N_{ab}^c c_{\mathbf{gh}} \quad (78)$$

Each topological charge $a_{\mathbf{g}}$ is accompanied by its unique conjugate $\bar{a}_{\mathbf{g}} \in \mathcal{C}_{\mathbf{g}^{-1}}$.

Since the conjugate charge is unique, we can see that $N_{a_{\mathbf{g}}b_{\mathbf{h}}}^0 = \delta_{\bar{a}_{\mathbf{g}}b_{\mathbf{h}}}$.

The quantum dimensions for each topological charge $d_{a_{\mathbf{g}}}$ obeys the relation

$$d_{a_{\mathbf{g}}} d_{b_{\mathbf{h}}} = \sum_c N_{ab}^c d_{c_{\mathbf{gh}}} \quad (79)$$

We also define the total quantum dimension of $\mathcal{C}_{\mathbf{g}}$ to be

$$\mathcal{D}_{\mathbf{g}} = \sqrt{\sum_{a \in \mathcal{C}_{\mathbf{g}}} d_{a_{\mathbf{g}}}^2} \quad (80)$$

We also see that, given this definition, the following relation holds

$$\mathcal{D}_0^2 = \sum_{a \in \mathcal{C}_0} d_{a_0}^2 = \sum_{\substack{a \in \mathcal{C}_0 \\ c \in \mathcal{C}_{\mathbf{g}}}} d_{a_0} d_{b_{\mathbf{g}}}^{-1} N_{ab}^c d_{c_{\mathbf{g}}} = \sum_{\substack{a \in \mathcal{C}_0 \\ c \in \mathcal{C}_{\mathbf{g}}}} d_{c_{\mathbf{g}}} N_{cb}^a d_{a_0} d_{b_{\mathbf{g}}}^{-1} = \sum_{c \in \mathcal{C}_{\mathbf{g}}} d_{c_{\mathbf{g}}}^2 = \mathcal{D}_{\mathbf{g}}^2 \quad (81)$$

In the second line of the equation above, we have used equation (79) and the fact that $N_{ab}^c = N_{cb}^a$. The above relation on the total quantum dimensions hold for any $\mathbf{g} \in G$ with nonempty $\mathcal{C}_{\mathbf{g}} \neq \emptyset$.

B 2. *G*-crossed Topological Eigenstates

In order to proceed with characterizing the topological properties and phases of a system, we need to begin with defining *G*-crossed topological eigenstates (bras) and their duals (kets) that label the fusion states

$$\left(\frac{d_c}{d_a d_b} \right)^{1/4} \begin{array}{c} c_{\mathbf{gh}} \\ \nearrow \mu \\ a_{\mathbf{g}} \quad b_{\mathbf{h}} \end{array} = \langle a_{\mathbf{g}}, b_{\mathbf{h}}; c_{\mathbf{gh}}, \mu | \in V_{ab}^c, \quad (82)$$

$$\left(\frac{d_c}{d_a d_b}\right)^{1/4 a_{\mathbf{g}}} \begin{array}{c} \swarrow a_{\mathbf{g}} \\ \mu \\ \searrow b_{\mathbf{h}} \\ \uparrow c_{\mathbf{gh}} \end{array} = |a_{\mathbf{g}}, b_{\mathbf{h}}; c_{\mathbf{gh}}, \mu\rangle \in V_c^{ab}, \quad (83)$$

As a result, we could specify an inner product on the topological states, by first considering the stacking of two fusion vertices on top of each other

$$\sqrt{\frac{d_c}{d_a d_b}} \begin{array}{c} \gamma_{\mathbf{gh}} \uparrow \nu \\ \uparrow a_{\mathbf{g}} \\ \downarrow b_{\mathbf{h}} \\ \uparrow c_{\mathbf{gh}} \mu \end{array} = \delta_{\gamma_c} \delta_{\nu\mu} \begin{array}{c} c_{\mathbf{gh}} \\ \uparrow \end{array} = |a_{\mathbf{g}}, b_{\mathbf{h}}; c_{\mathbf{gh}}, \mu\rangle \langle a_{\mathbf{g}}, b_{\mathbf{h}}; \gamma_{\mathbf{gh}}, \nu| \quad (84)$$

Taking the trace over the labels c of the category $\mathcal{C}_{\mathbf{gh}}$ and dividing by the dimension d_c , results in *orthonormality condition* of the topological states

$$\begin{aligned} \langle a_{\mathbf{g}}, b_{\mathbf{h}}; \gamma_{\mathbf{gh}}, \nu | a_{\mathbf{g}}, b_{\mathbf{h}}; c_{\mathbf{gh}}, \mu \rangle \\ = \delta_{\gamma_c} \delta_{\nu\mu} \frac{1}{d_c} \text{tr}_c \left[\begin{array}{c} c_{\mathbf{gh}} \\ \uparrow \end{array} \right] = \delta_{\gamma_c} \delta_{\nu\mu} \frac{1}{d_c} \text{tr}_{\mathcal{C}_{\mathbf{gh}}} = \delta_{\gamma_c} \delta_{\nu\mu} \quad (85) \end{aligned}$$

With this inner product, the identity operator in the on a pair of anyons with charges $a_{\mathbf{g}}$ and $b_{\mathbf{h}}$ is written (diagrammatically) as the partition of unity

$$\mathbf{1}(\mathbf{g}, \mathbf{h})_{ab} = \begin{array}{c} a_{\mathbf{g}} \\ \uparrow \\ b_{\mathbf{h}} \\ \uparrow \end{array} = \sum_{c, \mu} \sqrt{\frac{d_c}{d_a d_b}} \begin{array}{c} \swarrow a_{\mathbf{g}} \\ \mu \\ \searrow b_{\mathbf{h}} \\ \uparrow c_{\mathbf{gh}} \end{array} \quad (86)$$

It is worth noting that we may see this identity operator acting on the sector (\mathbf{g}, \mathbf{h}) of *G*-crossed fusion category and is thus a mapping from the sector (\mathbf{g}, \mathbf{h}) to itself.

B 3. *G*-Crossed Braiding

Braiding of defects is a group action on the system that is compatible with *G*-Graded fusion and is associated with the action of exchanging the positions of two defects. It must be noted that the usual notion of braiding in fusion categories is quite different than *G*-Crossed braiding as when the group *G* is non-Abelian, *G*-graded fusion

category is not commutative. This prevents any meaningful way of defining braiding in the usual sense of exchange of two topological charges. Thus, there must be a group action when the positions of defects, carrying non-trivial group elements, are exchanged.

We begin by defining the *G*-crossed braiding by the following

$$R^{a_g b_h} = \begin{array}{c} a_g \quad b_h \\ \diagdown \quad \diagup \\ b_h \quad \bar{h} a_g \end{array} = \sum_{c, \mu, \nu} \sqrt{\frac{d_c}{d_a d_b}} [R_{c_{gh}}^{a_g b_h}]_{\mu\nu} \begin{array}{c} a_g \quad b_h \\ \diagdown \quad \diagup \\ c_{gh} \quad \nu \\ \diagup \quad \diagdown \\ b_h \quad \mu \quad \bar{h} a_g \end{array} \quad (87)$$

where the *R*-symbols for a *G*-crossed theory are the maps $R_c^{ab} : V_{c_{gh}}^{b_h \bar{h} a_g} \rightarrow V_{c_{gh}}^{a_g b_h}$ that result from exchanging (in a counterclockwise manner) two objects of charges b_h and $\bar{h} a_g$, respectively, which are in the charge c_{gh} fusion channel.

The *G*-crossed *R*-symbols can equivalently be written in terms of the relation

$$\begin{array}{c} a_g \quad b_h \\ \diagdown \quad \diagup \\ c_{gh} \quad \mu \end{array} = \sum_{\nu} [R_{c_{gh}}^{a_g b_h}]_{\mu\nu} \begin{array}{c} a_g \quad b_h \\ \diagdown \quad \diagup \\ c_{gh} \quad \nu \end{array} . \quad (88)$$

Similarly, the clockwise *G*-crossed braiding exchange operator is

$$\left(R^{a_g b_h}\right)^{-1} = \begin{array}{c} b_h \quad \bar{h} a_g \\ \diagdown \quad \diagup \\ a_g \quad b_h \end{array} = \sum_{c, \mu, \nu} \sqrt{\frac{d_c}{d_a d_b}} \left[\left(R_{c_{gh}}^{a_g b_h}\right)^{-1}\right]_{\mu\nu} \begin{array}{c} b_h \quad \bar{h} a_g \\ \diagdown \quad \diagup \\ c_{gh} \quad \nu \\ \diagup \quad \diagdown \\ a_g \quad \mu \quad b_h \end{array} \quad (89)$$

In order for *G*-crossed braiding to be compatible with fusion, we wish to have the ability to slide lines over or under fusion vertices. However, unlike anyonic fusion category, we may not assume that such operations are completely trivial, since one must at least account for the group action on a vertex. The appropriate relations are

given by the unitary transformations

$$\begin{array}{c}
 \begin{array}{c} a_g \quad b_h \\ \diagup \quad \diagdown \\ x_k \quad \mu \\ \bar{k} \quad c_{gh} \end{array} \\
 = \sum_{\nu} [U_{\mathbf{k}}(a, b; c)]_{\mu\nu} \\
 \begin{array}{c} a_g \quad b_h \\ \diagdown \quad \diagup \\ x_k \quad \mu \\ \bar{k} \quad c_{gh} \end{array}
 \end{array} \quad (90)$$

$$\begin{array}{c}
 \begin{array}{c} a_g \quad b_h \quad \bar{h}\bar{g}x_k \\ \diagup \quad \diagdown \quad \diagup \\ x_k \quad \mu \\ \bar{g}x \quad c_{gh} \end{array} \\
 = \eta_x(\mathbf{g}, \mathbf{h}) \\
 \begin{array}{c} a_g \quad b_h \quad \bar{h}\bar{g}x_k \\ \diagdown \quad \diagup \quad \diagdown \\ x_k \quad \mu \\ c_{gh} \end{array}
 \end{array} \quad (91)$$

Here, we have used the notation $[U_{\mathbf{k}}(a, b; c)]_{\mu\nu}$ to signify the global symmetry action upon moving defect line with element \mathbf{k} over a fusion vertex, and the phase $\eta_x(\mathbf{g}, \mathbf{h})$ introduced upon moving the fusion vertex with elements \mathbf{g} and \mathbf{h} on top of the defect branch with topological charge x . The group actions U and the phases η can be thought of as gauge transformations on the topological states.

Sliding a line over a vertex, as in Eq. (90) is a unitary transformation between $V_{\bar{k}c}^{\bar{k}a\bar{k}b}$ and V_c^{ab} , as specified by the unitary operators $U_{\mathbf{k}}(a, b; c)$. This requires the dimensionality of the fusion spaces to be preserved under the corresponding symmetry action, giving

$$N_{\bar{k}a_g \bar{k}b_h}^{\bar{k}c_{gh}} = N_{a_g b_h}^{c_{gh}} \quad (92)$$

for any \mathbf{k} acting on a vertex. It follows that the quantum dimensions are also invariant

$$d_{a_g} = d_{\bar{k}a_g}. \quad (93)$$

Clearly, if the sliding line has vacuum charge $x_{\mathbf{k}} = 0$, the sliding transformations should be trivial, so

$$[U_{\mathbf{0}}(a, b; c)]_{\mu\nu} = \delta_{\mu\nu} \quad (94)$$

$$\eta_0(\mathbf{g}, \mathbf{h}) = 1. \quad (95)$$

We require that the sliding rules are compatible with the property that vacuum lines can be freely added or removed from a diagram, i.e. sliding over/under a vertex $|a, b; c\rangle$ with $a = 0$ or $b = 0$ should be trivial, since it is equivalent to simply sliding over a line. This imposes the conditions

$$U_{\mathbf{k}}(0, 0; 0) = U_{\mathbf{k}}(a, 0; a) = U_{\mathbf{k}}(0, b; b) = 1 \quad (96)$$

$$\eta_x(\mathbf{0}, \mathbf{0}) = \eta_x(\mathbf{g}, \mathbf{0}) = \eta_x(\mathbf{0}, \mathbf{h}) = 1. \quad (97)$$

Combining Eqs. (90) and (91) with trivial braidings, such as

$$\begin{array}{c} a \\ \uparrow \\ \uparrow \\ b \end{array} = \begin{array}{c} a \quad b \\ \diagdown \quad \diagup \\ \uparrow \\ \diagup \quad \diagdown \\ b \quad a \end{array}, \quad (98)$$

we see that sliding lines over or under vertices with the opposite braiding are given by

$$\begin{array}{c} a_g \quad b_h \\ \diagdown \quad \diagup \\ \mu \\ \diagup \quad \diagdown \\ c \quad x_k \\ \uparrow \\ k_{cgh} \end{array} = \sum_{\nu} [U_{\mathbf{k}}(\mathbf{k}a, \mathbf{k}b; \mathbf{k}c)]_{\mu\nu} \begin{array}{c} a_g \quad b_h \\ \uparrow \quad \uparrow \\ k_a \quad k_b \\ \diagdown \quad \diagup \\ \nu \\ \diagup \quad \diagdown \\ k_{cgh} \end{array} \quad (99)$$

$$\begin{array}{c} x_k \quad a_g \quad b_h \\ \diagdown \quad \diagup \\ \mu \\ \diagup \quad \diagdown \\ \bar{h}\bar{g}, x_k \\ \uparrow \\ c_{gh} \end{array} = \eta_x(\mathbf{g}, \mathbf{h}) \begin{array}{c} x_k \quad a_g \quad b_h \\ \uparrow \quad \uparrow \\ \bar{g}x \quad \bar{h}\bar{g}, x_k \\ \diagdown \quad \diagup \\ \mu \\ \diagup \quad \diagdown \\ c_{gh} \end{array}. \quad (100)$$

Compatibility of the sliding moves with the inner product Eq. (84) is obtained by sliding a line over a bubble diagram, as in Eq. (84)). In this way, we obtain the

corresponding relations for sliding over fusion (rather than splitting) vertices

$$\begin{array}{c}
 \begin{array}{c} c_{gh} \\ \uparrow \\ \begin{array}{c} \mu \\ \uparrow \\ a \end{array} \begin{array}{c} b \\ \uparrow \\ \end{array} \\ \diagup \quad \diagdown \\ \begin{array}{c} x_k \\ \uparrow \\ \bar{k}_{a_g} \end{array} \begin{array}{c} \bar{k}_{b_h} \\ \uparrow \\ \end{array} \end{array} \\
 = \sum_{\nu} [U_{\mathbf{k}}(a, b; c)]_{\nu\mu} \begin{array}{c} c_{gh} \\ \uparrow \\ \begin{array}{c} \nu \\ \uparrow \\ x_k \end{array} \begin{array}{c} \bar{k}_c \\ \uparrow \\ \end{array} \\ \diagup \quad \diagdown \\ \begin{array}{c} \bar{k}_{a_g} \\ \uparrow \\ \end{array} \begin{array}{c} \bar{k}_{b_h} \\ \uparrow \\ \end{array} \end{array}
 \end{array} \quad (101)$$

$$\begin{array}{c}
 \begin{array}{c} c_{gh} \\ \uparrow \\ \begin{array}{c} \mu \\ \uparrow \\ x_k \end{array} \begin{array}{c} \bar{k}_c \\ \uparrow \\ \end{array} \\ \diagup \quad \diagdown \\ \begin{array}{c} \bar{k}_{a_g} \\ \uparrow \\ \end{array} \begin{array}{c} \bar{k}_{b_h} \\ \uparrow \\ \end{array} \end{array} \\
 = \sum_{\nu} [U_{\mathbf{k}}(\bar{k}_a, \bar{k}_b; \bar{k}_c)]_{\nu\mu} \begin{array}{c} c_{gh} \\ \uparrow \\ \begin{array}{c} \nu \\ \uparrow \\ a \end{array} \begin{array}{c} b \\ \uparrow \\ \end{array} \\ \diagup \quad \diagdown \\ \begin{array}{c} \bar{k}_{a_g} \\ \uparrow \\ \end{array} \begin{array}{c} \bar{k}_{b_h} \\ \uparrow \\ \end{array} \end{array}
 \end{array} \quad (102)$$

A similar calculation gives the relations for sliding lines under fusion vertices

$$\begin{array}{c}
 \begin{array}{c} c_{gh} \quad \bar{h}\bar{g}x_k \\ \uparrow \quad \uparrow \\ \begin{array}{c} \mu \\ \uparrow \\ x_k \end{array} \begin{array}{c} \bar{g}x_k \\ \uparrow \\ \end{array} \\ \diagup \quad \diagdown \\ \begin{array}{c} a_g \\ \uparrow \\ \end{array} \begin{array}{c} b_h \\ \uparrow \\ \end{array} \end{array} \\
 = \eta_x(\mathbf{g}, \mathbf{h}) \begin{array}{c} c_{gh} \quad \bar{h}\bar{g}x_k \\ \uparrow \quad \uparrow \\ \begin{array}{c} \mu \\ \uparrow \\ x_k \end{array} \\ \diagup \quad \diagdown \\ \begin{array}{c} a_g \\ \uparrow \\ \end{array} \begin{array}{c} b_h \\ \uparrow \\ \end{array} \end{array}
 \end{array} \quad (103)$$

$$\begin{array}{c}
 \begin{array}{c} c_{gh} \\ \uparrow \\ \begin{array}{c} \mu \\ \uparrow \\ x_k \end{array} \begin{array}{c} \bar{h}\bar{g}x_k \\ \uparrow \\ \end{array} \\ \diagup \quad \diagdown \\ \begin{array}{c} a_g \\ \uparrow \\ \end{array} \begin{array}{c} b_h \\ \uparrow \\ \end{array} \end{array} \\
 = \eta_x(\mathbf{g}, \mathbf{h}) \begin{array}{c} c_{gh} \\ \uparrow \\ \begin{array}{c} \mu \\ \uparrow \\ x_k \end{array} \begin{array}{c} \bar{h}\bar{g}x_k \\ \uparrow \\ \end{array} \\ \diagup \quad \diagdown \\ \begin{array}{c} a_g \\ \uparrow \\ \end{array} \begin{array}{c} b_h \\ \uparrow \\ \end{array} \end{array} .
 \end{array} \quad (104)$$

We have the following consistency conditions arising from the compatibility of F -moves in G -crossed theory with sliding lines over and under fusion vertices

$$\begin{aligned}
 & \sum_{\alpha', \beta', \mu', \nu'} [U_{\mathbf{k}}(\bar{k}_a, \bar{k}_b; \bar{k}_e)]_{\alpha\alpha'} [U_{\mathbf{k}}(\bar{k}_e, \bar{k}_c; \bar{k}_d)]_{\beta\beta'} [F_{\bar{k}_d}^{\bar{k}_a \bar{k}_b \bar{k}_c}]^{(\bar{k}_e, \alpha', \beta')(\bar{k}_f, \mu', \nu')} \\
 & \times [U_{\mathbf{k}}(\bar{k}_b, \bar{k}_c; \bar{k}_f)^{-1}]_{\mu'\mu} [U_{\mathbf{k}}(\bar{k}_a, \bar{k}_f; \bar{k}_d)^{-1}]_{\nu'\nu} = [F_d^{abc}]_{(e, \alpha, \beta)(f, \mu, \nu)}. \quad (105)
 \end{aligned}$$

$$\eta_{\bar{g}x}(\mathbf{h}, \mathbf{k}) \eta_x(\mathbf{g}, \mathbf{hk}) = \eta_x(\mathbf{g}, \mathbf{h}) \eta_x(\mathbf{gh}, \mathbf{k}). \quad (106)$$

This is a central statement used throughout the paper, mainly for the proof of the modularity of the projective operators. The consistency condition above is also a statement of the fact that symmetry fractionalization is consistent in the G -crossed theory framework. A detailed discussion of this is done in [17].

We also have the G -crossed Yang-Baxter equation

$$\begin{array}{c}
\begin{array}{c}
\text{\scriptsize } k_{a_g} \quad \text{\scriptsize } k_{b_h} \quad \text{\scriptsize } x_k \\
\text{\scriptsize } x_k \quad \text{\scriptsize } b_h \quad \text{\scriptsize } \bar{h}_{a_g}
\end{array}
\end{array}
= \frac{\eta_{k_a}(\mathbf{k}\mathbf{h}\bar{\mathbf{k}}, \mathbf{k})}{\eta_{k_a}(\mathbf{k}, \mathbf{h})}
\begin{array}{c}
\begin{array}{c}
\text{\scriptsize } k_{a_g} \quad \text{\scriptsize } k_{b_h} \quad \text{\scriptsize } x_k \\
\text{\scriptsize } x_k \quad \text{\scriptsize } b_h \quad \text{\scriptsize } \bar{h}_{a_g}
\end{array}
\end{array}
. \quad (107)$$

Furthermore, the compatibility of G -crossed braiding with sliding lines over and under fusion vertices implies

$$\frac{\eta_{k_a}(\mathbf{k}\mathbf{h}\bar{\mathbf{k}}, \mathbf{k})}{\eta_{k_a}(\mathbf{k}, \mathbf{h})} \sum_{\mu', \nu'} [U_{\mathbf{k}}(\mathbf{k}b, \mathbf{k}\bar{h}a; \mathbf{k}c)]_{\mu\mu'} [R_{\mathbf{k}c}^{\mathbf{k}a\mathbf{k}b}]_{\mu'\nu'} [U_{\mathbf{k}}(\mathbf{k}a, \mathbf{k}b; \mathbf{k}c)^{-1}]_{\nu'\nu} = [R_c^{ab}]_{\mu\nu} \quad (108)$$

This is the G -crossed generalization of the statement that the R -symbols are invariant under the symmetry action.

Finally, we have the G -crossed ribbon identity

$$\sum_{\lambda} [R_{c_{\mathbf{g}\mathbf{h}}}^{b_{\mathbf{h}}\bar{h}_{a_{\mathbf{g}}}}]_{\mu\lambda} [R_{c_{\mathbf{g}\mathbf{h}}}^{a_{\mathbf{g}}b_{\mathbf{h}}}]_{\lambda\nu} = \frac{\theta_c}{\theta_a\theta_b} \frac{[U_{\mathbf{g}\mathbf{h}}(a, b; c)]_{\mu\nu}}{\eta_a(\mathbf{g}, \mathbf{h})\eta_b(\mathbf{h}, \bar{\mathbf{h}}\mathbf{g})}. \quad (109)$$

B 4. G -crossed Invariants and the S -matrix

As seen in Eq. (105) and (108), R and F matrices are invariant under the symmetry actions and so these quantities are the same in both BTC and G -crossed BTCs. We will discuss the invariance of various topological quantities and discuss the implications on the S -matrix.

Eq. (105) with $e = f = 0$ yields the relation

$$\frac{\varkappa_{k_a}}{\varkappa_a} = \frac{[F_{k_a}^{\mathbf{k}a\mathbf{k}\bar{a}\mathbf{k}a}]_{00}}{[F_a^{a\bar{a}a}]_{00}} = \frac{U_{\mathbf{k}}(\mathbf{k}\bar{a}, \mathbf{k}a; 0)}{U_{\mathbf{k}}(\mathbf{k}a, \mathbf{k}\bar{a}; 0)}. \quad (110)$$

The topological twists are defined the same way as before by taking the quantum

trace of a counterclockwise braid of a topological charge with itself

$$\theta_a = \frac{1}{d_a} \text{tr} \left(\text{braid}_a \right) = \sum_{c,\mu} \frac{d_c}{d_a} [R_c^{aa}]_{\mu\mu}. \quad (111)$$

Using Eq. (107) with the definition of the twist, we find the general relation between θ_a and $\theta_{\mathbf{k}_a}$ is

$$\theta_{a_{\mathbf{g}}} = \frac{\eta_{\mathbf{k}_{a_{\mathbf{g}}}}(\mathbf{k}_{\mathbf{g}}\bar{\mathbf{k}}, \mathbf{k})}{\eta_{\mathbf{k}_{a_{\mathbf{g}}}}(\mathbf{k}, \mathbf{g})} \theta_{\mathbf{k}_{a_{\mathbf{g}}}} = \frac{\eta_{a_{\mathbf{g}}}(\bar{\mathbf{k}}, \mathbf{k}_{\mathbf{g}}\bar{\mathbf{k}})}{\eta_{a_{\mathbf{g}}}(\mathbf{g}, \bar{\mathbf{k}})} \theta_{\mathbf{k}_{a_{\mathbf{g}}}}. \quad (112)$$

When $\mathbf{k}_a = a$, it follows that

$$\eta_{a_{\mathbf{g}}}(\mathbf{g}, \mathbf{k}) = \eta_{a_{\mathbf{g}}}(\mathbf{k}, \mathbf{g}). \quad (113)$$

We also note that Eq. (106) gives $\eta_{\mathbf{k}_x}(\mathbf{k}, \bar{\mathbf{k}}) = \eta_x(\bar{\mathbf{k}}, \mathbf{k})$ for any x and \mathbf{k} , so we also have

$$\eta_{a_{\mathbf{g}}}(\mathbf{k}, \bar{\mathbf{k}}) = \eta_{a_{\mathbf{g}}}(\bar{\mathbf{k}}, \mathbf{k}) \quad (114)$$

when $\mathbf{k}_a = a$.

The definition of topological twists can also be written in the form

$$\text{tr} \left(\text{braid}_a \right) = \theta_a \text{tr} \left(\text{strand}_a \right) = \text{tr} \left(\text{twist}_a \right), \quad (115)$$

as is the case with BTCs. It is clear that the inverse topological twists are similarly obtained from clockwise braidings

$$\text{tr} \left(\text{braid}_a^{-1} \right) = \theta_a^{-1} \text{tr} \left(\text{strand}_a \right) = \text{tr} \left(\text{twist}_a^{-1} \right). \quad (116)$$

Unlike a BTC, it is not necessarily the case that $\theta_{a_{\mathbf{g}}}$ and $\theta_{\bar{a}_{\mathbf{g}}}$ are equal in a *G*-crossed

BTC. In particular, we have

$$\theta_{a_{\mathbf{g}}} = U_{\mathbf{g}}(\bar{a}_{\mathbf{g}}, a_{\mathbf{g}}; 0) \eta_{\bar{a}_{\mathbf{g}}}(\bar{\mathbf{g}}, \mathbf{g}) \theta_{\bar{a}_{\mathbf{g}}}. \quad (117)$$

and

$$\theta_{a_{\mathbf{g}}} = U_{\mathbf{g}}(a_{\mathbf{g}}, \bar{a}_{\mathbf{g}}; 0) \varkappa_{a_{\mathbf{g}}} \left(R_0^{\bar{a}_{\mathbf{g}} a_{\mathbf{g}}} \right)^{-1} \quad (118)$$

$$= \eta_{a_{\mathbf{g}}}(\mathbf{g}, \bar{\mathbf{g}})^{-1} \varkappa_{a_{\mathbf{g}}}^{-1} \left(R_0^{a_{\mathbf{g}} \bar{a}_{\mathbf{g}}} \right)^{-1} \quad (119)$$

Consistency of sliding over and under fusion channels also gives us the following relations

$$[U_{\bar{\mathbf{k}}}(\bar{\mathbf{k}} a, \bar{\mathbf{k}} b; \bar{\mathbf{k}} c)]_{\mu\nu} = \frac{\eta_c(\mathbf{k}, \bar{\mathbf{k}})}{\eta_a(\mathbf{k}, \bar{\mathbf{k}}) \eta_b(\mathbf{k}, \bar{\mathbf{k}})} [U_{\mathbf{k}}(a, b; c)^{-1}]_{\mu\nu} \quad (120)$$

$$\eta_a(\mathbf{k}, \mathbf{l}) \eta_{\bar{a}}(\mathbf{k}, \mathbf{l}) = \frac{U_{\mathbf{k}\mathbf{l}}(a, \bar{a}; 0)}{U_{\mathbf{k}}(a, \bar{a}; 0) U_{\mathbf{l}}(\bar{\mathbf{k}} a, \bar{\mathbf{k}} \bar{a}; 0)}. \quad (121)$$

Previously in [17], the topological S-matrix was defined as follows

$$\begin{aligned} S_{a_{\mathbf{g}} b_{\mathbf{h}}} &= \frac{1}{\mathcal{D}_0} a \left(\begin{array}{c} \circlearrowleft \\ \circlearrowright \end{array} \right) b \\ &= \frac{1}{\mathcal{D}_0} \sum_{c, \mu, \nu} d_c [R_c^{b\bar{a}}]_{\mu\nu} [R_c^{\bar{a}b}]_{\nu\mu} \\ &= \frac{1}{\mathcal{D}_0} \sum_{c, \mu} d_c \frac{\theta_c}{\theta_{\bar{a}} \theta_b} \frac{[U_{\bar{\mathbf{g}}\mathbf{h}}(\bar{a}, b; c)]_{\mu\mu}}{\eta_{\bar{a}}(\bar{\mathbf{g}}, \mathbf{h}) \eta_b(\mathbf{h}, \bar{\mathbf{g}})}. \end{aligned} \quad (122)$$

One should note that the quantity above is only well-defined if $\mathbf{gh} = \mathbf{hg}$, otherwise the loops will not be able to close back upon themselves, as the topological charge values would change upon braiding.

Following from the definition of the topological S-matrix above, the following property follows

$$S_{\mathbf{k}_{a_{\mathbf{g}}} \mathbf{k}_{b_{\mathbf{h}}}} = \frac{\eta_{\mathbf{k}_{\bar{a}}}(\mathbf{k}, \mathbf{h}) \eta_{\mathbf{k}_b}(\mathbf{k}, \bar{\mathbf{g}})}{\eta_{\mathbf{k}_{\bar{a}}}(\mathbf{kh}\bar{\mathbf{k}}, \mathbf{k}) \eta_{\mathbf{k}_b}(\mathbf{k}\bar{\mathbf{g}}\bar{\mathbf{k}}, \mathbf{k})} S_{a_{\mathbf{g}} b_{\mathbf{h}}} \quad (123)$$

From these definitions, it also follows that when ${}^{\mathbf{h}}a_{\mathbf{g}} = a_{\mathbf{g}}$ and ${}^{\mathbf{g}}b_{\mathbf{h}} = b_{\mathbf{h}}$ (and hence $\mathbf{gh} = \mathbf{hg}$), so that the corresponding S -matrix element is well-defined, we have the loop-removal relation

$$\begin{array}{c} \uparrow b_{\mathbf{h}} \\ \circlearrowleft \\ \leftarrow a_{\mathbf{g}} \\ \downarrow \end{array} = \frac{S_{ab}}{S_{0b}} \begin{array}{c} \uparrow b_{\mathbf{h}} \\ | \\ \downarrow \end{array}, \quad (124)$$

which can be verified by closing the b line upon itself in this expression. In fact, if either ${}^{\mathbf{h}}a_{\mathbf{g}} \neq a_{\mathbf{g}}$ or ${}^{\mathbf{g}}b_{\mathbf{h}} \neq b_{\mathbf{h}}$, then left hand side of the equation evaluates to zero, so, for these purposes, we can consider $S_{ab} = 0$ when it is not well-defined. Thus, in order for the G -crossed theory to be consistent on a surface of arbitrary genus, we need to generalize the topological S-matrix defined above in Eq. (122) to be compatible with arbitrary defect lines enclosing the puncture on a punctured torus.

VII. MODULARITY OF $\mathcal{C}^{\times G}$ ON TORUS *

When the S -matrix of the G -crossed theory is unitary, the theory is said to be modular, and described by a G -crossed Modular Tensor Category (MTC). Modularity is an important property of the theory, as it allows us to define information preserving operators to map the topological state between various sectors of the G -crossed theory. Let us establish a few important properties when the original anyonic theory with only trivial defects, namely \mathcal{C}_0 , is an MTC. From this, one obtains the following relation

$$\delta_{a_{\mathbf{g}}a'_{\mathbf{g}}} = \sum_{x_0 \in \mathcal{C}_0^{\mathbf{g}}} S_{a_{\mathbf{g}}x_0} S_{a'_{\mathbf{g}}x_0}^* = \sum_{x_0 \in \mathcal{C}_0^{\mathbf{g}}} S_{x_0 a_{\mathbf{g}}} S_{x_0 a'_{\mathbf{g}}}^*. \quad (125)$$

Furthermore, we can write this relation in terms of defect lines enclosed by loops,

by defining the ω_a -loop enclosing a single defect line for a G -crossed theory

$$\begin{array}{c} \uparrow b_g \\ \circlearrowleft \\ \omega_{a_g} \\ | \end{array} = \sum_{x_0 \in \mathcal{C}_0^g} S_{0a_g} S_{x_0 a_g}^* \begin{array}{c} \uparrow b_g \\ \circlearrowleft \\ x_0 \\ | \end{array} = \delta_{a_g b_g} \begin{array}{c} \uparrow b_g \\ | \end{array}, \quad (126)$$

An MTC can be used to describe the topological phases of a theory. This description, however, depends heavily on the topology of the surface on which the theory is defined. The genus g and the number of boundary components n , define the important topological properties of the (2+1)-D surface. Topology determines important properties of the topological phases of the system, namely the ground state degeneracy. In the 2d toric code, for example, the ground state degeneracy is equal to 2^{2g} . Thus, it is important to define the (2+1)-D surface as a compact, orientable surface $\Sigma_{g,n}$, labeled by the genus and number of boundary components.

The ground state subspace of the system is finite and independent of the system size, as the dimension of the Hilbert space \mathcal{H}_Σ is determined by the topological aspects outlined above. In order to describe the topological phases hosted in the system, it is important to consider the homeomorphisms of the surface $\Sigma_{g,n}$ onto itself, and study their action on the ground states of the system. In particular, it is important to study the set of orientation preserving automorphisms of the surface Σ , modulo the continuous deformations (mappings that preserve the topology). These automorphisms are called ‘‘Mapping Class Groups’’ of Σ and are denoted by $\text{MCG}(\Sigma)$. We outline how the action of $\text{MCG}(\Sigma)$ on the ground state subspace forms a projective representation, and we show the specific form of these representations using the data describing the MTC.

The simplest nontrivial surface in consideration is a torus, and we shall denote

the surface with $\Sigma_{1,0}$ (genus-1 surface, with no boundaries). The mapping class group of a torus is also referred to as the ‘modular group’ and the action of its elements on the torus is called ‘modular transformations’. The modular group is isomorphic to $SL(2, Z)$ group, i.e.

$$MCG(\Sigma_{1,0}) \cong \{\mathfrak{s}, \mathfrak{t} | (\mathfrak{st})^3 = \mathfrak{s}^2, \mathfrak{s}^4 = \mathbb{1}\} \quad (127)$$

A torus can be described by a generating pair of oriented cycles, having algebraic intersection number +1. We will label the two generating cycles as l and m . As shown in the Fig. 8, l and m can represent the longitudinal and meridian cycles of the torus.

The action of the mapping class group on the pair of generating cycles (l, m) produces a new pair of generating cycles that provide an equivalent description of the torus. The generators of the modular group can be chosen to be the following

$$\mathfrak{s} \cong \begin{bmatrix} 0 & -1 \\ 1 & 0 \end{bmatrix} \quad (128)$$

$$\mathfrak{t} \cong \begin{bmatrix} 1 & 1 \\ 0 & 1 \end{bmatrix} \quad (129)$$

It is quite straightforward to notice that the matrices \mathfrak{s} and \mathfrak{t} defined above satisfy the properties of the modular group outlined in Eq.(127). We can also write the action of these matrices on the pair of generating cycles (l, m) as follows

$$\begin{bmatrix} l \\ m \end{bmatrix} = \begin{bmatrix} 0 & -1 \\ 1 & 0 \end{bmatrix} \begin{bmatrix} m \\ -l \end{bmatrix} \quad (130)$$

$$\begin{bmatrix} l \\ m \end{bmatrix} = \begin{bmatrix} 1 & 1 \\ 0 & 1 \end{bmatrix} \begin{bmatrix} l - m \\ m \end{bmatrix} \quad (131)$$

From the equations above, we can see that the choices of the generating cycles $(m, -l)$ and $(l - m, m)$ are related to (l, m) through the modular transformations presented in Eq.(127).

To describe the topological state on a torus, we shall label a set of basis states using the charges $a \in \mathcal{C}_{\mathbf{g}}$ and $b \in \mathcal{C}_{\mathbf{h}}$, along with the pair of generating cycles (l, m) of the torus. We can, thus, use the notation $|a_{\mathbf{g}}^{(\mathbf{g}, \mathbf{h})}\rangle_{(l, m)}$ to describe the topological state living on (\mathbf{g}, \mathbf{h}) -sector of the torus. One can equivalently describe the topological state using the flux-line \mathbf{h} in the (\mathbf{g}, \mathbf{h}) -sector, i.e. $|b_{\mathbf{h}}^{(\mathbf{h}, \bar{\mathbf{g}})}\rangle_{(m, -l)}$.

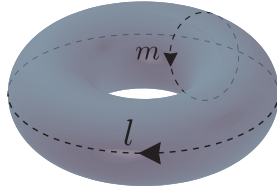


Figure 8: Longitudinal(l) and meridian (m) generating cycles of a torus in a particular embedding in 3D

In Fig. 9, two different basis $|a_{\mathbf{g}}^{(\mathbf{g}, \mathbf{h})}\rangle_{(l, m)}$ and $|b_{\mathbf{h}}^{(\mathbf{h}, \bar{\mathbf{g}})}\rangle_{(m, -l)}$ are drawn. They are related by a modular transformation $\mathcal{S}_{a_{\mathbf{g}} b_{\mathbf{h}}}^{(\mathbf{g}, \mathbf{h})}$. In FIG. 9, it can be seen that the topological states can be thought of as flux lines threading the torus across their corresponding cycle. Upon measurement of topological charge through the flux threading the torus (orthogonal to the direction of the cycle), one obtains the corresponding topological charges labeling the topological states. Note that, in FIG. 9, the torus is not punctured and so the only well-defined way one could relate (through the topological S-matrix) the two topological states, drawn in the figure, is if the two defect lines \mathbf{g} and \mathbf{h} commute.

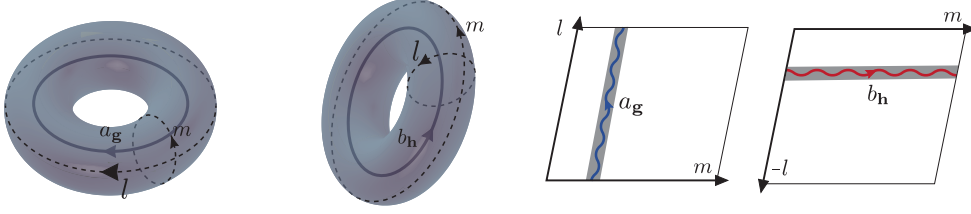


Figure 9: 3d and the corresponding 2d figure showing the two basis related by a modular $\mathcal{S}_{a_g b_h}^{(\mathbf{g}, \mathbf{h})}$ transformations. The generating cycle l corresponds to the defect line \mathbf{g} and m corresponds to \mathbf{h} . Measurement of topological charge along m on the left will result in a measurement charge value of a . Correspondingly, measurement across l on the right figure will result in a topological charge value of b .

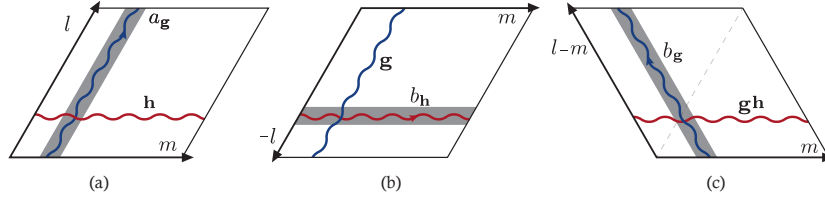


Figure 10: 2d diagrams showing the transformation $\mathcal{S}_{a_g b_g}^{(\mathbf{g}, \mathbf{h})}$ and $\mathcal{T}_{a_g b_g}^{(\mathbf{g}, \mathbf{h})}$ on the state $|a_{\mathbf{g}}^{(\mathbf{g}, \mathbf{h})}\rangle_{(l, m)}$. (a): 2d representation of the (\mathbf{g}, \mathbf{h}) -sector. (b): 2d representation of the $(\mathbf{h}, \bar{\mathbf{h}} \bar{\mathbf{g}})$ -sector given by \mathcal{S} transformation of the state $|a_{\mathbf{g}}^{(\mathbf{g}, \mathbf{h})}\rangle_{(l, m)}$. (c): $(\mathbf{g}, \mathbf{gh})$ -sector given by \mathcal{T} transformation of the state $|a_{\mathbf{g}}^{(\mathbf{g}, \mathbf{h})}\rangle_{(l, m)}$.

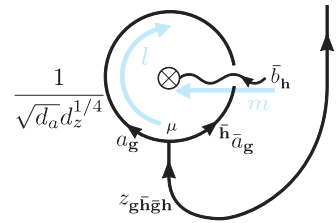
Similar to Eq.(127), we can write the following transformations relating the basis states describing the topological state

$$|a_{\mathbf{g}}^{(\mathbf{g}, \mathbf{h})}\rangle_{(l, m)} = \sum_{b \in \mathcal{C}_{\mathbf{h}}} \mathcal{S}_{a_{\mathbf{g}} b_{\mathbf{h}}}^{(\mathbf{g}, \mathbf{h})} |b_{\mathbf{h}}^{(\mathbf{h}, \bar{\mathbf{g}})}\rangle_{(m, -l)} \quad (132)$$

$$|a_{\mathbf{g}}^{(\mathbf{g}, \mathbf{h})}\rangle_{(l, m)} = \sum_{b \in \mathcal{C}_{\mathbf{g}}} \mathcal{T}_{a_{\mathbf{g}} b_{\mathbf{g}}}^{(\mathbf{g}, \mathbf{h})} |b_{\mathbf{g}}^{(\mathbf{g}, \mathbf{gh})}\rangle_{(l-m, m)} \quad (133)$$

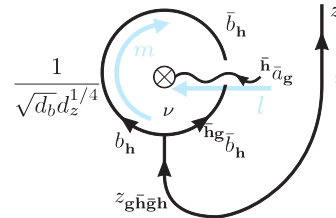
VIII. G -CROSSED MTC ON SURFACES OF ARBITRARY GENUS *

In order to construct a G -crossed MTC on higher genus surfaces, one can first construct the theory on a torus with a boundary (a punctured torus). This will provide the building block for higher genus as any surface of arbitrary genus can be constructed by gluing multiple punctured tori along their boundaries. We shall start by defining the topological states occupying the punctured torus with a given choice of generating cycles (l, m) , defined on a particular (\mathbf{g}, \mathbf{h}) -sector. We further specify how the defect line with label z connects the hole of the punctured torus to the two possible defect lines around the torus.



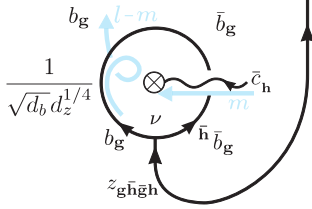
$$\frac{1}{\sqrt{d_a} d_z^{1/4}} \left(\text{Diagram} \right) = |a_{\mathbf{g}}, \bar{\mathbf{h}} \bar{a}_{\mathbf{g}}; z, \mu\rangle_{(l, m; w)} |z_{\mathbf{g} \bar{\mathbf{h}} \mathbf{g} \mathbf{h}}, \bar{z}_{\mathbf{g} \bar{\mathbf{h}} \mathbf{g} \mathbf{h}}; 0\rangle \quad (134)$$

Similarly, on the $(\mathbf{h}, \bar{\mathbf{h}} \bar{\mathbf{g}})$ -sector, the topological state is defined as



$$\frac{1}{\sqrt{d_b} d_z^{1/4}} \left(\text{Diagram} \right) = |b_{\mathbf{h}}, \bar{\mathbf{h}} \bar{b}_{\mathbf{h}}; z, \nu\rangle_{(m, -l; w + \frac{1}{4})} |z_{\mathbf{g} \bar{\mathbf{h}} \mathbf{g} \mathbf{h}}, \bar{z}_{\mathbf{g} \bar{\mathbf{h}} \mathbf{g} \mathbf{h}}; 0\rangle \quad (135)$$

and finally, on the $(\mathbf{g}, \mathbf{gh})$ -sector, we have the state



$$\frac{1}{\sqrt{d_b} d_z^{1/4}} \left| a_{\mathbf{g}}, \bar{\mathbf{h}} \bar{a}_{\mathbf{g}}; z, \mu \right\rangle_{(l,m;w)} = |b_{\mathbf{g}}, \bar{\mathbf{h}} \bar{b}_{\mathbf{g}}; z, \nu\rangle_{(l-m,m;w-1)} |z_{\mathbf{g}\bar{\mathbf{h}}\bar{\mathbf{g}}\mathbf{h}}, \bar{z}_{\mathbf{g}\bar{\mathbf{h}}\bar{\mathbf{g}}\mathbf{h}}; 0\rangle. \quad (136)$$

The torus with the defect lines drawn in FIG. 11 are a 2d graphical representation of the defects on the punctured torus. The generalization of the Eq. (132) and (133) on the punctured torus can thus be written as

$$\begin{aligned} \left| a_{\mathbf{g}}, \bar{\mathbf{h}} \bar{a}_{\mathbf{g}}; z, \mu \right\rangle_{(l,m;w)} &= \sum_{b \in \mathcal{C}_{\mathbf{h}}} \mathcal{S}_{(a_{\mathbf{g}}, \mu)(b_{\mathbf{h}}, \nu)}^{(z)} \left| b_{\mathbf{h}}, \bar{\mathbf{h}} \bar{b}_{\mathbf{h}}; z, \nu \right\rangle_{(m, -l; w + \frac{1}{4})} \\ &= \sum_{b \in \mathcal{C}_{\mathbf{g}}} \mathcal{T}_{(a_{\mathbf{g}}, \mu)(b_{\mathbf{g}}, \nu)}^{(z)} \left| b_{\mathbf{g}}, \bar{\mathbf{h}} \bar{b}_{\mathbf{g}}; z, \nu \right\rangle_{(l-m, m; w-1)} \end{aligned} \quad (137)$$

It is worth emphasizing that $\mathcal{S}_{(a_{\mathbf{g}}, \mu)(b_{\mathbf{h}}, \nu)}^{(z)}$ and $\mathcal{T}_{(a_{\mathbf{g}}, \mu)(b_{\mathbf{g}}, \nu)}^{(z)}$ are mappings that transform (\mathbf{g}, \mathbf{h}) -sector to $(\mathbf{h}, \bar{\mathbf{h}} \bar{\mathbf{g}})$ -sector and to $(\mathbf{g}, \mathbf{gh})$, respectively.

In order to consider the inner product between such states, one should cut along the corresponding generating cycles, make sure that the direction of the generating cycles l and m align, and then glue them. Taking the inner product of the states

defining Eq. (134) and (135) results in the following diagrammatic definition

$$\begin{aligned}
 & \frac{\sqrt{d_a d_b}}{\mathcal{D}} \langle b_{\mathbf{h}}, \bar{\mathbf{h}}_{\mathbf{g}} \bar{b}_{\mathbf{h}}; z, \nu | a_{\mathbf{g}}, \bar{\mathbf{h}}_{\mathbf{g}} \bar{a}_{\mathbf{g}}; z, \mu \rangle_{(l, m; w)} \\
 &= \frac{1}{\mathcal{D} \sqrt{d_z}} \langle \text{Diagram} \rangle = S_{(a_{\mathbf{g}}, \mu)(b_{\mathbf{h}}, \nu)}^{(z)} \quad (138)
 \end{aligned}$$

We have included the extra factors of dimensions of d_a and d_b for consistency with choices of normalization made in defining the topological states in Eqs. (82) and (83). The factor of \mathcal{D} is contained in the definition of the topological S-matrix for convenience.

Further, by taking the inner product between the states defined and note that this state and the original state defined in Eq. (134) and (136), gives us a diagrammatic definition of the modular transformation $\mathcal{T}_{(a_{\mathbf{g}}, \mu)(b_{\mathbf{g}}, \nu)}^{(z)}$

$$\begin{aligned}
 & \langle b_{\mathbf{g}}, \bar{\mathbf{h}}_{\mathbf{g}} \bar{b}_{\mathbf{g}}; z, \nu | a_{\mathbf{g}}, \bar{\mathbf{h}}_{\mathbf{g}} \bar{a}_{\mathbf{g}}; z, \mu \rangle_{(l, m; w)} \\
 &= \frac{1}{d_a \sqrt{d_z}} \delta_{ab} \delta_{\mu\nu} \langle \text{Diagram} \rangle = \mathcal{T}_{(a_{\mathbf{g}}, \mu)(b_{\mathbf{g}}, \nu)}^{(z)} \quad (139)
 \end{aligned}$$

The inner products defined in Eq.(138) and Eq.(139) motivates the definitions of a more general set of operators \mathbf{S} , \mathbf{T} , and \mathbf{C} which will be defined in the following section. In our paper, we show that these operators provide projective representation

of the mapping class group of the punctured torus, namely that

$$(\mathbf{S}\mathbf{T})^3 = \Theta_0 \mathbf{S}^2 \tag{140}$$

$$\mathbf{S} = \mathbf{C}\mathbf{S}^\dagger \tag{141}$$

$$\mathbf{C}^2 = \mathbf{Q}^{-1} \tag{142}$$

$$\mathbf{C}\mathbf{S} = \mathbf{S}\mathbf{C} \tag{143}$$

$$\mathbf{C}\mathbf{T} = \mathbf{T}\mathbf{C} \tag{144}$$

$$\mathbf{S}^2 = \mathbf{C}. \tag{145}$$

Note that these relations are quite similar to modular group properties in Eq. (127).

The relations above, however, these relations are more appropriately described by the mapping class group of the torus with a boundary (puncture), i.e. $MCG(\Sigma_{1,1}) \cong \{\mathfrak{s}, \mathfrak{t} | (\mathfrak{s}\mathfrak{t})^3 = \mathfrak{s}^2\}$. This mapping class group has an equivalent representation, using operators called ‘Dehn Twists’. The main distinction between $MCG(\Sigma_{1,0})$ and $MCG(\Sigma_{1,1})$ is that in $MCG(\Sigma_{1,1})$, unlike $MCG(\Sigma_{1,0})$, the relation $\mathfrak{s}^4 = \mathbf{1}$ is not satisfied. Instead, \mathfrak{s}^4 is equal to a Dehn Twist operator, which has infinite order. Given these properties of $MCG(\Sigma_{1,1})$, we can see how the relations given in Eqs. (140-144) provide a projective representation for $MCG(\Sigma_{1,1})$. Eqs. (143) and (144) show that the operators defined commute. Eqs. (145) and (142) indicate that $\mathbf{S}^4 = \mathbf{Q}^{-1}$, which as discussed above, is a relationship that is expected from operators representing $MCG(\Sigma_{1,1})$.

Another important observation is the following. Eqs. (141) and (145) indicate that $\mathbf{S}^{-1} = \mathbf{S}^\dagger$. This implies the unitarity of the \mathbf{S} operator, which means that the G -crossed theory on the punctured torus is modular. We need to reiterate that the only assumption made in showing the modularity of G -crossed theory, i.e. proving Eqs. (145), was that the underlying BTC theory \mathcal{C}_0 is modular. Thus, by proving

Eqs.(140 - 144), we prove that modularity of \mathcal{C}_0 implies the modularity of \mathcal{C}_G^\times .

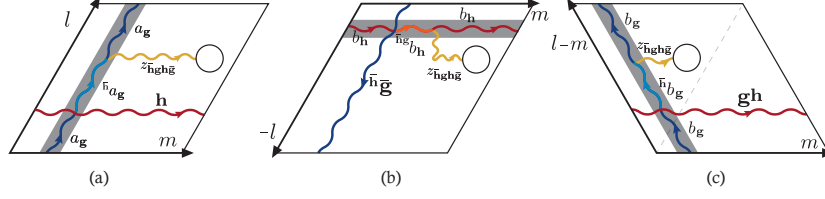


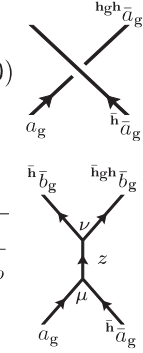
Figure 11: 2d figures representing the defect sectors on the punctured torus. The colored zig-zag lines represent specific symmetry line defects. (a): diagram of the (\mathbf{g}, \mathbf{h}) -sector on a punctured torus. The boundary of the puncture carries a charge that is equal to the charge of the defect line \mathbf{g} closing on itself after being conjugated by the loop \mathbf{h} (around the meridian). (b): diagram of $(\mathbf{h}, \bar{\mathbf{h}}\bar{\mathbf{g}})$ -sector on the punctured torus, given by a modular \mathcal{S} transformation. (c): diagram of $(\mathbf{g}, \mathbf{gh})$ -sector on the punctured torus, given by the \mathcal{T} transformation.

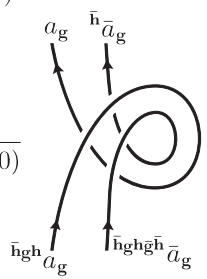
A. Modular transformations

Let us define the operators \mathcal{S} , \mathcal{T} , \mathcal{Q} , and \mathcal{C} explicitly.

$$\mathcal{S}(\mathbf{g}, \mathbf{h}) \equiv \sum_{a,b} \frac{\sqrt{d_a d_b}}{\mathcal{D}} \frac{1}{U_{\mathbf{h}}(a, \bar{a}; 0)} \begin{array}{c} \text{Diagram of } \mathcal{S}(\mathbf{g}, \mathbf{h}) \text{ with inputs } a_{\mathbf{g}}, \bar{h}\bar{a}_{\mathbf{g}} \text{ and outputs } b_{\mathbf{h}}, \bar{h}\bar{g}\bar{b}_{\mathbf{h}} \end{array} = \sum_{\substack{a,b \in \mathcal{C}_{\mathbf{g}}; \\ z, \mu, \nu}} \mathcal{S}_{(a_{\mathbf{g}}, \mu)(b_{\mathbf{h}}, \nu)}^{(z)} \sqrt{\frac{d_z}{d_a d_b}} \begin{array}{c} \text{Diagram of } \mathcal{S}(\mathbf{g}, \mathbf{h}) \text{ with inputs } a_{\mathbf{g}}, \bar{h}\bar{a}_{\mathbf{g}} \text{ and outputs } b_{\mathbf{h}}, \bar{h}\bar{g}\bar{b}_{\mathbf{h}} \end{array} \quad (146)$$

$$\mathcal{T}(\mathbf{g}, \mathbf{h}) \equiv \sum_{a \in \mathcal{C}_{\mathbf{g}}} \eta_a(\mathbf{g}, \mathbf{h}) \begin{array}{c} \text{Diagram of } \mathcal{T}(\mathbf{g}, \mathbf{h}) \text{ with inputs } a_{\mathbf{g}}, \bar{h}\bar{a}_{\mathbf{g}} \end{array} = \sum_{a \in \mathcal{C}_{\mathbf{g}}} \theta_a \eta_a(\mathbf{g}, \mathbf{h}) \begin{array}{c} \text{Diagram of } \mathcal{T}(\mathbf{g}, \mathbf{h}) \text{ with inputs } a_{\mathbf{g}}, \bar{h}\bar{a}_{\mathbf{g}} \end{array} = \sum_{\substack{a,b \in \mathcal{C}_{\mathbf{g}}; \\ z, \mu, \nu}} \mathcal{T}_{(a_{\mathbf{g}}, \mu)(b_{\mathbf{g}}, \nu)}^{(z)} \sqrt{\frac{d_z}{d_a d_b}} \begin{array}{c} \text{Diagram of } \mathcal{T}(\mathbf{g}, \mathbf{h}) \text{ with inputs } a_{\mathbf{g}}, \bar{h}\bar{a}_{\mathbf{g}} \text{ and outputs } b_{\mathbf{g}}, \bar{h}\bar{b}_{\mathbf{g}} \end{array} \quad (147)$$

$$\begin{aligned}
C(\mathbf{g}, \mathbf{h}) &\equiv \sum_{a \in \mathcal{C}_{\mathbf{g}}} R_0^{\bar{h} a \bar{g}} \eta_a(\mathbf{h}, \bar{h} \bar{\mathbf{g}}) \eta_a(\bar{\mathbf{g}} \mathbf{h}, \bar{h} \bar{\mathbf{g}}) U_{\bar{h} \bar{\mathbf{g}} \bar{h}}(\bar{h} \bar{a}, \bar{h} a; 0) \\
&= \sum_{\substack{a, b \in \mathcal{C}_{\mathbf{g}}; \\ z, \mu, \nu}} C_{(a_{\mathbf{g}}, \mu)(b_{\mathbf{g}}, \nu)}^{(z)} \sqrt{\frac{d_z}{d_a d_b}}
\end{aligned}$$

(148)

$$\begin{aligned}
Q(\mathbf{g}, \mathbf{h}) &\equiv \sum_{a \in \mathcal{C}_{\mathbf{g}}} \eta_a(\bar{h} \mathbf{g} \mathbf{h}, \bar{h} \mathbf{g} \bar{h} \bar{\mathbf{g}}) \frac{\eta_{\bar{a}}(\mathbf{h} \mathbf{g} \bar{h} \bar{\mathbf{g}}, \bar{h} \mathbf{g} \bar{h} \bar{\mathbf{g}}) \eta_{\bar{a}}(\bar{\mathbf{g}}, \mathbf{h}) \eta_{\bar{a}}(\bar{\mathbf{g}} \mathbf{h}, \bar{h} \mathbf{g})}{\eta_{\bar{a}}(\bar{\mathbf{g}}, \mathbf{g} \bar{h} \bar{\mathbf{g}}) \eta_{\bar{a}}(\bar{h} \bar{\mathbf{g}}, \bar{h} \mathbf{g} \bar{h} \bar{\mathbf{g}})} \\
&\times \frac{U_{\mathbf{h}}(\bar{a}, a; 0)}{U_{\bar{h} \mathbf{g} \bar{h} \bar{\mathbf{g}} \mathbf{h}}(\bar{h} \mathbf{g} a, \bar{h} \mathbf{g} \bar{a}; 0) U_{\bar{h} \mathbf{g}}(\bar{h} a, \bar{h} \bar{a}; 0) U_{\mathbf{g} \bar{h} \bar{\mathbf{g}} \mathbf{h}}(\bar{a}, a; 0)}
\end{aligned}$$

(149)

In the previous section we tried to provide a motivation for these definitions.

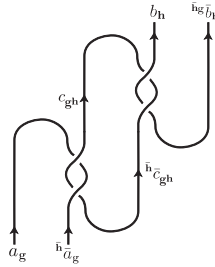
In our paper, we show that the operators defined above satisfy the mapping class group relations for the punctured torus in Eqs. (140-145). We further emphasize that Eqs. 145 and 141 imply that the S -matrix is unitary, and thus the G -crossed theory is modular. However, in our analysis, we show that Eq. (145) is valid only if the underlying fusion theory without defects (\mathcal{C}_0) is modular. This proves that modularity of \mathcal{C}_0 implies the modularity of $\mathcal{C}^{\times G}$, i.e. symmetry action on topological DOF does not destroy the modularity of the fusion theory.

IX. PROOF OF MODULAR GROUP RELATIONS *

$$\text{A. } (\mathbf{ST})^3 = \Theta_0 \mathbf{S}^2$$

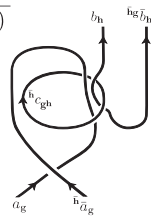
In order to prove this identity, we will prove an equivalent relation, namely that $\mathbf{TSTST} = \Theta_0 \mathbf{S}$. Starting with the definition of \mathbf{TSTST}

$$T(\mathbf{g}, \mathbf{h})S(\mathbf{g}, \mathbf{gh})T(\mathbf{gh}, \bar{\mathbf{h}}\bar{\mathbf{g}})S(\mathbf{gh}, \mathbf{h})T(\mathbf{h}, \bar{\mathbf{h}}\bar{\mathbf{h}}\bar{\mathbf{g}}) =$$

$$\sum_{\substack{a \in C_{\mathbf{g}}; \\ c \in C_{\mathbf{gh}}; \\ b \in C_{\mathbf{h}}}} \frac{\theta_a \theta_b \theta_c}{\mathcal{D}^2} \sqrt{d_a d_b d_c} \eta_a(\mathbf{g}, \mathbf{h}) \frac{1}{U_{\mathbf{gh}}(a, \bar{a}; 0)} \eta_c(\mathbf{gh}, \bar{\mathbf{h}}\bar{\mathbf{g}}) \frac{1}{U_{\mathbf{h}}(c, \bar{c}; 0)} \eta_b(\mathbf{h}, \bar{\mathbf{h}}\bar{\mathbf{h}}\bar{\mathbf{g}})$$

(150)

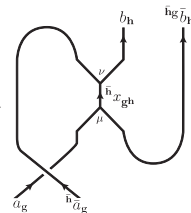
Using our defined actions upon crossing lines over and under vertices, as shown in FIG. 12 of Appendix-A, we obtain

$$= \sum_{a,b,c} \theta_a \theta_b \theta_c \frac{\sqrt{d_a d_b d_c}}{\mathcal{D}^2} R_0^{\bar{h}_a \bar{h}_b \bar{h}_c} \frac{\eta_a(\mathbf{g}, \mathbf{h}) \eta_a(\mathbf{gh}, \bar{\mathbf{h}}\bar{\mathbf{g}}) \eta_{\bar{h}_c \bar{h}_a}(\bar{\mathbf{h}}\bar{\mathbf{gh}}, \bar{\mathbf{h}}\bar{\mathbf{h}}\bar{\mathbf{g}})}{\eta_a(\bar{\mathbf{h}}\bar{\mathbf{g}}, \bar{\mathbf{h}}\bar{\mathbf{gh}})} \frac{U_{\bar{\mathbf{h}}\bar{\mathbf{g}}}(c, \bar{c}; 0)}{U_{\mathbf{h}}(c, \bar{c}; 0)}$$

$$\times \eta_c(\mathbf{gh}, \bar{\mathbf{h}}\bar{\mathbf{g}}) \eta_{\bar{c}}(\bar{\mathbf{h}}\bar{\mathbf{g}}, \bar{\mathbf{h}}\bar{\mathbf{g}}) \eta_b(\mathbf{h}, \bar{\mathbf{h}}\bar{\mathbf{h}}\bar{\mathbf{g}})$$

(151)

Then by fusing the lines wrapped around by the loop $\bar{\mathbf{h}}\bar{c}_{\mathbf{gh}}$, and summing over all the topological labels c , we get

$$= \Theta_0 \sum_{a,b} \sum_{\substack{x \in C_{\mathbf{gh}}, \\ \mu, \nu}} \theta_a \theta_b \frac{\sqrt{d_a d_b}}{\mathcal{D}^2} R_0^{\bar{h}_a \bar{h}_b \bar{h}_x} \frac{\eta_a(\mathbf{g}, \mathbf{h}) \eta_a(\mathbf{gh}, \bar{\mathbf{h}}\bar{\mathbf{g}}) \eta_{\bar{h}_x \bar{h}_a}(\bar{\mathbf{h}}\bar{\mathbf{gh}}, \bar{\mathbf{h}}\bar{\mathbf{h}}\bar{\mathbf{g}})}{\eta_a(\bar{\mathbf{h}}\bar{\mathbf{g}}, \bar{\mathbf{h}}\bar{\mathbf{gh}})}$$

$$\times \eta_b(\mathbf{h}, \bar{\mathbf{h}}\bar{\mathbf{h}}\bar{\mathbf{g}}) \frac{[U_{\bar{\mathbf{h}}\bar{\mathbf{g}}}(\bar{\mathbf{h}}\bar{a}_g, b_{\mathbf{h}}, \bar{\mathbf{h}}x_{\mathbf{gh}})]_{\mu\nu}}{\theta_x \eta_x(\mathbf{gh}, \bar{\mathbf{h}}\bar{\mathbf{g}})}$$

(152)

Using the inverse of G -crossed ribbon identity Eq.(109) (by summing over $x, \mu,$

and ν) and noting that

$$[U_{\bar{h}\bar{h}\bar{g}}(\bar{h}a_g, b_h, \bar{h}x_{gh})]_{\mu\nu} = \frac{\eta_{\bar{h}x}(\bar{h}gh, \bar{h}\bar{h}\bar{g})}{\eta_{\bar{h}gh_a}(\bar{h}gh, \bar{h}\bar{h}\bar{g})\eta_{\bar{h}gb}(\bar{h}gh, \bar{h}\bar{h}\bar{g})} [U_{\bar{h}gh}(\bar{h}gh a_g, \bar{h}g b_h, \bar{h}x_{gh})^{-1}]_{\mu\nu},$$

our expression simplifies to

$$= \Theta_0 \sum_{a,b} \sum_{\substack{x \in \mathcal{C}_{gh}, \\ \mu, \nu}} \theta_a \theta_b \frac{\sqrt{d_a d_b}}{\mathcal{D}^2} R_0^{\bar{h}a_g \bar{h}\bar{a}_g} \frac{\eta_a(\mathbf{g}, \mathbf{h}) \eta_a(\mathbf{g}\mathbf{h}, \bar{h}\bar{g})}{\eta_a(\mathbf{g}, \bar{h}\bar{g}) \eta_a(\mathbf{g}\bar{h}\bar{g}, \bar{h}\mathbf{g}\mathbf{h})} \times \frac{1}{\eta_a(\mathbf{h}, \bar{h}\bar{g}) \eta_a(\bar{g}\mathbf{h}, \bar{h}\mathbf{g})} \text{Diagram} \quad (153)$$

$$= \Theta_0 \sum_{a,b} \frac{\sqrt{d_a d_b}}{\mathcal{D}} \frac{1}{U_{\mathbf{h}}(a, \bar{a}; 0)} \text{Diagram} = \Theta_0 S(\mathbf{g}, \mathbf{h}) \quad (154)$$

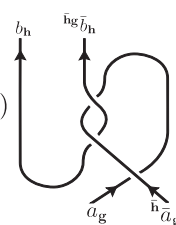
To follow the details of the last step, refer to the appendix. This proves our first relation.

B. $S = CS^\dagger$

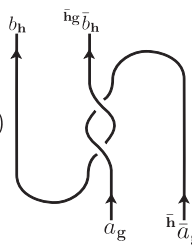
Starting from the definition of $S(\mathbf{g}, \mathbf{h})$

$$S(\mathbf{g}, \mathbf{h}) = \sum_{a,b} \frac{\sqrt{d_a d_b}}{\mathcal{D}} \frac{1}{U_{\mathbf{h}}(a, \bar{a}; 0)} \text{Diagram} \\ = \sum_{\substack{a \in \mathcal{C}_{\mathbf{g}}; \\ b \in \mathcal{C}_{\mathbf{h}}}} \frac{\sqrt{d_a d_b}}{\mathcal{D}} R_0^{\bar{h}a_g \bar{h}\bar{a}_g} \frac{\eta_a(\mathbf{h}, \bar{h})}{\eta_{\bar{h}a}(\bar{h}, \bar{h}\bar{g})} \eta_{\bar{h}a}(\bar{h}\bar{g}, \bar{h}\mathbf{g}\bar{h}) \\ \times U_{\bar{h}\bar{g}}(b, \bar{b}; 0) U_{\bar{h}\mathbf{g}\bar{h}}(\bar{h}\bar{a}, \bar{h}a; 0) \text{Diagram} \quad (155)$$

For details of steps, refer to the appendix. By noting that $\frac{\eta_a(\mathbf{h}, \bar{\mathbf{h}})\eta_{\bar{\mathbf{h}}_a}(\bar{\mathbf{h}}\bar{\mathbf{g}}, \bar{\mathbf{h}}\bar{\mathbf{g}}\bar{\mathbf{h}})}{\eta_{\bar{\mathbf{h}}_a}(\bar{\mathbf{h}}, \bar{\mathbf{h}}\bar{\mathbf{g}})} = \eta_a(\mathbf{h}, \bar{\mathbf{h}}\bar{\mathbf{g}})\eta_a(\bar{\mathbf{g}}\mathbf{h}, \bar{\mathbf{h}}\bar{\mathbf{g}}\bar{\mathbf{h}})$, we can rewrite this as

$$= \sum_{\substack{a \in \mathcal{C}_{\mathbf{g}}; \\ b \in \mathcal{C}_{\bar{\mathbf{h}}}}} \frac{\sqrt{d_a d_b}}{\mathcal{D}} R_0^{\bar{\mathbf{h}}_a \bar{\mathbf{h}}_a} \eta_a(\mathbf{h}, \bar{\mathbf{h}}\bar{\mathbf{g}})\eta_a(\bar{\mathbf{g}}\mathbf{h}, \bar{\mathbf{h}}\bar{\mathbf{g}}\bar{\mathbf{h}}) U_{\bar{\mathbf{h}}\bar{\mathbf{g}}}(b, \bar{b}; 0) \\ \times U_{\bar{\mathbf{h}}\bar{\mathbf{g}}\bar{\mathbf{h}}}(\bar{\mathbf{h}}\bar{a}, \bar{\mathbf{h}}a; 0) = C(\mathbf{g}, \mathbf{h}) S^\dagger(\mathbf{h}, \bar{\mathbf{h}}\bar{\mathbf{g}})$$


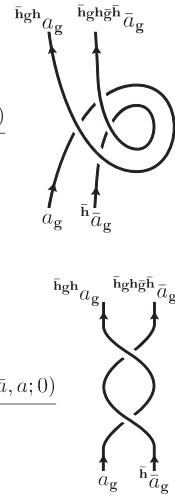
Noting that the last equality follows from the definition of $S^\dagger(\mathbf{h}, \bar{\mathbf{h}}\bar{\mathbf{g}})$

$$S^\dagger(\mathbf{h}, \bar{\mathbf{h}}\bar{\mathbf{g}}) = \sum_{\substack{a \in \mathcal{C}_{\mathbf{g}}; \\ b \in \mathcal{C}_{\bar{\mathbf{h}}}}} \frac{\sqrt{d_a d_b}}{\mathcal{D}} U_{\bar{\mathbf{h}}\bar{\mathbf{g}}}(b, \bar{b}; 0)$$

(156)

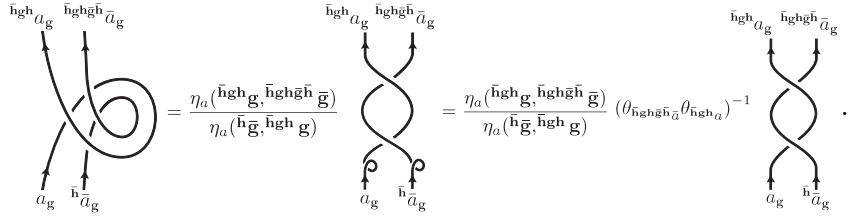
and that of $C(\mathbf{g}, \mathbf{h})$ introduced in Eq. (148). This concludes the proof.

C. $C^2 = Q^{-1}$

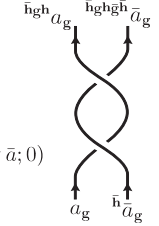
By using the inverse of Eq. (149), we have the following

$$\begin{aligned}
\mathcal{Q}^{-1}(\mathbf{g}, \mathbf{h}) &= \sum_{a \in \mathcal{C}_{\mathbf{g}}} \frac{1}{\eta_a(\bar{\mathbf{h}}\mathbf{g}\bar{\mathbf{g}}, \bar{\mathbf{h}}\mathbf{g}\bar{\mathbf{h}}\bar{\mathbf{g}})} \frac{\eta_a(\bar{\mathbf{g}}, \mathbf{g}\bar{\mathbf{h}}\bar{\mathbf{g}})\eta_a(\bar{\mathbf{h}}\bar{\mathbf{g}}, \bar{\mathbf{h}}\mathbf{g}\bar{\mathbf{h}}\bar{\mathbf{h}})}{\eta_a(\mathbf{h}\mathbf{g}\bar{\mathbf{h}}\bar{\mathbf{g}}, \bar{\mathbf{h}}\mathbf{g}\bar{\mathbf{h}}\bar{\mathbf{g}})\eta_a(\bar{\mathbf{g}}, \mathbf{h})\eta_a(\bar{\mathbf{g}}\mathbf{h}, \bar{\mathbf{h}}\mathbf{g}\bar{\mathbf{h}}\bar{\mathbf{g}})} \\
&\quad \times \frac{U_{\bar{\mathbf{h}}\mathbf{g}\bar{\mathbf{h}}\bar{\mathbf{g}}}(\bar{\mathbf{h}}\mathbf{g}a, \bar{\mathbf{h}}\mathbf{g}\bar{a}; 0)U_{\bar{\mathbf{h}}\bar{\mathbf{g}}}(\bar{\mathbf{h}}a, \bar{\mathbf{h}}\bar{a}; 0)U_{\mathbf{g}\bar{\mathbf{h}}\bar{\mathbf{g}}\bar{\mathbf{h}}}(\bar{a}, a; 0)}{U_{\mathbf{h}}(\bar{a}, a; 0)} \\
&= \sum_{a \in \mathcal{C}_{\mathbf{g}}} \frac{(\theta_{\bar{\mathbf{h}}\mathbf{g}\bar{\mathbf{h}}\bar{\mathbf{g}}\bar{a}}\theta_{\bar{\mathbf{h}}\mathbf{g}\mathbf{h}a})^{-1}}{\eta_a(\bar{\mathbf{h}}\bar{\mathbf{g}}, \bar{\mathbf{h}}\mathbf{g}\bar{\mathbf{g}})} \frac{\eta_a(\bar{\mathbf{g}}, \mathbf{g}\bar{\mathbf{h}}\bar{\mathbf{g}})\eta_a(\bar{\mathbf{h}}\bar{\mathbf{g}}, \bar{\mathbf{h}}\mathbf{g}\bar{\mathbf{h}}\bar{\mathbf{h}})}{\eta_a(\mathbf{h}\mathbf{g}\bar{\mathbf{h}}\bar{\mathbf{g}}, \bar{\mathbf{h}}\mathbf{g}\bar{\mathbf{h}}\bar{\mathbf{g}})\eta_a(\bar{\mathbf{g}}, \mathbf{h})\eta_a(\bar{\mathbf{g}}\mathbf{h}, \bar{\mathbf{h}}\mathbf{g}\bar{\mathbf{h}}\bar{\mathbf{g}})} \\
&\quad \times \frac{U_{\bar{\mathbf{h}}\mathbf{g}\bar{\mathbf{h}}\bar{\mathbf{g}}}(\bar{\mathbf{h}}\mathbf{g}a, \bar{\mathbf{h}}\mathbf{g}\bar{a}; 0)U_{\bar{\mathbf{h}}\bar{\mathbf{g}}}(\bar{\mathbf{h}}a, \bar{\mathbf{h}}\bar{a}; 0)U_{\mathbf{g}\bar{\mathbf{h}}\bar{\mathbf{g}}\bar{\mathbf{h}}}(\bar{a}, a; 0)}{U_{\mathbf{h}}(\bar{a}, a; 0)}
\end{aligned}$$

(157)

The last equality follows from the following relation

$$\begin{aligned}
&\text{Diagram 1} = \frac{\eta_a(\bar{\mathbf{h}}\mathbf{g}\bar{\mathbf{g}}, \bar{\mathbf{h}}\mathbf{g}\bar{\mathbf{h}}\bar{\mathbf{g}})}{\eta_a(\bar{\mathbf{h}}\bar{\mathbf{g}}, \bar{\mathbf{h}}\mathbf{g}\bar{\mathbf{g}})} \text{Diagram 2} = \frac{\eta_a(\bar{\mathbf{h}}\mathbf{g}\bar{\mathbf{g}}, \bar{\mathbf{h}}\mathbf{g}\bar{\mathbf{h}}\bar{\mathbf{g}})}{\eta_a(\bar{\mathbf{h}}\bar{\mathbf{g}}, \bar{\mathbf{h}}\mathbf{g}\bar{\mathbf{g}})} (\theta_{\bar{\mathbf{h}}\mathbf{g}\bar{\mathbf{h}}\bar{\mathbf{g}}\bar{a}}\theta_{\bar{\mathbf{h}}\mathbf{g}\mathbf{h}a})^{-1} \text{Diagram 3}
\end{aligned}$$

(158)

Using Eq. (148), we note that \mathcal{C}^2 is given by the following expression

$$\begin{aligned}
\mathcal{C}(\mathbf{g}, \mathbf{h})\mathcal{C}(\bar{\mathbf{h}}\bar{\mathbf{g}}, \bar{\mathbf{h}}\mathbf{g}\bar{\mathbf{h}}) &= \sum_{a \in \mathcal{C}_{\mathbf{g}}} R_0^{\bar{\mathbf{h}}a\bar{\mathbf{h}}a} R_0^{\bar{\mathbf{h}}\mathbf{g}\bar{a}\bar{\mathbf{h}}\mathbf{g}a} \eta_a(\mathbf{h}, \bar{\mathbf{h}}\bar{\mathbf{g}})\eta_a(\bar{\mathbf{g}}\mathbf{h}, \bar{\mathbf{h}}\bar{\mathbf{g}}\bar{\mathbf{h}}) \\
&\quad \times \eta_{\bar{\mathbf{h}}\bar{a}}(\bar{\mathbf{h}}\mathbf{g}\bar{\mathbf{h}}, \bar{\mathbf{h}}\mathbf{g}\bar{\mathbf{g}})\eta_{\bar{\mathbf{h}}\bar{a}}(\bar{\mathbf{h}}\mathbf{g}\bar{\mathbf{h}}, \bar{\mathbf{h}}\mathbf{g}\bar{\mathbf{h}}\bar{\mathbf{h}}) U_{\bar{\mathbf{h}}\bar{\mathbf{g}}\bar{\mathbf{h}}}(\bar{\mathbf{h}}\bar{a}, \bar{\mathbf{h}}a; 0)U_{\bar{\mathbf{h}}\mathbf{g}\bar{\mathbf{h}}\bar{\mathbf{g}}}(\bar{\mathbf{h}}\mathbf{g}a, \bar{\mathbf{h}}\mathbf{g}\bar{a}; 0)
\end{aligned}$$

(159)

Using the relations between G-crossed braids R and the twist angles given by equations (117) and (119), together with the G -crossed ribbon identity, we note the following

$$R_0^{\bar{\mathbf{h}}\mathbf{g}\bar{a}\bar{\mathbf{h}}\mathbf{g}a} = \frac{U_{\bar{\mathbf{h}}\mathbf{g}\bar{\mathbf{h}}\bar{\mathbf{g}}}(\bar{\mathbf{h}}\mathbf{g}a, \bar{\mathbf{h}}\mathbf{g}\bar{a}; 0)}{\theta_{\bar{\mathbf{h}}\mathbf{g}\bar{\mathbf{h}}\bar{\mathbf{g}}\bar{a}}} \quad (160)$$

$$R_0^{\bar{\mathbf{h}}a\bar{\mathbf{h}}a} = \frac{1}{\theta_{\bar{\mathbf{h}}\bar{a}}\eta_{\bar{\mathbf{h}}\bar{a}}(\bar{\mathbf{h}}\bar{\mathbf{g}}, \bar{\mathbf{h}}\bar{\mathbf{g}})\eta_{\bar{\mathbf{h}}\bar{a}}(\bar{\mathbf{h}}\bar{\mathbf{g}}, \bar{\mathbf{h}}\bar{\mathbf{g}})}. \quad (161)$$

Using these relations, we can now rewrite the algebraic expression in Eq. (159) as

$$\begin{aligned}
& R_0^{\bar{h}_a \bar{h}_a} R_0^{\bar{h} g \bar{h}_a} \eta_a(\mathbf{h}, \bar{\mathbf{g}}) \eta_a(\bar{\mathbf{g}} \mathbf{h}, \bar{\mathbf{h}}) \eta_{\bar{h}_a}(\bar{\mathbf{h}} \bar{\mathbf{g}}, \bar{\mathbf{h}} g) \\
& \quad \times \eta_{\bar{h}_a}(\bar{\mathbf{h}} g \bar{\mathbf{h}}, \bar{\mathbf{h}} g \bar{\mathbf{h}} \mathbf{h}) U_{\bar{h}_a}(\bar{h}_a, \bar{h}_a; 0) U_{\bar{h}_a}(\bar{\mathbf{h}} g \bar{\mathbf{h}}, \bar{\mathbf{h}} g \bar{h}_a; 0) \\
& = \frac{U_{\bar{h}_a}(\bar{\mathbf{h}} g \bar{\mathbf{h}}, \bar{\mathbf{h}} g \bar{h}_a; 0)}{\theta_{\bar{h}_a} \theta_{\bar{h}_a} \eta_{\bar{h}_a}(\bar{\mathbf{h}} \bar{\mathbf{g}}, \bar{\mathbf{h}} \mathbf{g}) \eta_{\bar{h}_a}(\bar{\mathbf{h}} \bar{\mathbf{g}}, \bar{\mathbf{h}} \mathbf{g})} \eta_a(\mathbf{h}, \bar{\mathbf{h}}) \eta_a(\bar{\mathbf{g}} \mathbf{h}, \bar{\mathbf{h}}) \eta_{\bar{h}_a}(\bar{\mathbf{h}} \bar{\mathbf{g}}, \bar{\mathbf{h}} g) \\
& \quad \times \eta_{\bar{h}_a}(\bar{\mathbf{h}} g \bar{\mathbf{h}}, \bar{\mathbf{h}} g \bar{\mathbf{h}} \mathbf{h}) U_{\bar{h}_a}(\bar{h}_a, \bar{h}_a; 0) U_{\bar{h}_a}(\bar{\mathbf{h}} g \bar{\mathbf{h}}, \bar{\mathbf{h}} g \bar{h}_a; 0) \\
& = \frac{1}{\theta_{\bar{h}_a} \theta_{\bar{h}_a}} \frac{\eta_a(\mathbf{h}, \bar{\mathbf{h}}) \eta_a(\bar{\mathbf{g}} \bar{\mathbf{h}}, \bar{\mathbf{h}} g) \eta_a(\mathbf{g} \bar{\mathbf{h}} \bar{\mathbf{g}}, \bar{\mathbf{h}} g \bar{\mathbf{h}})}{\eta_a(\mathbf{h}, \bar{\mathbf{h}}) \eta_a(\bar{\mathbf{g}} \mathbf{h}, \bar{\mathbf{h}}) \eta_a(\mathbf{h}, \bar{\mathbf{h}} g)} \\
& \quad \times \frac{\eta_a(\bar{\mathbf{g}} \mathbf{h}, \bar{\mathbf{h}}) U_{\bar{h}_a}(\bar{\mathbf{h}} g \bar{\mathbf{h}}, \bar{\mathbf{h}} g \bar{h}_a; 0) U_{\bar{h}_a}(\bar{h}_a, \bar{h}_a; 0) U_{\bar{h}_a}(\bar{\mathbf{h}} g \bar{\mathbf{h}}, \bar{\mathbf{h}} g \bar{h}_a; 0)}{\eta_a(\bar{\mathbf{g}} \mathbf{h}, \bar{\mathbf{h}})} \quad (162)
\end{aligned}$$

The last equality follows from the following relations

$$\begin{aligned}
\eta_{\bar{h}_a}(\bar{\mathbf{h}} \bar{\mathbf{g}}, \bar{\mathbf{h}} \mathbf{g}) &= \eta_a(\mathbf{h}, \bar{\mathbf{h}}) \eta_a(\bar{\mathbf{g}} \mathbf{h}, \bar{\mathbf{h}} \mathbf{g}) \\
\eta_{\bar{h}_a}(\bar{\mathbf{h}} \bar{\mathbf{g}}, \bar{\mathbf{h}} \mathbf{g}) &= \eta_a(\mathbf{h}, \bar{\mathbf{h}}) \eta_a(\bar{\mathbf{g}} \mathbf{h}, \bar{\mathbf{h}} \mathbf{g}) \\
\eta_{\bar{h}_a}(\bar{\mathbf{h}} g \bar{\mathbf{h}}, \bar{\mathbf{h}} g \bar{\mathbf{h}} \mathbf{h}) &= \frac{\eta_a(\mathbf{h}, \bar{\mathbf{h}}) \eta_a(\bar{\mathbf{g}} \bar{\mathbf{h}}, \bar{\mathbf{h}} g \bar{\mathbf{h}})}{\eta_a(\mathbf{h}, \bar{\mathbf{h}} g \bar{\mathbf{h}})} \\
\eta_{\bar{h}_a}(\bar{\mathbf{h}} g \bar{\mathbf{h}}, \bar{\mathbf{h}} g \bar{\mathbf{h}} \mathbf{h}) &= \frac{\eta_a(\mathbf{h}, \bar{\mathbf{h}} g \bar{\mathbf{h}}) \eta_a(\mathbf{g} \bar{\mathbf{h}} \bar{\mathbf{g}}, \bar{\mathbf{h}} g \bar{\mathbf{h}} \mathbf{h})}{\eta_a(\mathbf{h}, \bar{\mathbf{h}} g \bar{\mathbf{h}})}.
\end{aligned}$$

Noting the following identities

$$\begin{aligned}
\eta_a(\mathbf{g} \bar{\mathbf{h}} \bar{\mathbf{g}}, \bar{\mathbf{h}} g \bar{\mathbf{h}} \mathbf{h}) &= \frac{\eta_a(\bar{\mathbf{g}}, \mathbf{g} \bar{\mathbf{h}} \bar{\mathbf{g}}) \eta_a(\mathbf{g} \bar{\mathbf{h}} \bar{\mathbf{g}}, \bar{\mathbf{h}} g \bar{\mathbf{h}} \mathbf{h})}{\eta_a(\bar{\mathbf{g}}, \mathbf{g} \bar{\mathbf{h}} \bar{\mathbf{g}})} \\
\eta_a(\mathbf{g} \bar{\mathbf{h}} \bar{\mathbf{g}}, \bar{\mathbf{h}} g \bar{\mathbf{h}} \mathbf{h}) &= \frac{\eta_a(\bar{\mathbf{g}}, \mathbf{g} \bar{\mathbf{h}} \bar{\mathbf{g}}) \eta_a(\bar{\mathbf{h}} \bar{\mathbf{g}}, \bar{\mathbf{h}} g \bar{\mathbf{h}} \mathbf{h})}{\eta_a(\bar{\mathbf{g}}, \mathbf{g} \bar{\mathbf{h}} \bar{\mathbf{g}})} \\
\eta_a(\mathbf{h}, \bar{\mathbf{h}} g \bar{\mathbf{h}}) &= \frac{\eta_a(\bar{\mathbf{g}}, \mathbf{h}) \eta_a(\bar{\mathbf{g}} \mathbf{h}, \bar{\mathbf{h}} g \bar{\mathbf{h}})}{\eta_a(\bar{\mathbf{g}}, \mathbf{g} \bar{\mathbf{h}} \bar{\mathbf{g}})} \\
\eta_a(\mathbf{h}, \bar{\mathbf{h}} g \bar{\mathbf{h}} \mathbf{h}) &= \frac{\eta_a(\bar{\mathbf{g}}, \mathbf{h}) \eta_a(\bar{\mathbf{g}} \mathbf{h}, \bar{\mathbf{h}} g \bar{\mathbf{h}} \mathbf{h})}{\eta_a(\bar{\mathbf{g}}, \mathbf{g} \bar{\mathbf{h}} \bar{\mathbf{g}})}
\end{aligned}$$

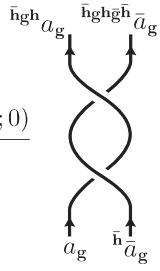
we can simplify the terms with η_a in the outermost right terms in Eq. (162), as

follows

$$\frac{\eta_{\bar{a}}(\mathbf{h}, \bar{\mathbf{h}}\mathbf{g}, \bar{\mathbf{h}})}{\eta_{\bar{a}}(\mathbf{h}, \bar{\mathbf{h}}\bar{\mathbf{g}})} \frac{\eta_{\bar{a}}(\mathbf{g}, \bar{\mathbf{h}}\bar{\mathbf{g}}, \bar{\mathbf{h}}\mathbf{g}\mathbf{h}, \bar{\mathbf{h}})}{\eta_{\bar{a}}(\mathbf{g}\mathbf{g}, \bar{\mathbf{h}}\bar{\mathbf{g}}, \bar{\mathbf{h}}\mathbf{g}\mathbf{h}\mathbf{g}\mathbf{h}, \bar{\mathbf{h}})} = \frac{\eta_{\bar{a}}(\bar{\mathbf{g}}\mathbf{h}, \bar{\mathbf{h}}\mathbf{g}, \bar{\mathbf{h}})}{\eta_{\bar{a}}(\bar{\mathbf{g}}\mathbf{h}, \bar{\mathbf{h}}\mathbf{g})} \frac{\eta_{\bar{a}}(\bar{\mathbf{h}}\bar{\mathbf{g}}, \bar{\mathbf{h}}\mathbf{g}\mathbf{h}, \bar{\mathbf{h}})}{\eta_{\bar{a}}(\bar{\mathbf{h}}\mathbf{g}, \bar{\mathbf{h}}\bar{\mathbf{g}})} \frac{\eta_{\bar{a}}(\bar{\mathbf{g}}, \mathbf{g}, \bar{\mathbf{h}}\bar{\mathbf{g}})}{\eta_{\bar{a}}(\bar{\mathbf{g}}\mathbf{h}, \bar{\mathbf{h}}\mathbf{g}\mathbf{h}, \bar{\mathbf{h}})} \frac{\eta_{\bar{a}}(\bar{\mathbf{h}}\bar{\mathbf{g}}, \bar{\mathbf{h}}\mathbf{g}\mathbf{h}\mathbf{g}\mathbf{h}, \bar{\mathbf{h}})}{\eta_{\bar{a}}(\bar{\mathbf{g}}, \mathbf{h}\mathbf{g}, \bar{\mathbf{h}}\bar{\mathbf{g}})}. \quad (163)$$

Finally, by noting that $\theta_{\bar{\mathbf{h}}\bar{\mathbf{a}}} = \frac{\eta_{\bar{a}}(\bar{\mathbf{g}}, \mathbf{h})\eta_{\bar{a}}(\mathbf{h}\mathbf{g}, \bar{\mathbf{h}}\bar{\mathbf{g}}, \bar{\mathbf{h}}\mathbf{g}\mathbf{h}\bar{\mathbf{g}}\bar{\mathbf{h}})}{\eta_{\bar{a}}(\mathbf{h}, \bar{\mathbf{h}}\bar{\mathbf{g}})\eta_{\bar{a}}(\bar{\mathbf{g}}, \mathbf{h}\mathbf{g}\bar{\mathbf{h}}\bar{\mathbf{g}})}\theta_{\bar{\mathbf{h}}\mathbf{g}\mathbf{h}\bar{\mathbf{g}}\bar{\mathbf{h}}\bar{\mathbf{a}}}$, $\eta_{\bar{a}}(\bar{\mathbf{g}}\mathbf{h}, \bar{\mathbf{h}}\mathbf{g}, \bar{\mathbf{h}})}{\eta_{\bar{a}}(\bar{\mathbf{g}}\mathbf{h}, \bar{\mathbf{h}}\mathbf{g})} = \frac{U_{\bar{\mathbf{h}}\bar{\mathbf{g}}}(\bar{a}, a; 0)}{U_{\bar{\mathbf{g}}\mathbf{h}}(\bar{a}, a; 0)U_{\bar{\mathbf{h}}\bar{\mathbf{g}}\bar{\mathbf{h}}}(\bar{\mathbf{h}}\bar{\mathbf{a}}, \bar{\mathbf{h}}a; 0)}$, and $\eta_{\bar{a}}(\bar{\mathbf{g}}\mathbf{h}, \bar{\mathbf{h}}\mathbf{g})\eta_{\bar{a}}(\bar{\mathbf{g}}\mathbf{h}, \bar{\mathbf{h}}\mathbf{g}) = \frac{U_{\mathbf{h}}(\bar{a}, a; 0)}{U_{\bar{\mathbf{g}}\mathbf{h}}(\bar{a}, a; 0)U_{\bar{\mathbf{h}}\bar{\mathbf{g}}}(\bar{\mathbf{h}}\bar{\mathbf{a}}, \bar{\mathbf{h}}a; 0)}$, we rewrite C^2 as

$$C^2 = \sum_{a \in C_{\mathbf{g}}} \frac{(\theta_{\bar{\mathbf{h}}\mathbf{g}\mathbf{h}\bar{\mathbf{g}}\bar{\mathbf{h}}\bar{\mathbf{a}}}\theta_{\bar{\mathbf{h}}\mathbf{g}\mathbf{h}\bar{\mathbf{a}}})^{-1}}{\eta_{\bar{a}}(\bar{\mathbf{h}}\bar{\mathbf{g}}, \bar{\mathbf{h}}\mathbf{g}\mathbf{h}, \bar{\mathbf{h}})} \frac{\eta_{\bar{a}}(\bar{\mathbf{g}}, \mathbf{g}, \bar{\mathbf{h}}\bar{\mathbf{g}})\eta_{\bar{a}}(\bar{\mathbf{h}}\bar{\mathbf{g}}, \bar{\mathbf{h}}\mathbf{g}\mathbf{h}\bar{\mathbf{g}}\bar{\mathbf{h}})}{\eta_{\bar{a}}(\mathbf{h}\mathbf{g}, \bar{\mathbf{h}}\bar{\mathbf{g}}, \bar{\mathbf{h}}\mathbf{g}\mathbf{h}\bar{\mathbf{g}}\bar{\mathbf{h}})\eta_{\bar{a}}(\bar{\mathbf{g}}, \mathbf{h})\eta_{\bar{a}}(\bar{\mathbf{g}}\mathbf{h}, \bar{\mathbf{h}}\mathbf{g}\mathbf{h}, \bar{\mathbf{h}})}$$

$$\times \frac{U_{\bar{\mathbf{h}}\bar{\mathbf{g}}\bar{\mathbf{h}}\bar{\mathbf{h}}}(\bar{\mathbf{h}}\mathbf{g}\mathbf{h}\bar{\mathbf{a}}, \bar{\mathbf{h}}\mathbf{g}\mathbf{h}\bar{\mathbf{a}}; 0)U_{\bar{\mathbf{h}}\bar{\mathbf{g}}}(\bar{\mathbf{h}}\bar{\mathbf{a}}, \bar{\mathbf{h}}\bar{\mathbf{a}}; 0)U_{\bar{\mathbf{g}}\bar{\mathbf{h}}\bar{\mathbf{g}}\bar{\mathbf{h}}}(\bar{a}, a; 0)}{U_{\mathbf{h}}(\bar{a}, a; 0)}$$


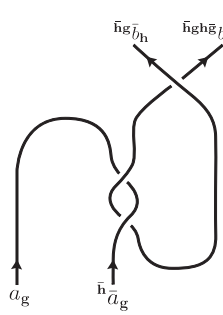
$$= Q^{-1}. \quad (164)$$

proving that $C^2 = Q^{-1}$.

D. $CS = SC$

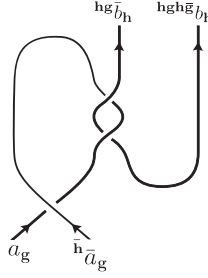
We first start by noting that

$$S(\mathbf{g}, \mathbf{h})C(\mathbf{h}, \bar{\mathbf{h}}\bar{\mathbf{g}}) = \sum_{a, b} \frac{\sqrt{d_a d_b}}{\mathcal{D}^2} R_0^{\bar{\mathbf{h}}\mathbf{g}b\mathbf{h}, \bar{\mathbf{h}}\mathbf{g}\bar{b}\mathbf{h}} \eta_b(\bar{\mathbf{h}}\bar{\mathbf{g}}, \bar{\mathbf{h}}\mathbf{g}, \bar{\mathbf{h}})}$$

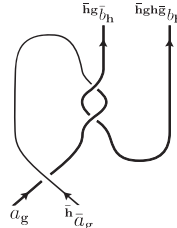
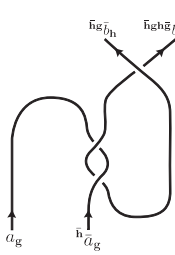
$$\times \eta_b(\bar{\mathbf{h}}\bar{\mathbf{h}}\bar{\mathbf{g}}, \bar{\mathbf{h}}\mathbf{g}\mathbf{h}, \bar{\mathbf{h}}) \frac{U_{\bar{\mathbf{h}}\bar{\mathbf{g}}\bar{\mathbf{h}}\bar{\mathbf{h}}}(\bar{\mathbf{h}}\mathbf{g}\bar{b}, \bar{\mathbf{h}}\mathbf{g}b; 0)}{U_{\mathbf{h}}(a, \bar{a}; 0)}$$


Now, we can start from the definition of $CS = C(\mathbf{g}, \mathbf{h})S(\bar{\mathbf{h}}\bar{\mathbf{g}}, \bar{\mathbf{h}}\mathbf{g}, \bar{\mathbf{h}})$ and show that after sliding some appropriate lines over and under vertices, we get an expression that

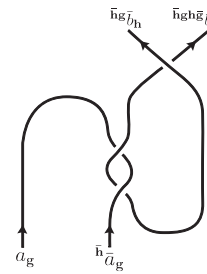
is equivalent to SC .

$$C(g, h)S(\bar{h}\bar{g}, \bar{h}g\bar{h}) = \sum_{a,b} \frac{\sqrt{d_a d_b}}{\mathcal{D}^2} R_0^{\bar{h}a_g \bar{h}a_g} \times \eta_a(\mathbf{h}, \bar{h}\bar{g})\eta_a(\bar{g}\mathbf{h}, \bar{h}g\bar{h}) \quad (165)$$


We can manipulate the diagram in Eq.(165), as laid out in the FIG. 14 of Appendix-C , and note that

$$\begin{aligned} & \text{Diagram} = \frac{R_0^{\bar{h}g\bar{h}h, \bar{h}g\bar{h}h}}{R_0^{\bar{h}a_g \bar{h}a_g}} \frac{\eta_a(\bar{h}\bar{g}, \bar{h}g\bar{h})}{\eta_a(\mathbf{h}, \bar{h}\bar{g})\eta_{\bar{h}g\bar{h}a}(\bar{h}g\mathbf{h}, \bar{h}g\bar{h})} \\ & \times \frac{\eta_b(\bar{h}\bar{g}, \bar{h}g)\eta_{\bar{h}g\bar{h}b}(\bar{h}g\bar{h}, \bar{h}g\mathbf{g})}{\eta_{\bar{h}g\bar{h}b}(\bar{h}g, \bar{h}g\bar{h})} \frac{U_{\bar{h}g\bar{h}g}(\bar{h}g\bar{h}, \bar{h}g\bar{h}; 0)}{U_{\mathbf{h}}(a, \bar{a}; 0)} \text{Diagram} \end{aligned} \quad (166)$$



Substituting the diagram obtained in Eq.(166) into Eq.(165), we get

$$C(g, h)S(\bar{h}\bar{g}, \bar{h}g\bar{h}) = \sum_{a,b} \frac{\sqrt{d_a d_b}}{\mathcal{D}} R_0^{\bar{h}g\bar{h}h, \bar{h}g\bar{h}h} \frac{\eta_a(\bar{g}\mathbf{h}, \bar{h}g\bar{h})\eta_a(\bar{h}\bar{g}, \bar{h}g\bar{h})}{\eta_{\bar{h}g\bar{h}a}(\bar{h}g\mathbf{h}, \bar{h}g\bar{h})} \times \frac{\eta_{\bar{h}g\bar{h}b}(\bar{h}g\bar{h}, \bar{h}g\mathbf{g})}{\eta_{\bar{h}g\bar{h}b}(\bar{h}g, \bar{h}g\bar{h})} \frac{U_{\bar{h}g\bar{h}g}(\bar{h}g\bar{h}, \bar{h}g\bar{h}; 0)}{U_{\mathbf{h}}(a, \bar{a}; 0)} \text{Diagram} \quad (167)$$


Using Eq.(106), we see that $\eta_{\bar{h}g\bar{h}a}(\bar{h}g\mathbf{h}, \bar{h}g\bar{h}) = \eta_a(\bar{g}\mathbf{h}, \bar{h}g\bar{h})\eta_a(\bar{h}\bar{g}, \bar{h}g\bar{h})$ and $\frac{\eta_{\bar{h}g\bar{h}b}(\bar{h}g\bar{h}, \bar{h}g\mathbf{g})}{\eta_{\bar{h}g\bar{h}b}(\bar{h}g, \bar{h}g\bar{h})} = \eta_b(\bar{h}\bar{g}, \bar{h}g\bar{h})\eta_b(\bar{h}\bar{h}\bar{g}, \bar{h}g\mathbf{g})$. Using these relations, it follows that

$$C(\mathbf{g}, \mathbf{h})S(\bar{\mathbf{h}}\bar{\mathbf{g}}, \bar{\mathbf{h}}\mathbf{g}\bar{\mathbf{h}}) = \sum_{a,b} \frac{\sqrt{d_a d_b}}{\mathcal{D}} R_0^{\bar{\mathbf{h}}\mathbf{g}\bar{\mathbf{h}}\bar{\mathbf{h}}\bar{\mathbf{g}}\bar{\mathbf{h}}} \eta_b(\bar{\mathbf{h}}\bar{\mathbf{g}}, \bar{\mathbf{h}}\mathbf{g}\bar{\mathbf{h}}) \eta_b(\bar{\mathbf{h}}\bar{\mathbf{h}}\bar{\mathbf{g}}, \bar{\mathbf{h}}\mathbf{g}\bar{\mathbf{h}}) \times \frac{U_{\bar{\mathbf{h}}\mathbf{g}\bar{\mathbf{h}}\bar{\mathbf{g}}}(\bar{\mathbf{h}}\bar{\mathbf{g}}\bar{\mathbf{h}}, \bar{\mathbf{h}}\mathbf{g}\bar{\mathbf{h}}; 0)}{U_{\mathbf{h}}(a, \bar{a}; 0)} = S(\mathbf{g}, \mathbf{h})C(\mathbf{h}, \bar{\mathbf{h}}\bar{\mathbf{g}})$$

This concludes the proof of commutativity of C with S .

E. $CT = TC$

From the definition of given in Eqs. (147) and (148), we first note that

$$T(\mathbf{g}, \mathbf{h})C(\mathbf{g}, \mathbf{gh}) = \sum_a R_0^{\bar{\mathbf{h}}\mathbf{a}\bar{\mathbf{h}}\bar{\mathbf{a}}\bar{\mathbf{h}}} \eta_a(\mathbf{g}, \mathbf{h}) \eta_a(\mathbf{gh}, \bar{\mathbf{h}}\bar{\mathbf{g}}) \eta_a(\mathbf{h}, \bar{\mathbf{h}}\bar{\mathbf{h}}\bar{\mathbf{g}}) U_{\bar{\mathbf{h}}\bar{\mathbf{h}}\bar{\mathbf{g}}}(\bar{\mathbf{h}}\bar{a}, \bar{\mathbf{h}}a; 0)$$

$$= \sum_a R_0^{\bar{\mathbf{h}}\mathbf{a}\bar{\mathbf{h}}\bar{\mathbf{a}}\bar{\mathbf{h}}} \eta_a(\mathbf{g}, \mathbf{h}) \eta_a(\mathbf{gh}, \bar{\mathbf{h}}\bar{\mathbf{g}}) \eta_a(\mathbf{h}, \bar{\mathbf{h}}\bar{\mathbf{h}}\bar{\mathbf{g}}) U_{\bar{\mathbf{h}}\bar{\mathbf{h}}\bar{\mathbf{g}}}(\bar{\mathbf{h}}\bar{a}, \bar{\mathbf{h}}a; 0) \theta_{a_g}$$
(168)

We begin the proof by simplifying CT , and showing that it equals TC .

$$C(\mathbf{g}, \mathbf{h})T(\bar{\mathbf{h}}\bar{\mathbf{g}}, \bar{\mathbf{h}}\mathbf{g}\bar{\mathbf{h}}) = \sum_a R_0^{\bar{\mathbf{h}}\mathbf{a}\bar{\mathbf{h}}\bar{\mathbf{a}}\bar{\mathbf{h}}} \eta_a(\mathbf{h}, \bar{\mathbf{h}}\bar{\mathbf{g}}) \eta_a(\bar{\mathbf{g}}\mathbf{h}, \bar{\mathbf{h}}\mathbf{g}\bar{\mathbf{h}}) U_{\bar{\mathbf{h}}\bar{\mathbf{h}}\bar{\mathbf{g}}}(\bar{\mathbf{h}}\bar{a}_g, \bar{\mathbf{h}}a_g; 0) \eta_{\bar{\mathbf{h}}\bar{a}}(\bar{\mathbf{h}}\bar{\mathbf{g}}, \bar{\mathbf{h}}\mathbf{g}\bar{\mathbf{h}})$$

$$= \sum_a R_0^{\bar{\mathbf{h}}\mathbf{a}\bar{\mathbf{h}}\bar{\mathbf{a}}\bar{\mathbf{h}}} \eta_a(\mathbf{h}, \bar{\mathbf{h}}\bar{\mathbf{g}}) \eta_a(\bar{\mathbf{g}}\mathbf{h}, \bar{\mathbf{h}}\mathbf{g}\bar{\mathbf{h}}) U_{\bar{\mathbf{h}}\bar{\mathbf{h}}\bar{\mathbf{g}}}(\bar{\mathbf{h}}\bar{a}_g, \bar{\mathbf{h}}a_g; 0) \eta_{\bar{\mathbf{h}}\bar{a}}(\bar{\mathbf{h}}\bar{\mathbf{g}}, \bar{\mathbf{h}}\mathbf{g}\bar{\mathbf{h}}) \theta_{\bar{\mathbf{h}}\bar{a}_g}$$
(169)

We first note that $\theta_{\bar{\mathbf{h}}\bar{a}} = \frac{\eta_a(\mathbf{g}, \mathbf{h})\theta_a}{U_{\bar{\mathbf{h}}\bar{\mathbf{g}}}(\bar{\mathbf{h}}\bar{a}, \bar{\mathbf{h}}a; 0)\eta_a(\mathbf{h}, \bar{\mathbf{h}}\bar{\mathbf{g}})\eta_{\bar{\mathbf{h}}\bar{a}}(\bar{\mathbf{h}}\bar{\mathbf{g}}, \bar{\mathbf{h}}\mathbf{g}\bar{\mathbf{h}})}$. Furthermore, using Eq. (112), the algebraic expression inside the sum can be simplified as follows (ignoring $R_0^{\bar{\mathbf{h}}\mathbf{a}\bar{\mathbf{h}}\bar{\mathbf{a}}\bar{\mathbf{h}}}$,

as it is the same in both expressions SC and CS)

$$\begin{aligned} & \eta_a(\mathbf{h}, \bar{\mathbf{h}} \bar{\mathbf{g}}) \eta_a(\bar{\mathbf{g}} \mathbf{h}, \bar{\mathbf{h}} \mathbf{g} \bar{\mathbf{h}}) U_{\bar{\mathbf{h}} \mathbf{g} \bar{\mathbf{h}}}(\bar{\mathbf{h}} \bar{a}_{\mathbf{g}}, \bar{\mathbf{h}} a_{\mathbf{g}}; 0) \eta_{\bar{\mathbf{h}} \bar{a}}(\bar{\mathbf{h}} \bar{\mathbf{g}}, \bar{\mathbf{h}} \mathbf{g} \bar{\mathbf{h}}) \theta_{\bar{\mathbf{h}} \bar{a}_{\mathbf{g}}} \\ &= \eta_a(\mathbf{h}, \bar{\mathbf{h}} \bar{\mathbf{g}}) \eta_a(\bar{\mathbf{g}} \mathbf{h}, \bar{\mathbf{h}} \mathbf{g} \bar{\mathbf{h}}) U_{\bar{\mathbf{h}} \mathbf{g} \bar{\mathbf{h}}}(\bar{\mathbf{h}} \bar{a}_{\mathbf{g}}, \bar{\mathbf{h}} a_{\mathbf{g}}; 0) \eta_{\bar{\mathbf{h}} \bar{a}}(\bar{\mathbf{h}} \bar{\mathbf{g}}, \bar{\mathbf{h}} \mathbf{g} \bar{\mathbf{h}}) \frac{\eta_a(\mathbf{g}, \mathbf{h}) \theta_a}{U_{\bar{\mathbf{h}} \mathbf{g}}(\bar{\mathbf{h}} \bar{a}, \bar{\mathbf{h}} a; 0) \eta_{\bar{\mathbf{h}} \bar{a}}(\bar{\mathbf{h}} \bar{\mathbf{g}}, \bar{\mathbf{h}} \mathbf{g})}. \end{aligned} \quad (170)$$

We also acknowledge that Eqs. (120) and (121) imply the following relations

$$\begin{aligned} U_{\bar{\mathbf{h}} \mathbf{g} \bar{\mathbf{h}}}(\bar{\mathbf{h}} \bar{a}, \bar{\mathbf{h}} a; 0) &= \frac{U_{\bar{\mathbf{h}} \mathbf{g} \bar{\mathbf{h}}}(\bar{\mathbf{h}} \mathbf{g} \bar{a}, \bar{\mathbf{h}} \mathbf{g} \bar{a}; 0)^{-1}}{\eta_{\bar{\mathbf{h}} \mathbf{g} \bar{a}}(\bar{\mathbf{h}} \mathbf{g} \bar{\mathbf{h}}, \bar{\mathbf{h}} \mathbf{g} \bar{\mathbf{h}}) \eta_{\bar{\mathbf{h}} \mathbf{g} \bar{a}}(\bar{\mathbf{h}} \mathbf{g} \bar{\mathbf{h}}, \bar{\mathbf{h}} \mathbf{g} \bar{\mathbf{h}})} \\ \frac{U_{\bar{\mathbf{h}} \bar{\mathbf{g}}}(\bar{\mathbf{h}} \bar{a}, \bar{\mathbf{h}} a; 0)}{U_{\bar{\mathbf{h}} \bar{\mathbf{h}} \bar{\mathbf{g}}}(\bar{\mathbf{h}} \bar{a}, \bar{\mathbf{h}} a; 0) U_{\bar{\mathbf{h}} \mathbf{g} \bar{\mathbf{h}}}(\bar{\mathbf{h}} \mathbf{g} \bar{a}, \bar{\mathbf{h}} \mathbf{g} \bar{a}; 0)} &= \eta_{\bar{\mathbf{h}} \bar{a}}(\bar{\mathbf{h}} \bar{\mathbf{h}} \bar{\mathbf{g}}, \bar{\mathbf{h}} \mathbf{g} \bar{\mathbf{h}}) \eta_{\bar{\mathbf{h}} a}(\bar{\mathbf{h}} \bar{\mathbf{h}} \bar{\mathbf{g}}, \bar{\mathbf{h}} \mathbf{g} \bar{\mathbf{h}}). \end{aligned}$$

Using the two equations, we see that

$$U_{\bar{\mathbf{h}} \mathbf{g} \bar{\mathbf{h}}}(\bar{\mathbf{h}} \bar{a}, \bar{\mathbf{h}} a; 0) = \frac{\eta_{\bar{\mathbf{h}} \bar{a}}(\bar{\mathbf{h}} \bar{\mathbf{h}} \bar{\mathbf{g}}, \bar{\mathbf{h}} \mathbf{g} \bar{\mathbf{h}}) \eta_{\bar{\mathbf{h}} a}(\bar{\mathbf{h}} \bar{\mathbf{h}} \bar{\mathbf{g}}, \bar{\mathbf{h}} \mathbf{g} \bar{\mathbf{h}})}{\eta_{\bar{\mathbf{h}} \mathbf{g} \bar{a}}(\bar{\mathbf{h}} \mathbf{g} \bar{\mathbf{h}}, \bar{\mathbf{h}} \mathbf{g} \bar{\mathbf{h}}) \eta_{\bar{\mathbf{h}} \mathbf{g} \bar{a}}(\bar{\mathbf{h}} \mathbf{g} \bar{\mathbf{h}}, \bar{\mathbf{h}} \mathbf{g} \bar{\mathbf{h}})} \frac{U_{\bar{\mathbf{h}} \bar{\mathbf{h}} \bar{\mathbf{g}}}(\bar{\mathbf{h}} \bar{a}, \bar{\mathbf{h}} a; 0)}{U_{\bar{\mathbf{h}} \bar{\mathbf{g}}}(\bar{\mathbf{h}} \bar{a}, \bar{\mathbf{h}} a; 0)}. \quad (171)$$

Substituting Eq. (171) in the right hand side of Eq. (170), we see that the original algebraic expression in Eq. (169) reduces to

$$\begin{aligned} & \eta_a(\mathbf{h}, \bar{\mathbf{h}} \bar{\mathbf{g}}) \eta_a(\bar{\mathbf{g}} \mathbf{h}, \bar{\mathbf{h}} \mathbf{g} \bar{\mathbf{h}}) U_{\bar{\mathbf{h}} \mathbf{g} \bar{\mathbf{h}}}(\bar{\mathbf{h}} \bar{a}_{\mathbf{g}}, \bar{\mathbf{h}} a_{\mathbf{g}}; 0) \eta_{\bar{\mathbf{h}} \bar{a}}(\bar{\mathbf{h}} \bar{\mathbf{g}}, \bar{\mathbf{h}} \mathbf{g} \bar{\mathbf{h}}) \theta_{\bar{\mathbf{h}} \bar{a}_{\mathbf{g}}} \\ &= \eta_a(\mathbf{h}, \bar{\mathbf{h}} \bar{\mathbf{g}}) \eta_a(\bar{\mathbf{g}} \mathbf{h}, \bar{\mathbf{h}} \mathbf{g} \bar{\mathbf{h}}) \eta_{\bar{\mathbf{h}} a}(\bar{\mathbf{h}} \mathbf{g}, \bar{\mathbf{h}} \bar{\mathbf{g}}) \frac{\eta_a(\mathbf{g}, \mathbf{h}) \eta_{\bar{\mathbf{h}} a}(\bar{\mathbf{h}} \bar{\mathbf{h}} \bar{\mathbf{g}}, \bar{\mathbf{h}} \mathbf{g} \bar{\mathbf{h}})}{\eta_a(\mathbf{h}, \bar{\mathbf{h}} \bar{\mathbf{g}}) \eta_{\bar{\mathbf{h}} \mathbf{g} \bar{a}}(\bar{\mathbf{h}} \mathbf{g} \bar{\mathbf{h}}, \bar{\mathbf{h}} \mathbf{g} \bar{\mathbf{h}})} \\ &\quad \times \frac{\eta_{\bar{\mathbf{h}} \bar{a}}(\bar{\mathbf{h}} \bar{\mathbf{h}} \bar{\mathbf{g}}, \bar{\mathbf{h}} \mathbf{g} \bar{\mathbf{h}})}{\eta_{\bar{\mathbf{h}} \mathbf{g} \bar{a}}(\bar{\mathbf{h}} \mathbf{g} \bar{\mathbf{h}}, \bar{\mathbf{h}} \mathbf{g} \bar{\mathbf{h}})} \eta_{\bar{\mathbf{h}} \bar{a}}(\bar{\mathbf{h}} \bar{\mathbf{g}}, \bar{\mathbf{h}} \mathbf{g} \bar{\mathbf{h}}) U_{\bar{\mathbf{h}} \bar{\mathbf{h}} \bar{\mathbf{g}}}(\bar{\mathbf{h}} \bar{a}, \bar{\mathbf{h}} a; 0) \theta_a \end{aligned} \quad (172)$$

Now that we rewrote $\theta_{\bar{\mathbf{h}} \bar{a}_{\mathbf{g}}}$ in terms of θ_a , we can simplify many of the η terms in the expression above, using Eq. (106). First, we simplify η -terms containing the label

\bar{a}

$$\frac{\eta_{\bar{\mathbf{h}} \bar{a}}(\bar{\mathbf{h}} \bar{\mathbf{h}} \bar{\mathbf{g}}, \bar{\mathbf{h}} \mathbf{g} \bar{\mathbf{h}}) \eta_{\bar{\mathbf{h}} \bar{a}}(\bar{\mathbf{h}} \bar{\mathbf{g}}, \bar{\mathbf{h}} \mathbf{g} \bar{\mathbf{h}})}{\eta_{\bar{\mathbf{h}} \mathbf{g} \bar{a}}(\bar{\mathbf{h}} \mathbf{g} \bar{\mathbf{h}}, \bar{\mathbf{h}} \mathbf{g} \bar{\mathbf{h}})} = \frac{\left(\frac{\eta_{\bar{a}}(\mathbf{h}, \bar{\mathbf{h}} \bar{\mathbf{g}}) \eta_{\bar{a}}(\bar{\mathbf{g}} \mathbf{h}, \bar{\mathbf{h}} \mathbf{g} \bar{\mathbf{h}})}{\eta_{\bar{a}}(\mathbf{h}, \bar{\mathbf{h}} \bar{\mathbf{g}})} \right) \left(\frac{\eta_{\bar{a}}(\mathbf{h}, \bar{\mathbf{h}} \bar{\mathbf{h}} \bar{\mathbf{g}}) \eta_{\bar{a}}(\bar{\mathbf{h}} \bar{\mathbf{g}}, \bar{\mathbf{h}} \mathbf{g} \bar{\mathbf{h}})}{\eta_{\bar{a}}(\mathbf{h}, \bar{\mathbf{h}} \bar{\mathbf{g}})} \right)}{\left(\eta_{\bar{a}}(\bar{\mathbf{h}} \bar{\mathbf{g}}, \bar{\mathbf{h}} \mathbf{g} \bar{\mathbf{h}}) \eta_{\bar{a}}(\bar{\mathbf{g}} \mathbf{h}, \bar{\mathbf{h}} \mathbf{g} \bar{\mathbf{h}}) \right)} = 1.$$

Then, we can simplify the η -terms with the label a

$$\begin{aligned}
& \frac{\eta_a(\mathbf{h}, \bar{\mathbf{h}} \bar{\mathbf{g}}) \eta_a(\bar{\mathbf{g}} \mathbf{h}, \bar{\mathbf{h}} \mathbf{g} \bar{\mathbf{h}}) \eta_{\bar{h}_a}(\bar{\mathbf{h}} \bar{\mathbf{h}} \bar{\mathbf{g}}, \bar{\mathbf{h}} \mathbf{g} \mathbf{h}) \eta_{\bar{h}_a}(\bar{\mathbf{h}} \mathbf{g}, \bar{\mathbf{h}} \bar{\mathbf{g}}) \eta_a(\mathbf{g}, \mathbf{h})}{\eta_a(\mathbf{h}, \bar{\mathbf{h}} \mathbf{g}) \eta_{\bar{h}_a}(\bar{\mathbf{h}} \mathbf{g} \mathbf{h}, \bar{\mathbf{h}} \mathbf{g} \bar{\mathbf{h}})} \\
&= \frac{\eta_a(\mathbf{h}, \bar{\mathbf{h}} \bar{\mathbf{g}}) \eta_a(\bar{\mathbf{g}} \mathbf{h}, \bar{\mathbf{h}} \mathbf{g} \bar{\mathbf{h}}) \left(\frac{\eta_a(\mathbf{h}, \bar{\mathbf{h}} \bar{\mathbf{g}}) \eta_a(\bar{\mathbf{h}} \bar{\mathbf{g}}, \bar{\mathbf{h}} \mathbf{g} \bar{\mathbf{h}})}{\eta_a(\mathbf{h}, \bar{\mathbf{h}} \bar{\mathbf{g}})} \right) \left(\eta_a(\mathbf{h}, \bar{\mathbf{h}} \mathbf{g}) \eta_a(\mathbf{g} \mathbf{h}, \bar{\mathbf{h}} \bar{\mathbf{g}}) \right) \eta_a(\mathbf{g}, \mathbf{h})}{\eta_a(\mathbf{h}, \bar{\mathbf{h}} \mathbf{g}) \left(\eta_a(\bar{\mathbf{h}} \bar{\mathbf{g}}, \bar{\mathbf{h}} \mathbf{g} \mathbf{h}) \eta_a(\bar{\mathbf{g}} \mathbf{h}, \bar{\mathbf{h}} \mathbf{g} \bar{\mathbf{h}}) \right)} \\
&= \eta_a(\mathbf{g}, \mathbf{h}) \eta_a(\mathbf{h}, \bar{\mathbf{h}} \bar{\mathbf{h}} \bar{\mathbf{g}}) \eta_a(\mathbf{g} \mathbf{h}, \bar{\mathbf{h}} \bar{\mathbf{g}}) \quad (173)
\end{aligned}$$

We see that the U -term obtained in Eq. (172) is the same as the U -term in Eq. (168).

Using the results of Eq. (173), we have our desired relation

$$\begin{aligned}
C(\mathbf{g}, \mathbf{h}) T(\bar{\mathbf{h}} \bar{\mathbf{g}}, \bar{\mathbf{h}} \mathbf{g} \bar{\mathbf{h}}) &= \sum_a R_0^{\bar{h}_a \bar{h}_g \bar{a}_g} \eta_a(\mathbf{g}, \mathbf{h}) \eta_a(\mathbf{g} \mathbf{h}, \bar{\mathbf{h}} \bar{\mathbf{g}}) \eta_a(\mathbf{h}, \bar{\mathbf{h}} \bar{\mathbf{h}} \bar{\mathbf{g}}) \\
&\times U_{\bar{h}_a \bar{h}_g}(\bar{h}_a, \bar{h}_g; 0) \theta_{a_g} \quad \begin{array}{c} \nearrow^{\bar{h}_g \bar{h}_g} \\ \searrow_{\bar{h}_g \bar{h}_g} \\ \nearrow_{a_g} \\ \searrow^{\bar{h}_g \bar{h}_g} \end{array} = T(\mathbf{g}, \mathbf{h}) C(\mathbf{g}, \mathbf{g} \mathbf{h}) \quad (174)
\end{aligned}$$

F. $S^2 = C$

We emphasize that $S^2 = C$ implies that $S^\dagger = S^{-1}$, given that we have already shown that $S = CS^\dagger$ in subsection B.. This implies that S is unitary and so $\mathcal{C}^{\times G}$ is modular on higher genus surfaces. However, as we will demonstrate shortly, in order to show that $S^2 = C$, we must require that \mathcal{C}_0 is modular. Therefore, our analysis implies that modularity of the underlying UMTC \mathcal{C}_0 , implies G-crossed modularity of $\mathcal{C}^{\times G}$. In the earlier derivations, we manipulated the diagram to be able to sum over the middle loop and use the Ribbon property due to presence of twist terms θ in the sum. However, we do not have any twist terms in the expression S^2 , so we must employ a different strategy. We restate relevant identities that will be used for the proof. From

the MTC Verlinde formula, Eqs. (125) and (126), we have

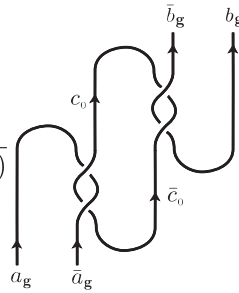
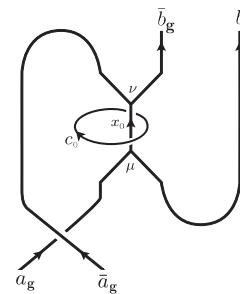
$$\sum_{c \in \mathcal{C}_0} \frac{d_c}{\mathcal{D}} \text{loop}_{c_0} = \sum_{c \in \mathcal{C}_0} \frac{S_{c_0 x_0}}{S_{0 x_0}} S_{c_0} S_{00}^* \left| \begin{array}{c} \uparrow x_0 \\ \downarrow x_0 \end{array} \right. = \delta_{x_0} \left| \begin{array}{c} \uparrow x_0 \\ \downarrow x_0 \end{array} \right.$$

We start the proof by assuming the modularity of $\mathbf{S}(\mathbf{0}, \mathbf{0})$, and showing that $\mathbf{S}(\mathbf{g}, \mathbf{0})\mathbf{S}(\mathbf{0}, \bar{\mathbf{g}}) = \mathbf{C}(\mathbf{g}, \mathbf{0})$. Then, using the fact that $\mathbf{S} = \mathbf{C}\mathbf{S}^\dagger$, we see that this implies the modularity of $\mathbf{S}(\mathbf{g}, \mathbf{0})$, i.e. $\mathbf{S}^{-1}(\mathbf{g}, \mathbf{0}) = \mathbf{S}^\dagger(\mathbf{g}, \mathbf{0})$. We can then use a similar identity for the sum of the ω_a -loop on the $(\mathbf{g}, \mathbf{0})$ sector, i.e.

$$\sum_{c \in \mathcal{C}_h} \frac{d_c}{\mathcal{D}} \text{loop}_{c_h} = \sum_{c \in \mathcal{C}_h} \frac{S_{c_h x_0}}{S_{0 x_0}} S_{c_0} S_{00}^* \left| \begin{array}{c} \uparrow x_0 \\ \downarrow x_0 \end{array} \right. = \delta_{x_0} \left| \begin{array}{c} \uparrow x_0 \\ \downarrow x_0 \end{array} \right.$$

To show that, in general, $\mathbf{S}^2 = \mathbf{C}$.

F 1. $\mathbf{S}(\mathbf{g}, \mathbf{0})\mathbf{S}(\mathbf{0}, \bar{\mathbf{g}}) = \mathbf{C}(\mathbf{g}, \mathbf{0})$

$$\begin{aligned} \mathbf{S}(\mathbf{g}, \mathbf{0})\mathbf{S}(\mathbf{0}, \bar{\mathbf{g}}) &= \sum_{\substack{a, b \in \mathcal{C}_g; \\ c \in \mathcal{C}_0}} \frac{\sqrt{d_a d_b}}{\mathcal{D}^2} d_c \frac{1}{U_{\bar{\mathbf{g}}}(c, \bar{c}; 0)} \text{diagram}_1 \\ &= \sum_{a, b} \frac{\sqrt{d_a d_b}}{\mathcal{D}^2} R_0^{a_g \bar{a}_g} \sum_{\substack{c, x \in \mathcal{C}_0; \\ \nu}} d_c \sqrt{\frac{d_x}{d_a d_b}} \text{diagram}_2 \end{aligned} \quad (175)$$



Using the modularity properties above, the sum over c results in a kronecker delta δ_{x0} , and so the expression simplifies to

$$= \sum_{a \in \mathcal{C}_{\mathbf{g}}} R_0^{a_{\mathbf{g}} \bar{a}_{\mathbf{g}}} \text{ (diagram) } = C(\mathbf{g}, \mathbf{0}) \quad (176)$$

Note that the last equality follows from straightening the bends on the diagram above. This results in a trivial ratio of Frobenius coefficients. The reason this factor is trivial is because we have to bend two conjugate defect lines, each of which have Frobenius factors that are conjugates (inverses) of each other.

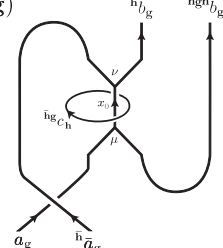
This proves our first result.

F 2. $S(\mathbf{g}, \mathbf{h})S(\mathbf{h}, \bar{\mathbf{h}} \bar{\mathbf{g}}) = C(\mathbf{g}, \mathbf{h})$

Starting with

$$S(\mathbf{g}, \mathbf{h})S(\mathbf{h}, \bar{\mathbf{h}} \bar{\mathbf{g}}) = \sum_{a,b,c} \frac{\sqrt{d_a d_b}}{\mathcal{D}^2} \frac{d_c}{U_{\mathbf{h}}(a, \bar{a}; 0) U_{\bar{\mathbf{h}} \bar{\mathbf{g}}}(c, \bar{c}; 0)} \text{ (diagram) } \quad (177)$$

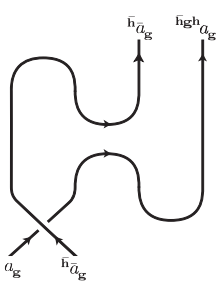
We can reduce the diagram to the following, similar to the method explained in FIG. 12 in Appendix.

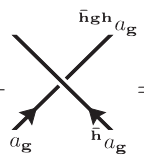
$$\begin{aligned}
&= \sum_{a,b,c} \frac{\sqrt{d_a d_b}}{\mathcal{D}^2} d_c R_0^{\bar{h} a_g \bar{h} \bar{a}_g} \frac{\eta_a(\mathbf{h}, \bar{\mathbf{h}} \bar{\mathbf{g}})}{\eta_a(\bar{\mathbf{h}} \bar{\mathbf{g}}, \bar{\mathbf{h}} \mathbf{g})} \eta_{\bar{\mathbf{h}} \mathbf{g} \mathbf{h} a}(\bar{\mathbf{h}} \mathbf{g} \mathbf{h}, \bar{\mathbf{h}} \mathbf{g} \bar{\mathbf{h}}) \eta_{\bar{c}}(\bar{\mathbf{h}} \bar{\mathbf{g}}, \bar{\mathbf{h}} \mathbf{g}) \\
&\quad \times \sum_{\substack{x \in \mathcal{C}_0; \\ \mu, \nu}} \sqrt{\frac{d_x}{d_a d_b}} \frac{[U_{\bar{\mathbf{h}} \mathbf{g} \bar{\mathbf{h}}}(\bar{h} a, \bar{h} \bar{b}; x)]_{\mu\nu}}{\eta_{\bar{\mathbf{h}} \mathbf{g} \bar{c}}(\bar{\mathbf{h}} \mathbf{g}, \bar{\mathbf{h}} \bar{\mathbf{g}})}
\end{aligned}
\tag{178}$$


Noting that $\eta_{\bar{\mathbf{h}} \mathbf{g} \bar{c}}(\bar{\mathbf{h}} \mathbf{g}, \bar{\mathbf{h}} \bar{\mathbf{g}}) = \eta_{\bar{c}}(\bar{\mathbf{g}} \mathbf{h}, \bar{\mathbf{h}} \mathbf{g}) \eta_{\bar{c}}(\mathbf{h}, \bar{\mathbf{h}} \bar{\mathbf{g}}) = \eta_{\bar{c}}(\bar{\mathbf{h}} \bar{\mathbf{g}}, \bar{\mathbf{h}} \mathbf{g})$, we see that the $\eta_{\bar{c}}$ terms cancel, and we can simply sum over c using the ω_c loop relation mentioned above, as we showed that $\mathbf{S}(\mathbf{h}, \mathbf{0})$ is modular, i.e.

$$\sum_{c \in \mathcal{C}_h} \frac{S_{c_h x_0}}{S_{0x_0}} \frac{d_c}{\mathcal{D}} = \sum_{c \in \mathcal{C}_h} \frac{S_{c_h x_0}}{S_{0x_0}} S_{c_0} S_{00}^* = \delta_{0x}
\tag{179}$$

Using these relations, and noting that $\eta_{\bar{\mathbf{h}} \mathbf{g} \mathbf{h} a}(\bar{\mathbf{h}} \mathbf{g} \mathbf{h}, \bar{\mathbf{h}} \mathbf{g} \bar{\mathbf{h}}) = \eta_a(\bar{\mathbf{h}} \bar{\mathbf{g}}, \bar{\mathbf{h}} \mathbf{g} \mathbf{h}) \eta_a(\bar{\mathbf{g}} \mathbf{h}, \bar{\mathbf{h}} \mathbf{g} \bar{\mathbf{h}})$, the expression for \mathbf{S}^2 reduces to

$$\begin{aligned}
&= \sum_{a \in \mathcal{C}_g} R_0^{\bar{h} a_g \bar{h} \bar{a}_g} \eta_a(\mathbf{h}, \bar{\mathbf{h}} \bar{\mathbf{g}}) \eta_a(\bar{\mathbf{g}} \mathbf{h}, \bar{\mathbf{h}} \mathbf{g} \bar{\mathbf{h}}) U_{\bar{\mathbf{h}} \mathbf{g} \bar{\mathbf{h}}}(\bar{h} a, \bar{h} \bar{a}; 0)
\end{aligned}$$


$$= \sum_{a \in \mathcal{C}_g} R_0^{\bar{h} a_g \bar{h} \bar{a}_g} \eta_a(\mathbf{h}, \bar{\mathbf{h}} \bar{\mathbf{g}}) \eta_a(\bar{\mathbf{g}} \mathbf{h}, \bar{\mathbf{h}} \mathbf{g} \bar{\mathbf{h}}) U_{\bar{\mathbf{h}} \mathbf{g} \bar{\mathbf{h}}}(\bar{h} a, \bar{h} \bar{a}; 0) \frac{\chi_{\bar{h} a_g}}{\chi_{\bar{\mathbf{h}} \mathbf{g} \mathbf{h} a_g}} = C(\mathbf{g}, \mathbf{h})
\tag{180}$$


Note that to get the last equality, we used the fact that $\frac{\chi_{\bar{h} a_g}}{\chi_{\bar{\mathbf{h}} \mathbf{g} \mathbf{h} a_g}} = \frac{\chi_{\bar{\mathbf{h}} \mathbf{g} \bar{\mathbf{h}} \bar{\mathbf{g}} \mathbf{h}(\bar{\mathbf{h}} \mathbf{g} \mathbf{h} a_g)}}{\chi_{\bar{\mathbf{h}} \mathbf{g} \mathbf{h} a_g}} = \frac{U_{\bar{\mathbf{h}} \mathbf{g} \bar{\mathbf{h}}}(\bar{h} \bar{a}, \bar{h} a; 0)}{U_{\bar{\mathbf{h}} \mathbf{g} \bar{\mathbf{h}}}(\bar{h} a, \bar{h} \bar{a}; 0)}$. Thus, we see that our expression reduces to $\mathbf{C}(\mathbf{g}, \mathbf{h})$ defined earlier. This concludes the proof.

X. CONCLUDING REMARKS

We shall emphasize that the most important results of our work was to show that unitarity of the topological S -matrix is not destroyed by the action of the symmetry group on the topological degrees of freedom. Further research will be done to investigate whether similar relationships hold in a context where the underlying theory is purely fermionic. This is especially interesting as systems such as fractional quantum hall (FQH) effect are built by an underlying fermionic structure (electrons), however, the additional structure imposed by magnetic fluxes and fractional occupation induces a topological anyonic phases on top of the underlying fermionic system. Even though there have been attempts in understanding the algebraic structure of FQH systems and the role of symmetries in enriching the topological phases using G -crossed MTCs [42], further research is required to understand the exotic FQH phases such as $\nu = 5/2$.

A $(ST)^3 = \Theta_0 S^2$: DETAILED DIAGRAMMATIC STEPS

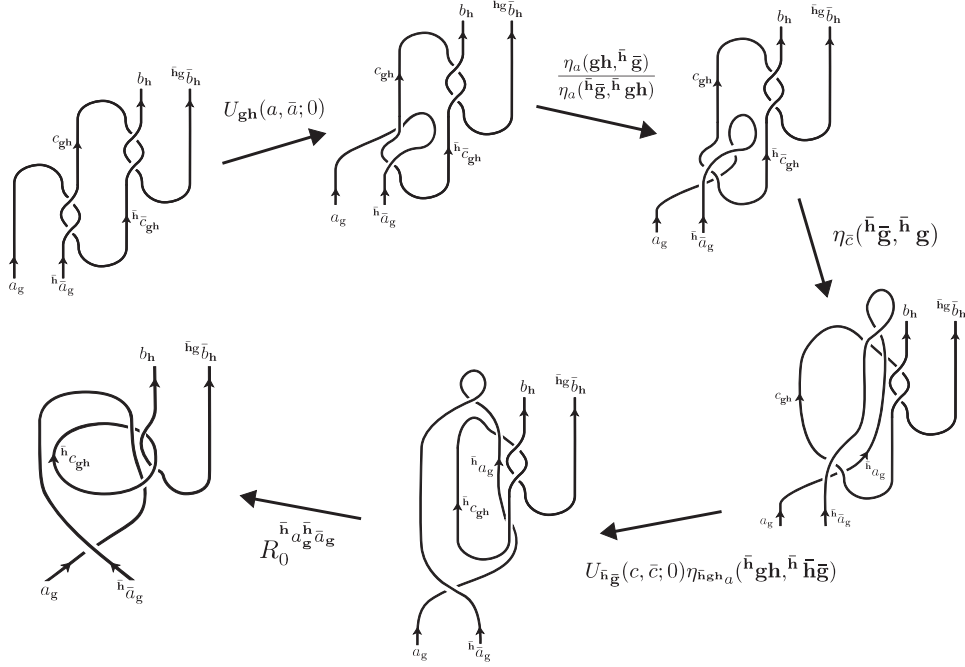


Figure 12: Diagrammatic steps in deriving equation (152) from (151)

By collecting all the terms in c in equation (152), we have

$$\begin{aligned}
 & \sum_{c \in \mathcal{C}_{\mathbf{gh}}} \theta_c d_c \frac{U_{\bar{\mathbf{h}}\bar{\mathbf{g}}}(c, \bar{c}; 0)}{U_{\mathbf{h}}(c, \bar{c}; 0)} \eta_c(\mathbf{gh}, \bar{\mathbf{h}}\bar{\mathbf{g}}) \eta_{\bar{c}}(\bar{\mathbf{h}}\bar{\mathbf{g}}, \bar{\mathbf{h}}\bar{\mathbf{g}}) \\
 & = \sum_{c \in \mathcal{C}_{\mathbf{gh}}} \theta_c d_c \frac{U_{\bar{\mathbf{h}}\bar{\mathbf{g}}}(c, \bar{c}; 0)}{U_{\mathbf{h}}(c, \bar{c}; 0)} \eta_c(\mathbf{gh}, \bar{\mathbf{h}}\bar{\mathbf{g}}) \eta_{\bar{c}}(\bar{\mathbf{h}}\bar{\mathbf{g}}, \bar{\mathbf{h}}\bar{\mathbf{g}}) \sum_{\substack{x \in \mathcal{C}_{\mathbf{gh}} \\ \nu}} \sqrt{\frac{dx}{d_a d_b}}
 \end{aligned}$$

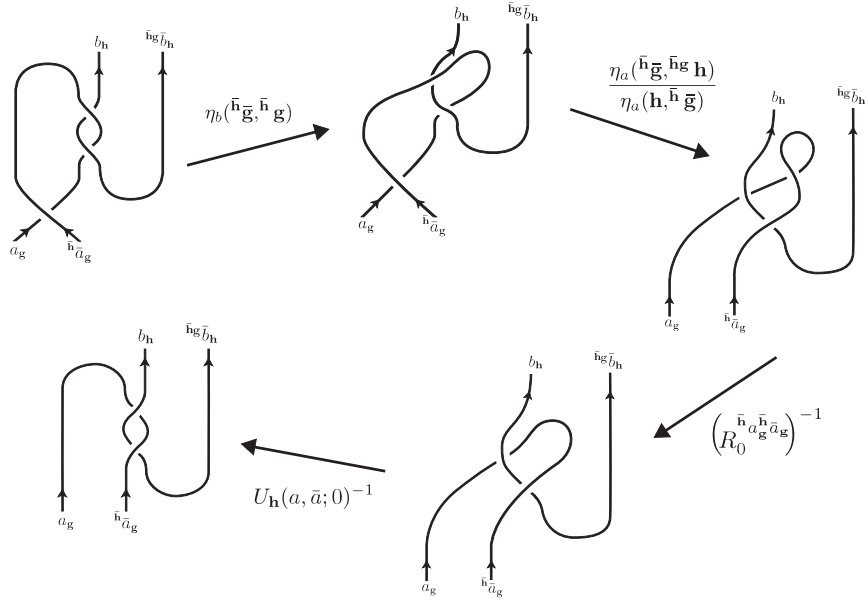


Figure 13: Diagrammatic steps in deriving equation (153) from (154)

B $S = CS^\dagger$: DETAILED DIAGRAMMATIC STEPS

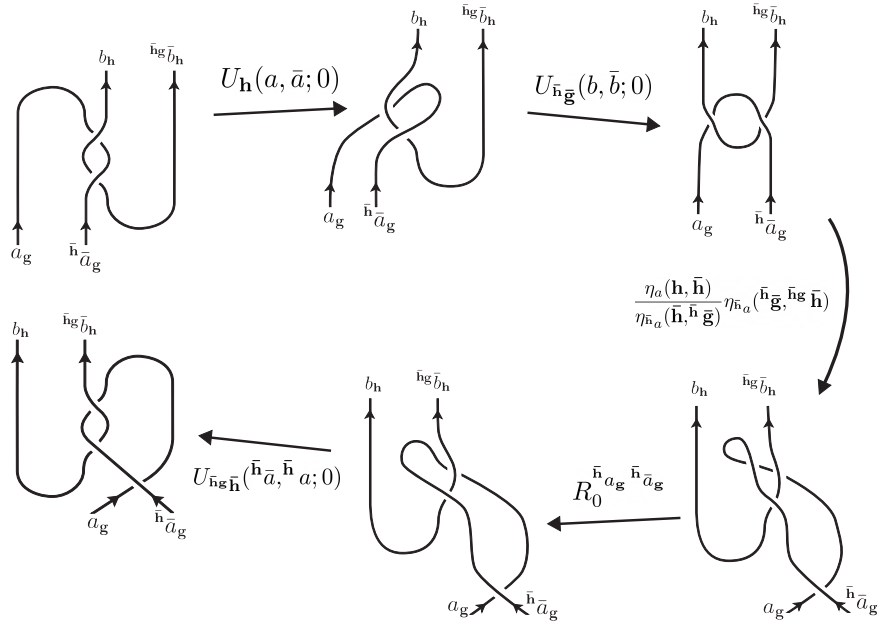


Figure 14: Diagrammatic steps in deriving equation (155)

C $CS = CS$: DETAILED DIAGRAMMATIC STEPS

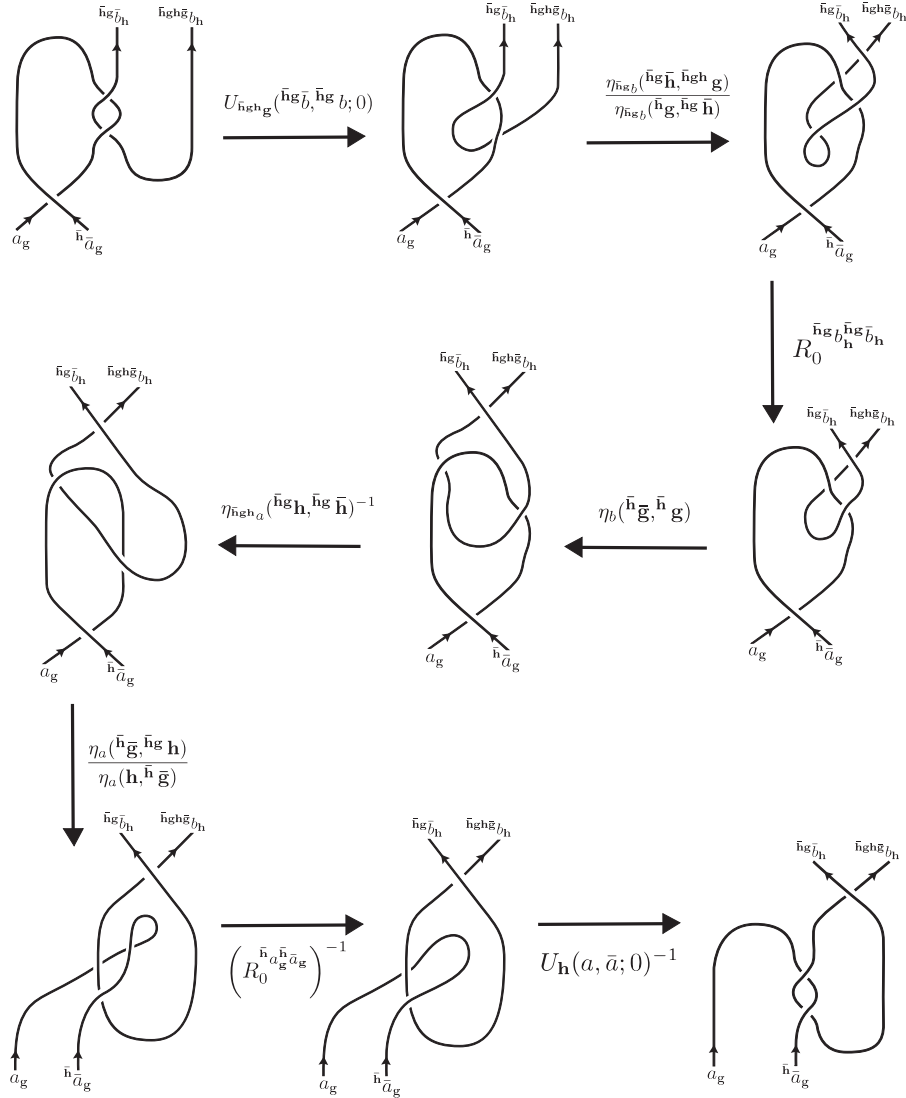


Figure 15: Diagrammatic steps in deriving equation (166) from (165).

REFERENCES

- [1] Parsa Bonderson. “Measuring topological order”. In: *Physical Review Research* 3.3 (Aug. 2021). ISSN: 2643-1564. DOI: 10.1103/physrevresearch.3.033110. URL: <http://dx.doi.org/10.1103/PhysRevResearch.3.033110>.
- [2] J. J. Sakurai and Jim Napolitano. *Modern Quantum Mechanics*. 2nd ed. Cambridge University Press, 2017. DOI: 10.1017/9781108499996.

- [3] Luigi E. Picasso, Luciano Bracci, and Emilio d’Emilio. “Perturbation Theory in Quantum Mechanics”. In: *Mathematics of Complexity and Dynamical Systems*. Ed. by Robert A. Meyers. New York, NY: Springer New York, 2011, pp. 1351–1375. ISBN: 978-1-4614-1806-1. DOI: 10.1007/978-1-4614-1806-1_85. URL: https://doi.org/10.1007/978-1-4614-1806-1_85.
- [4] Alfred Shapere and Frank Wilczek. *Geometric Phases in Physics*. World Scientific, 1989.
- [5] Y. Aharonov and D. Bohm. “Significance of Electromagnetic Potentials in the Quantum Theory”. In: *Phys. Rev.* 115 (3 Aug. 1959), pp. 485–491. DOI: 10.1103/PhysRev.115.485. URL: <https://link.aps.org/doi/10.1103/PhysRev.115.485>.
- [6] G. Herzberg and H. C. Longuet-Higgins. “Intersection of potential energy surfaces in polyatomic molecules”. In: *Discuss. Faraday Soc.* 35 (0 1963), pp. 77–82. DOI: 10.1039/DF9633500077. URL: <http://dx.doi.org/10.1039/DF9633500077>.
- [7] Ilya G. Ryabinkin, Loïc Joubert-Doriol, and Artur F. Izmaylov. “Geometric Phase Effects in Nonadiabatic Dynamics near Conical Intersection”. In: *Accounts of Chemical Research* 50.7 (2017). DOI: 10.1021/acs.accounts.7b00220. URL: <https://doi.org/10.1021/acs.accounts.7b00220>.
- [8] B. K. Kendrick. “Geometric Phase Effects in Chemical Reaction Dynamics and Molecular Spectra”. In: *The Journal of Physical Chemistry A* 107.35 (2003). DOI: 10.1021/jp021865x. URL: <https://doi.org/10.1021/jp021865x>.
- [9] J. Nakamura et al. “Direct observation of anyonic braiding statistics”. In: *Nature Physics* 16.9 (Sept. 2020), pp. 931–936. ISSN: 1745-2481. DOI: 10.1038/s41567-020-1019-1. URL: <http://dx.doi.org/10.1038/s41567-020-1019-1>.
- [10] Mikio Nakahara. *Geometry, Topology, and Physics*. Institute of Physics Publishing, 2003.
- [11] Alexander Altland and Ben D. Simons. *Condensed Matter Field Theory*. 2nd ed. Cambridge University Press, 2010. DOI: 10.1017/CB09780511789984.
- [12] Mark Srednicki. *Quantum Field Theory*. Cambridge University Press, 2007. DOI: 10.1017/CB09780511813917.

- [13] Edward Witten. “Topological Quantum Field Theory”. In: *Communications in Mathematical Physics* (1988). DOI: 10.1007/BF01223371. URL: <https://doi.org/10.1007/BF01223371>.
- [14] Edward Witten. “Quantum field theory and the Jones polynomial”. In: *Communications in Mathematical Physics* 121.3 (1989), pp. 351–399. DOI: [cmp/1104178138](https://doi.org/10.1007/BF01223371). URL: <https://doi.org/>.
- [15] B. Bakalov and A. Kirillov. “Lectures on Tensor Categories and Modular Functors”. In: *American Mathematical Society* (2001). URL: <http://theory.caltech.edu/~preskill/ph219/topological.pdf>.
- [16] John Preskill. “Lecture Notes for physics 219: Quantum Computation”. In: (2004). URL: <http://theory.caltech.edu/~preskill/ph219/topological.pdf>.
- [17] Maissam Barkeshli et al. “Symmetry fractionalization, defects, and gauging of topological phases”. In: *Physical Review B* 100.11 (Sept. 2019). ISSN: 2469-9969. DOI: 10.1103/physrevb.100.115147. URL: <http://dx.doi.org/10.1103/PhysRevB.100.115147>.
- [18] Michael V. Berry. “Quantal phase factors accompanying adiabatic changes”. In: *Proc. Roy. Soc. Lond. A* 392 (1984), pp. 45–57. DOI: 10.1098/rspa.1984.0023.
- [19] Barry Simon. “Holonomy, the Quantum Adiabatic Theorem, and Berry’s Phase”. In: *Phys. Rev. Lett.* 51 (24 Dec. 1983), pp. 2167–2170. DOI: 10.1103/PhysRevLett.51.2167. URL: <https://link.aps.org/doi/10.1103/PhysRevLett.51.2167>.
- [20] Frank Wilczek and A. Zee. “Appearance of Gauge Structure in Simple Dynamical Systems”. In: *Phys. Rev. Lett.* 52 (24 June 1984), pp. 2111–2114. DOI: 10.1103/PhysRevLett.52.2111. URL: <https://link.aps.org/doi/10.1103/PhysRevLett.52.2111>.
- [21] John Von-Neumann and P. Eugene Wigner. In: *Phys. Z* 30 (1929), pp. 467–70.
- [22] C. Alden Mead and Donald G. Truhlar. “On the determination of Born–Oppenheimer nuclear motion wave functions including complications due to conical intersections and identical nuclei”. In: *The Journal of Chemical Physics* 70.5 (1979), pp. 2284–2296. DOI: 10.1063/1.437734. eprint: <https://doi.org/10.1063/1.437734>. URL: <https://doi.org/10.1063/1.437734>.

- [23] Yingyue Hong et al. “Exclusive Neural Network Representation of the Quasi-Diabatic Hamiltonians Including Conical Intersections”. In: *The Journal of Physical Chemistry Letters* 11.18 (2020). PMID: 32835486, pp. 7552–7558. DOI: 10.1021/acs.jpcllett.0c02173. eprint: <https://doi.org/10.1021/acs.jpcllett.0c02173>. URL: <https://doi.org/10.1021/acs.jpcllett.0c02173>.
- [24] Spiridoula Matsika and David R. Yarkony. “Spin–Orbit Coupling and Conical Intersections. IV. A Perturbative Determination of the Electronic Energies, Derivative Couplings, and a Rigorous Diabatic Representation near a Conical Intersection. The General Case†”. In: *The Journal of Physical Chemistry B* 106.33 (2002), pp. 8108–8116. DOI: 10.1021/jp020396w. eprint: <https://doi.org/10.1021/jp020396w>. URL: <https://doi.org/10.1021/jp020396w>.
- [25] Ming-Che Chang and Qian Niu. “Berry phase, hyperorbits, and the Hofstadter spectrum: Semiclassical dynamics in magnetic Bloch bands”. In: *Phys. Rev. B* 53 (11 Mar. 1996), pp. 7010–7023. DOI: 10.1103/PhysRevB.53.7010. URL: <https://link.aps.org/doi/10.1103/PhysRevB.53.7010>.
- [26] J.M. Ziman. “Electrons and phonons: the theory of transport phenomena in solids”. In: (2001).
- [27] Lukasz Fidkowski, T. S. Jackson, and Israel Klich. “Model Characterization of Gapless Edge Modes of Topological Insulators Using Intermediate Brillouin-Zone Functions”. In: *Physical Review Letters* 107.3 (July 2011). ISSN: 1079-7114. DOI: 10.1103/physrevlett.107.036601. URL: <http://dx.doi.org/10.1103/PhysRevLett.107.036601>.
- [28] Liang Fu and C. L. Kane. “Topological insulators with inversion symmetry”. In: *Phys. Rev. B* 76 (4 July 2007), p. 045302. DOI: 10.1103/PhysRevB.76.045302. URL: <https://link.aps.org/doi/10.1103/PhysRevB.76.045302>.
- [29] Andreas P. Schnyder et al. “Classification of topological insulators and superconductors in three spatial dimensions”. In: *Physical Review B* 78.19 (Nov. 2008). ISSN: 1550-235X. DOI: 10.1103/physrevb.78.195125. URL: <http://dx.doi.org/10.1103/PhysRevB.78.195125>.
- [30] Subir Sachdev. *Quantum Phase Transitions*. 2nd ed. Cambridge University Press, 2011. DOI: 10.1017/CB09780511973765.

- [31] Xiao-Gang Wen. “Topological Order: From Long-Range Entangled Quantum Matter to a Unified Origin of Light and Electrons”. In: *ISRN Condensed Matter Physics* 2013 (Mar. 2013), pp. 1–20. ISSN: 2090-7400. DOI: 10.1155/2013/198710. URL: <http://dx.doi.org/10.1155/2013/198710>.
- [32] Alexei Kitaev. “Anyons in an exactly solved model and beyond”. In: *Annals of Physics* 321.1 (Jan. 2006), pp. 2–111. ISSN: 0003-4916. DOI: 10.1016/j.aop.2005.10.005. URL: <http://dx.doi.org/10.1016/j.aop.2005.10.005>.
- [33] D. C. Tsui, H. L. Stormer, and A. C. Gossard. “Two-Dimensional Magnetotransport in the Extreme Quantum Limit”. In: *Phys. Rev. Lett.* 48 (22 May 1982), pp. 1559–1562. DOI: 10.1103/PhysRevLett.48.1559. URL: <https://link.aps.org/doi/10.1103/PhysRevLett.48.1559>.
- [34] Horst L. Stormer. “Nobel Lecture: The fractional quantum Hall effect”. In: *Rev. Mod. Phys.* 71 (4 July 1999), pp. 875–889. DOI: 10.1103/RevModPhys.71.875. URL: <https://link.aps.org/doi/10.1103/RevModPhys.71.875>.
- [35] David Tong. *Lectures on the Quantum Hall Effect*. 2016. arXiv: 1606.06687 [hep-th].
- [36] Parsa Bonderson, Victor Gurarie, and Chetan Nayak. “Plasma analogy and non-Abelian statistics for Ising-type quantum Hall states”. In: *Phys. Rev. B* 83 (7 Feb. 2011), p. 075303. DOI: 10.1103/PhysRevB.83.075303. URL: <https://link.aps.org/doi/10.1103/PhysRevB.83.075303>.
- [37] Chetan Nayak et al. “Non-Abelian anyons and topological quantum computation”. In: *Reviews of Modern Physics* 80.3 (Sept. 2008), pp. 1083–1159. ISSN: 1539-0756. DOI: 10.1103/revmodphys.80.1083. URL: <http://dx.doi.org/10.1103/RevModPhys.80.1083>.
- [38] J. K. Jain. “Composite-fermion approach for the fractional quantum Hall effect”. In: *Phys. Rev. Lett.* 63 (2 July 1989), pp. 199–202. DOI: 10.1103/PhysRevLett.63.199. URL: <https://link.aps.org/doi/10.1103/PhysRevLett.63.199>.
- [39] Gregory Moore and Nicholas Read. “Nonabelions in the fractional quantum hall effect”. In: *Nuclear Physics B* 360.2 (1991), pp. 362–396. ISSN: 0550-3213. DOI: [https://doi.org/10.1016/0550-3213\(91\)90160-3](https://doi.org/10.1016/0550-3213(91)90160-3).

- 1016/0550-3213(91)90407-0. URL: <https://www.sciencedirect.com/science/article/pii/0550321391904070>.
- [40] F. D. M. Haldane and E. H. Rezayi. “Spin-singlet wave function for the half-integral quantum Hall effect”. In: *Phys. Rev. Lett.* 60 (10 Mar. 1988), pp. 956–959. DOI: 10.1103/PhysRevLett.60.956. URL: <https://link.aps.org/doi/10.1103/PhysRevLett.60.956>.
- [41] Cumrun Vafa. “Toward classification of conformal theories”. In: *Physics Letters B* 206.3 (1988), pp. 421–426. ISSN: 0370-2693. DOI: [https://doi.org/10.1016/0370-2693\(88\)91603-6](https://doi.org/10.1016/0370-2693(88)91603-6). URL: <https://www.sciencedirect.com/science/article/pii/0370269388916036>.
- [42] Naren Manjunath and Maissam Barkeshli. *Classification of fractional quantum Hall states with spatial symmetries*. 2020. arXiv: 2012.11603 [cond-mat.str-el].